The Relationship between Shear Strength and the Optical Spectral Behaviour of Different Soils

DOI: 10.54598/006460

PhD Dissertation

Alaa El Hariri
PhD Student

Supervisor:
Prof. Dr. Péter Kiss

Mechanical Engineering Doctoral School
MATE University – Gödöllő

2025

Doctoral school

Denomination: Doctoral School of Mechanical Engineering

Science: Mechanical Engineering Sciences

Leader: Prof. Dr. Gábor Kalácska

Institute of Technology, Hungarian University of Agriculture and Life Sciences (MATE), Szent Istvan Campus, Gödöllő, Hungary

Supervisor: Prof. Dr. Péter Kiss

Institute of Technology, Hungarian University of Agriculture and Life Sciences (MATE), Szent Istvan Campus, Gödöllő, Hungary

…… ……

Supervisor affirmation Head of school affirmation

Table of contents

Nomenclature and abbreviations

A' (m^2): area at the contact patch between the wheel/track and the soil.

A: wheel-soil interaction initial contact point.

B: wheel-soil interaction rear contact point.

b (m): width of the tractive element (wheel or track).

c (Pa, kPa): shear cohesion.

c_0 (m/s): speed of light in vacuum.

D (m): diameter of the sheared cylinder in the soil (from the vane).

d (m): diameter of the vane shaft.

e: void ratio.

F_g (N): gross traction.

F_{gh} (N): horizontal component of the gross traction.

F_n (N): net traction.

F (N): tangential force from the wheel/track on the soil.

F_1 (N): force needed for breaking the cohesive bonding.

F_2 (N): force needed to overcome the friction inbetween the soil.

$F_{shear\ strength}$ (N): force needed to shear the soil till failure.

G_1 and G_2 (MPa/m): elastic modulus.

H (m): height of the soil sheared cylinder (height of the vane).

j (m, mm): shear displacement.

k (Pa): sinkage modulus.

k_0 (Pa): static modulus.

M (Nm): torque applied on the vane to shear the soil.

M_s (Nm): torque applied at the surface between the vane and the soil.

M_{e1} (Nm): torque applied at the upper part of the vane.

M_{e2} (Nm): torque applied at the lower part of the vane.

m: exponent of the penetration velocity.

E': soil shear parameter.

n: sinkage exponent.

p_o (Pa): pressure at a point in the soil.

p (Pa): pressure applied on soil; the pressure-sinkage relationship.

P: considered contact point between the wheel and the soil at time t.

P' (Pa): spherical pressure.

R (section 3.3.1) (m): distance of the considered point from the origin.

r (section 3.3.1) (m): distance from the vertical axis (z-axis) to the considered point.

R (section 3.5.3) (m): radius of the soil sheared cylinder (radius of the vane).

r (section 3.7 a) (m): radius of the wheel.

R (section 3.7.1) (m): wheel radius.

R' (Pa): deviatoric stress.

r_1 (m): radius of the vane shaft.

s: wheel slippage.

t (s): time.

T_r (s): relaxation time.

t_{gr} (m): grouser pitch.

V: specific volume.

v (m/s, km/h): wheel driving speed.

v_j (m/s): shearing velocity.

v_z (m/s): sinkage velocity.

W_0 (N): vertical load used in the iteration.

W_1 (N): an approximation to the vertical load W.

W (N): normal load applied on the soil.

x (section 3.7.1) (m): distance of point P from the vertical line passing at the center of the wheel.

x_A (m): distance of point A from the vertical line passing at the center of the wheel.

x_B (m): distance of point B from the vertical line passing at the center of the wheel.

X, Y, and Z: tristimulus values of the spectrophotometric measurement.

x (in the colour reflectance equations): moisture content in the reflectance-moisture equation.

y (in the colour reflectance equations): change in the colour reflectance record at 700 nm as function of moisture content.

Y_1: change in the soil shear strength as function of moisture content.

Y_2: change in the soil shear cohesion as function of moisture content.

Y_3: change in the soil internal friction angle as function of moisture content.

z (m): sinkage or the depth.

ż: velocity vertical exponent.

z_0 (m): maximum sinkage.

α' and β': model parameters.

α (radian): angle of the peripheral point with the vertical axis.

ς: model parameter.

η (MPas/m^2): coefficient of viscosity.

θ (radian): angle of point P relative to the positive horizontal axis.

θ_A (radian): angle of point A relative to the positive horizontal axis.

θ_B (radian): angle of point B relative to the positive horizontal axis.

θ (section 3.3.1) (radian): angle of the distance (R) with the vertical axis.

μ: friction coefficient.

ν: moisture concentration factor.

σ_z (Pa): vertical stress at a point in the soil.

σ_r (Pa): radial stress at a point in the soil.

σ (Pa): normal stress applied at the contact zone between the machine and the soil.

σ' (Pa): undrained shear strength obtained by the vane.

σ'' (Pa): major principal stress.

σ_1', σ_2', and σ_3' (Pa): principal stresses acting on a soil cubic element.

σ_1 and σ_2 (Pa, kPa): normal stresses under different masses.

τ (Pa, kPa): soil shear strength.

τ' (Pa): soil shear sress.

ϕ (degree): internal friction angle.

ω (rad/s): angular velocity.

The units of the symbols provided above are in the international system (as meter and pascal), where each unit is changeable along its scale dependent on the application (as m to cm or mm).

Abbreviations:

ISTVS: International Society for Terrain-Vehicle Systems.

LCD: liquid crystal display.

mc: moisture content.

MSCC: Munsell soil colour chart.

CIV: CRREL instrumented vehicle.

CRREL: Cold Regions Research Engineering Laboratory.

ASTM: American Society for Testing and Materials.

OCR: overconsolidation ratio.

M-C: Mohr-Coulomb.

1. Introduction

Studies related to terramechanics are grabbing the interest of too many researches from different fields to deal with terramechanics cases especially when it comes to the performance of vehicles (wheeled and tracked) on soil terrains. The pressurizing interests in developing principles for studying the land locomotion mechanics, in addition to the work and the development contributed to this field, settled the modern foundation for an independent discipline in applied mechanics known by terramechanics. Terramechanics science aims to study the principles of the interaction between the terrain and machines by studying the performance of the vehicles in the operating environment, modeling the terrain behaviour, measuring the characteristics of terrain properties, and identifying pertinent parameters of the interaction between the vehicle and the terrain. The performance of the machines moving on the terrain is affected by the terrain itself, so studying the behaviour of different terrains under the machines will serve in enhancing the driving and the vehicle performance by improving the effective traction, decreasing the slippage, and limiting or avoiding the sinkage of the wheel/s upon moving on a soft terrain. The study data of the terrain behaviour will help in the enhancement of the vehicle drive on the studied terrain, through adjusting the design of the vehicle parts and systems as the suspension system, tire's material, differential, powertrain, etc.

By the movement of the vehicle on the terrain, the weight of the vehicle will lead to pressing the wheels downward, so upon moving on soft terrains the wheels will sink, and thus the pressure-sinkage relationship is important to be studied, also when the axle applies torque to rotate the wheel it will be faced by the resistance resulting from shearing the soil (the soil material strength), so might lead to the slippage of the vehicle, thus the shear-slip relationship is also important to be studied when dealing with terramechanics case. The combination of the both upper drags (slip and sinkage) will weaken the consumption of the vehicle's output power leading to many consequences such as non-safe drive, exhausting the vehicle systems (wheels, suspension, brakes, drive train...) and consuming fuel.

Terramechanics is divided into two branches; the first is terrain vehicle mechanics and is concerned with tractive performance of the vehicle over unprepared terrain, ride quality over undulated surface, obstacle negotiation and water crossing avoidance. The second branch is terrain implement machines, and it deals with the performance of the implements (work machinery, not vehicular machines) over the terrains. Studying the terrain behaviour will help in taking the decision go/no-go on the terrain as in military move and might serve in enhancing the designs of the vehicles, and if not enhancing at least will help in choosing the suitable machine for a specific terrain. Terramechanics will not only benefit the performance of the vehicles and its users, but will be good science in protecting the environment by preserving the lands structures, so not getting ruined by the machines passing over them (soil compaction, tearing surfaces such as vegetation areas).

This research concentrates on measuring the shear strength of different soil textures. The interaction between the machine specifically between the wheel or track (tractive force) and the terrain will lead to shearing the terrain, so studying the shear force at the interaction level is a required step for studying the vehicle mobility, especially that this load might lead to the slippage of the machine, thus weakens its performance. Off-road, agriculture, military, and other fields have a big interest in such study, especially when it comes to choosing the right machine to be used, and also to the manufacturing costs of machines. Focusing on studying the normal load applied from the vehicle on the soil (load bearing capacity), with the shear

interaction load (wheel/traction), will improve the performance and the industry of the production.

For determining these forces, methods relating the weight and thrust of the machine to certain mechanical properties of the soil are required. The influence of terrain roughness on the vehicle's speed must be considered. The carried out research is pure empirical work; experiments were carried out in the laboratory for measuring the shear strength of different soil textures at different moisture contents. Soil textures data (mechanical composition with GPS coordinates, location in Hungary) were taken from a research institute, afterwards laboratory instruments (as spectrophotometer) and machines (direct shear test) were used for carrying out the measurements, in addition to that a field measurement was carried out (in situ).

Measuring the shear strength of the soil will help in analyzing the shear loads interacting between the machines and the soil terrain mainly the tested soil types, thus the study will be beneficial to some researchers by relying on the obtained data and/or findings to be used in new terramechanics designs or technology. The techniques followed and used for measuring the mechanical properties of the terrain when it comes to terramechanics are the cone penetrometer, bevameter, and the techniques used in civil engineering soil mechanics (are of limited use in terramechanics). Each of these techniques doesn't provide all the mechanical properties of the terrain, but they might give some mechanical properties, or end up with values (cone index number) used in calculating mechanical properties. Methods of approach to terramechanics are through empirical, semi-empirical, and theoretical approach. The empirical method relies on experimental results of both the vehicle moving and the terrain, and the outputs are correlated. In case of dealing with too many terrains and with vehicles of different types, such as tracked vehicles, the experiments will consume too much effort and this step requires many experiments, but ends with actual results (might not benefit in tracked heavy vehicles). The semi-empirical is the combination of both, empirical and theoretical, through having experimental data used in theoretical models, and the theoretical approach relies on theoretical methods.

2. Aim of the research

The target behind the research is that after carrying out laboratory shear tests on different soil samples (different textures) at different moisture contents, and recording the colour reflectance of the different soils (colour influenced by moisture content), the shear strength values (shear strength and its parameters) of each soil texture will be related to its colour reflectance. Relating the shear strength values of a soil to its colour reflectance, provides simplicity in detecting the shear strength values from the colour of the soil. The shear strength values of the soil textures will be measured in the laboratory using the direct shear test, the shearing mechanism that emulates the shear beneath the vehicle tractive element (translational shearing). The colour reflectance will be measured using the visible range spectrophotometer, that measures by sending light wave in the visible band (400-700 nm spectrum).

This research is pioneer (new idea in the field), it will serve in enhancing the mobilty of a vehicle on a soil terrain especially in autonomous vehicles where there is no operator to deal with the surrounding environment of the vehicle during the vehicle maneuverability. This project part (my research) is linked to a comprehensive project (university project) in off-road autonomous vehicles, so before the vehicle goes on unprepared terrain, a drone will provide the vehicle with data about the soil colour (reflectance), thus adjusting the tractive element output torque or at least take go/no-go decision over the terrain (not to get immobilized).

In vehicle mobility on soil terrain, slippage occurs at three different locations, a small portion of the slippage occurs in the tyre since it is made of rubber (elastic) compounds (despite containing metals), the second slip is at the interaction zone and is the main slippage portion, and the third slippage occurs inside the soil - in the layer beneath the tyre - due to the slippage of the soil particles over each other.

For the tyre deformation slip, and has to do with the design and the materials of the tyre, can be enhanced through adjustment on the tyre design and/or the materials used.

For the slippage at the contact zone, it can be decreased through using grabbing geometries designs at the tractive element circumference, as using lugs/treads on the tyre.

The remaining slipping doubted zone that might have influence on the mobility is the soil inner zone beneath the wheel or track. The slippage resisting strength of this zone is the shear strength of the soil. This is the sensitive zone that will be considered in our research.

Shearing this zone is emulated using the direct shear test machine, similar shearing mechanism. The shear strength and its parameters will be related to the colour reflectance through the moisture content, since both, the strength and the colour, change as function of moisture content.

3. Literature review

3.1 Background

The interaction between machines and terrains studies are of interest to terramechanics researchers. Off-road vehicles are designed to move on unprepared terrains (such as unpaved roads), and such kind of vehicles are used daily in many fields. Terramechanics is a significant element in the engineer-manufacturer-user chain aiming to improve the vehicle's stability, design, performance, handling, riding and safety. The technical term terramechanics reflects the interaction between terrains and vehicles, and the aim behind this science is to enhance the design in the soil working machinery, thus ending with designs and innovations that improve the performance of the machines complying with the terrain characteristics (Taghavifar and Mardani, 2017). Terramechanics concept was first settled by (Bekker, 1956) through his book "Theory of land locomotion" (Taghavifar and Mardani, 2017). Vehicle's performance is described by its acceleration, deceleration, and tractive parameters such as drawbar pull and net traction when moving on unprepared terrain (with irregularities and cleats) (Taghavifar and Mardani, 2017). Regardless of the fast technological improvements, studies related to the movement of off-road vehicles on terrains did not receive a valuable consideration until the middle of the twentieth century (Wanjii et al., 1997).

Bekker and other scientists guided terramechanics engineers to the right path for studying system's traction, afterwards a model was developed to predict thrust, motion resistance, and net traction or drawbar pull on soil terrains, but the complexity in dealing with measuring the soil properties and the insufficient knowledge in soil mechanics ended with non-precise equations (Bekker, 1956, 1960). When it comes to the machine's performance over a terrain, this performance is faced by the limitations that the terrain imposes on the machine's traction device (wheels and tracks) (Wanjii et al., 1997). Studying the soil conditions and properties will enhance the performance of a vehicle over the soil since matching the tire inflation and the dynamic loads to the soil conditions will increase the tractive efficiency (Lyne and Burt, 1987). Vehicle's manufacturers worked and are working on finding tractive equations relating soil to the vehicle's traction device (wheel or track). Deere and Company Technical Center developed series of traction equations relating soil conditions to tire characteristics. The developed equations are for pneumatic tires with tread design (conventional design), and the equations have been used as models in the computer simulations of vehicles (Kahle and Hung, 1967), (Pershing, 1971), (Berenyi and Pershing, 1972). The challenge for engineers when it comes to designing agriculture machinery is to reduce the compaction of the soil resulting from the machine weight, and increase traction and the tillage speed, and that is achieved by determining the traction properties of soil (Mckeys, 1985). In spite of soil mechanics is a study founded since over a century, till now there are no fixed rules to follow for choosing the suitable soil shear strength measurement methods (Mckyes, 1985), but when it comes to off-road engineering the best method for finding the soil properties is the approach that emulates (duplicates) the field conditions (Karafiath and Nowatzki, 1978). Micklethwait (1944) mentioned that tractive forces acting on a vehicle are estimated using the coulomb's equation which relates the shear strength to cohesion, pressure, and friction, and that the bearing capacity is what keeps the vehicle on surface and resists the sinkage, and is estimated by a bearing capacity formula as the formula proposed by Prandtl (1920) and Terzaghi (1943). The possibility of locomotion on a given terrain is described by the ability of soil to provide resistance to the gravity loads and produce necessary thrust (Bekker, 1957).

3.2 Modelling of the terrain behaviour

When studying the interaction between the machine and the terrain, understanding the behaviour of the terrain at the interaction zone will help in determining the properties of the terrain. Dealing with the terrain as an elastic medium has built theoretical basis for studying the resulting soil compaction, but that is real in case of dense terrains and if the applied load isn't exceeding a limit which is the terrain bearing capacity (Wong, 2010). Considering the terrain as a rigid, perfectly plastic material, served in estimating the maximum traction of an off-road vehicle, predicting the forces acting on a bulldozer blade, and assessing the tractive forces developed by the lugs or wheel's grousers. This modelling can be applied for estimating the forces acting on the engaging element supported by the terrain, but cannot predict the terrain deformation (Wong, 2010). The soil deformation resulting from a load on the soil terrain is non-linear, and the strain consists of both regions, the elastic which is recoverable and the plastic or viscous and is irrecoverable. The change in the intensity of strain resulting from the applied stress represents the non-linearity; the elastic region in the stress-strain behaviour is the recoverable deformation of the soil, and the plastic region is the irrecoverable deformation describing the volumetric change, while viscosity is the deformation capacity developing with time (Wanjii et al., 1997). Different element's combinations have been used for ending up with models expressing the visco-elastic behaviour of soil depending on the type of the research problem (Wanjii et al., 1997). Tan dealt with the soil behaviour depending on rheological models using a Poynting-Thomson model (connecting Hookean element with a Maxwell element) (Tan, 1957). Pan in his study used a four-element model, also there are other models designed by researchers to deal with various types of stress-strain relationships (Pan, 1986) (Oida, 1986). Karafiath and his colleagues used the continuum mechanics and soil plasticity theory in modeling the soil-wheel interactions (Karafiath, 1970). Perumpral et al. (1971), Yong and Fattah (1976, 1978), and Raper et al. (1990) relied on the finite element method in the prediction systems of mobility and soil compaction. Wanjii et al. (1997) used a visco-elastic soil model based on the three-element Maxwell model for evaluating the normal stress distribution under the wheel, and for the evaluation of the tangential shear stress distribution, a rigid wheel-soil interface model was used. When studying the interaction between the vehicle and the terrain, the visco-elastic problems should be taken into consideration.

Sitkei (1972b, 1997) has shown that the soil can be modelled as a viscoelastic medium, thus when dealing with soil calculations rheological approach may be used. The performance of a vehicle enters a critical stage when moving on a very soft ground where the sinkage, slippage and other resistances (motion resitance) should be given an account. Dealing with a vehicle on a very soft soil terrain is much different than when having the vehicle operating on a soil surface without having deformation in the soil. The tyre tractive coefficient value ranges from 0.85 when moving on a paved surface to a coefficient less than 0.4 on soft terrains (Liljedahl et al., 1979).

3.3 Evaluation of the terrain

Evaluating the terrain settles the basic laws to assess a vehicle's mobility and its performance on the terrain. The majority of the laws that are used in scientific and engineering disciplines are constructed based on idealizations and simplifications (an example, Figure 3.1). These physical laws and principles must always be exploited for improving mobility on the terrains.

Baladi (1987) prepared a report for the 9th conference of ISTVS about the mechanical soil responses, the terrain data types, and the methods used for finding the data. Tanaka (1984)

using soil rheological models described the behaviour of paddy fields. Taylor and Gill (1984) worked on a review about the compaction of soil (intentional and incidental) in different fields (agricultural, forestry, and military). The turning resistance of soil on a vehicle was considered by Dudzinski (1984) through a review. Sigiyama and Kondo (1984) represented a paper on terrain evaluation. These are examples showing the importance of the terrain data and the measuring methods (data acquisition methods), dependent on the application/s. Describing the terrain profile by mechanical characteristics resulting from compression and tension loads under the tyres helps in estimating the combined behaviour of the vehicle and the terrain (Taghavifar and Mardani, 2017).

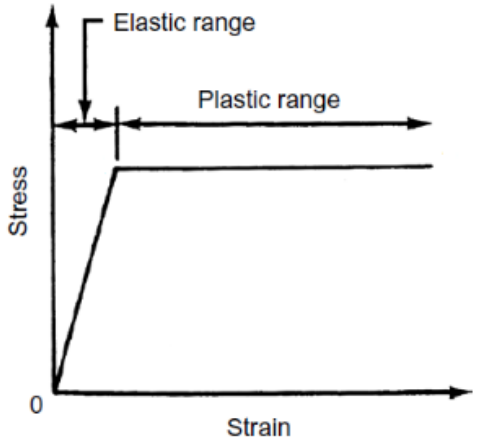

Fig. 3.1. Idealized stress-strain relationship of an elastoplastic material (Wong, 2010).

3.3.1 Terrain as an elastic region

For the case of not exceeding the yielding point upon having a load applied on the soil, the behaviour of the soil is known by the linear/non-linear elastic material. For this case the stress distribution in the soil medium can be estimated using the theory of elasticity by simplifying the stress distribution resulting from the load in a homogeneous, isotropic semi-infinite elastic medium using the Boussinesq equation defining the radial and vertical stresses (stresses in Figure 3.2) (Taghavifar and Mardani, 2017).

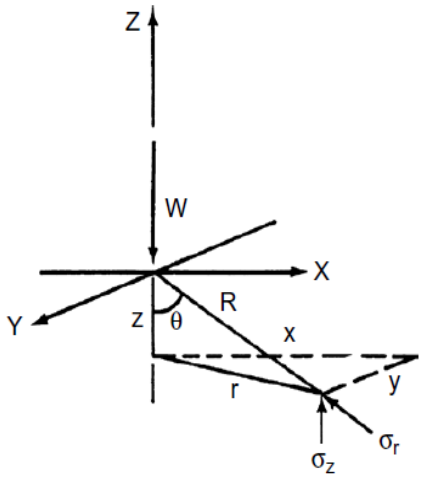

Fig. 3.2. Stresses resulting due to a point load on the surface of a semi-infinite elastic medium (Wong, 2010).

With,

$$\mathbf{r} = \sqrt{\mathbf{x^2 + y^2}} \qquad \mathbf{R} = \sqrt{\mathbf{z^2 + r^2}}$$

$$\sigma_z = \frac{3W}{2\pi\left[1 + \left(\frac{r}{z}\right)^2\right]^{\frac{5}{2}} z^2} = \frac{3W}{2\pi R^2} \cdot \left(\frac{z}{R}\right)^3 = \frac{3W}{2\pi R^2} \cdot \cos^3\theta \tag{3.1}$$

$$\sigma_r = \frac{3W}{2\pi R^2} \cdot \cos\theta \tag{3.2}$$

This model doesn't take into consideration the elastic behaviour of the soil and its characteristics, and the stress in this model is as function of distance from the point where the external load is applied and the applied load value, also this model is limited to distances where elastic behaviour is applicable, and upon crossing this distance, the model becomes invalid (Wong, 1989). Summing some discrete point loads (differential from the surface area) using the superposition effect will result in the load applied on the surface (Taghavifar and Mardani, 2017).

So, replacing W in the equation by $dW = p_0\, dA$ for finding $d\sigma_z$

$$d\sigma_z = \frac{3p_0 \cdot r dr d\theta}{2\pi\left[1 + \left(\frac{r}{z}\right)^2\right]^{\frac{5}{2}} \cdot z^2} \tag{3.3}$$

Double integration with respect to r and θ

$$\sigma_z = \frac{3p_0}{2\pi}\int_0^{r_0}\int_0^{2\pi} \frac{r dr d\theta}{\left[1 + \left(\frac{r}{z}\right)^2\right]^{\frac{5}{2}} \cdot z^2} = 3p_0 \int_0^{r_0} \frac{r dr}{\left[1 + \left(\frac{r}{z}\right)^2\right]^{\frac{5}{2}} \cdot z^2} \tag{3.4}$$

The pressure bulbs (Figure 3.3) are lines of different stress values, each of them describes (embeds) the points receiving the same level of stress in the medium.

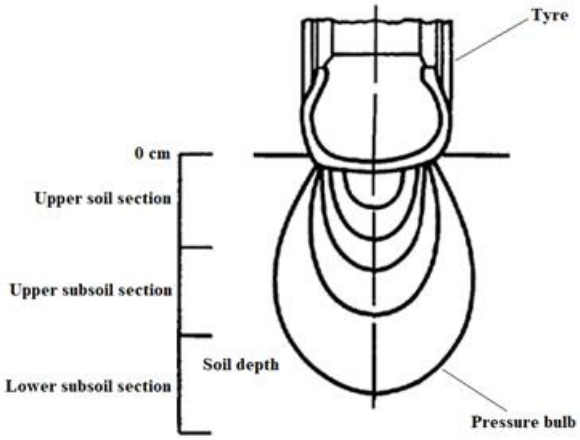

Fig. 3.3. Pressure bulbs under the wheel of a vehicle in a semi-infinite elastic medium (Wong, 2010).

Since the soil conditions such as moisture content influence the calculations, Frohlich introduced a moisture concentration factor ν (depends on the terrain) to the Boussinesq equation (Sohne, 1958), (Wong, 1989), (Boussinesq, 1885):

$$\sigma_z = \frac{W\nu}{2\pi R^2} \cdot (\cos^{\nu}\theta) = \frac{\nu W}{2\pi z^2} \cdot (\cos^{\nu+2}\theta) \tag{3.5}$$

$$\sigma_r = \frac{W\nu}{2\pi R^2} \cdot (\cos^{\nu-2}\theta) = \frac{\nu W}{2\pi . z^2} \cdot (\cos^{\nu}\theta) \tag{3.6}$$

3.3.2 Terrain as a plastic region

The Mohr-Coulomb failure criterion is implemented in the plasticity region defining the failure of the terrain. The criterion expresses the failure point of the soil, relating the shear strength to the cohesion and internal friction angle taking into consideration the applied normal stress, through the following equation (Taghavifar and Mardani, 2017).

$$\tau = c + \sigma \cdot \tan\phi \tag{3.7}$$

τ is the shear strength, c is the cohesion, σ is the normal stress applied on the sheared surface, and ϕ is the internal friction angle of the material.

The envelope (just one line) passing tangentially at the circumferences of the stress Mohr circles, shown in the Figure 3.4, is used to find the cohesion c (intercept with shear strength axis) and the angle of internal friction resistance (internal friction angle, the angle between the envelope line and the horizontal dashed line) (Taghavifar and Mardani, 2017).

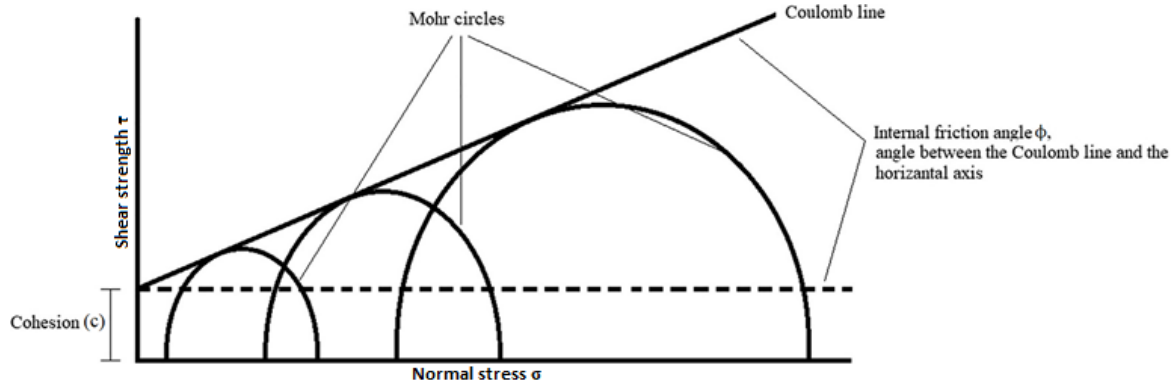

Fig. 3.4. Mohr-Coulomb failure criterion.

From a conceptual point this criterion means that if a Mohr circle representing the state of stress at a point touches the envelope line, the failure will occur at this point.

Using the cohesion c and the internal friction angle ϕ obtained from the Mohr-Coulomb envelope, the bearing capacity, maximum thrust, and the maximum drag on a tracked or wheeled vehicle system can be calculated.

Assuming the pressure acting on the area (patch) is uniform, then the maximum traction (thrust) is calculated using the following equation (scheme in Figure 3.5) (Taghavifar and Mardani, 2017).

$$F = \tau \cdot A' = (c + \sigma \cdot \tan\phi) \cdot A' = c \cdot A' + W \cdot \tan\phi \tag{3.8}$$

A’ is the contact area between tyre/track and the soil.
W is the normal load and is equal to the product of the contact pressure and the contact area.

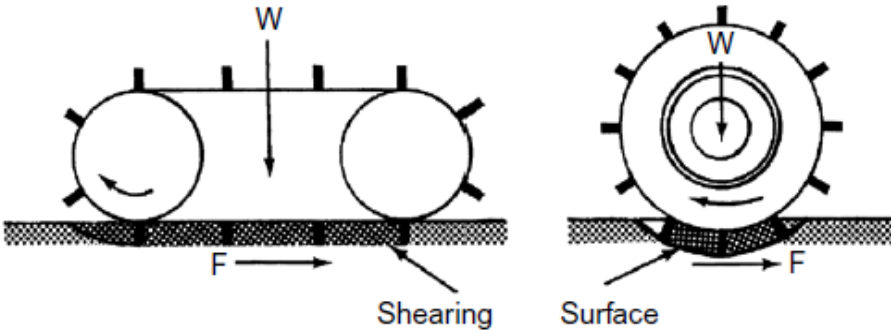

Fig. 3.5. Shearing action of a track and a wheel (Wong, 2010).

It is important to take into consideration that some of the soils are cohesionless (neglected cohesion value) as for dry sand, also there are types that are of neglected internal friction angle such as saturated clay (Taghavifar and Mardani, 2017).

Uffelmann (1961) has improved that for clay soils the vehicle performance can be represented in terms of cohesion, and Reece (1964) has shown that it is possible to express the vehicle performance on frictional soil (at least in dense state). Soil-implement mechanics has shown that soil forces and modes of failure rely on the cohesion, internal friction angle, and density (Payne, 1956), (Osman, 1964).

3.3.3 Evaluating the terrain using the critical state soil mechanics

Critical state soil mechanics was developed by Roscoe et al. (1958) and his associates at Cambridge University as a step aiming to solve the limitations that the models resulting from treating the terrains as elastic or rigid mediums aren’t able to solve (Schofield and Wroth, 1968), (Kurtay and Reece, 1970). Classical soil mechanics theories are applied to solve problems having the soil in dense state, but in case of problems having the soil in loose state it is dealt with it empirically. Critical state soil mechanics deals with the soil behaviour in whole states range by establishing a relationship between the specific volume V, spherical pressure P’, and the deviatoric stress R’ of the soil. The specific volume is equal to 1+e (e is the void ratio of the soil; ratio of the volume of voids to the solid’s volume) (Wong, 2010).

P’ and R’ are calculated using the following equations:

$$P' = \frac{\sigma_1' + \sigma_2' + \sigma_3'}{\sqrt{3}} \tag{3.9}$$

$$R' = \frac{1}{\sqrt{3}}[(\sigma_1' - \sigma_2')^2 + (\sigma_2' - \sigma_3')^2 + (\sigma_3' - \sigma_1')^2]^{\frac{1}{2}} \tag{3.10}$$

Where σ_1', σ_2', and σ_3' are principal stresses acting on a cubic element of the soil.

When using critical state soil mechanics in a study case, the soil is assumed to be homogeneous and isotropic. In off-road cases the vehicle is subjected to a variety of natural terrains, such as snow and organic terrains (tundra, muskeg), these terrains under most circumstances cannot be

treated as homogeneous and isotropic. Classical soil mechanics has so far found few practical applications for studying infield vehicle-terrain interaction (Wong, 2010).

3.4 Soil moisture content

The moisture content present in soil influences its properties, thus resulting in different soil behaviour. Komandi (1992) mentioned in his article that both, the shear strength and bearing capacity depend on the physical state of the soil. The moisture content and the void ratio are factors influencing the mechanical properties of the soil, through influencing the cohesion and the internal friction angle. Low moisture content means high interparticles friction, and the high mositure content decreases the soil friction. For loam soils cohesion decreases with the increase in the moisture content, and inversely the cohesion in sandy and clay soils increases with increasing the moisture (Komandi, 1992). Increasing the void ratio dercreases the cohesion and friction in all soils (Komandi, 1992). Shoop (1993) mentioned that the moisture content is the most influencing soil condition on the soil strength. The traction increases or remains constant with the increase in the moisture content until reaching the liquid limit. Liquid limit is the water content where the soil becomes as liquid (Rajapakse, 2015). Beyond the liquid limit, the traction decreases rapidly, this is applicable at all tyre contact pressures, but before the liquid limit, the contact pressure has influence on the traction (Shoop, 1993). At moisture content more than the liquid limit, the traction becomes insensitive to contact pressure (Shoop, 1993). Ayers (1987) and Harrison (1966) in their reports ended with results showing that the internal friction angle increases with water content till reaching liquid limit and afterwards the value drops. Other researchers have mentioned the influence of moisture on cohesion (Komandi, 1992), (Zydron and Zgoda, 2012), (Dafalla, 2013). Mulqueen et al. (1977) has shown that the change in water content influences the cone resistance value (cone index) in numerous ways. Pillinger et al. (2018) mentioned in their article that soil deformation resulting from the passage of a vehicle depends on the physical composition of the soil, dampness (water content), density, and the initial compression state, and also mentioned that with the increase in moisture the soil becomes more compact.

3.4.1 Gravimetric method for measuring the soil moisture content

Among the most accurate methods used for measuring the moisture content of the soil is the gravimetric method. This method depends on the masses of the soil before and after drying. The drying occurs either using oven for 24 hours (sufficient time for drying the soil) or using the moisture analyzer. The oven entitles to dry a bigger amount of soil (kg) when compared to the usage of the analyzer (g). Both of them dry the soil at fixed temperature (104-105 °Celsius). The temperature used is approximately at the boiling point of the water content, exceeding this temperature might lead to burning some of the soil constituents. The aim is just to evaporate the water reaching unchanged mass of the dry soil.

An analyzer is equipped with a system to hold a certain capacity (grams) and is of specific measuring resolution. Below the covering panel, the lid, on the inside of the hood there is a halogen heating bulb (or heating plate) for drying the soil sample, also for providing accuracy in the temperature control. Inside the analyzer there is a builtin temperature sensor that transfers the actual temperature to the electronic components for regulating the temperature. The hood is always checked that it is closed by a mechanical contact (process doesn't start or stops incase the hood is open). The mass of the sample appears on the LCD, and depending on the set parameters, additional information is displayed (temperature, time elapsed, required time, display mode, momentary result). At the start of moisture determination (start of the heating

process), the inside chamber is heated till temperature is reached. The amount of moisture evaporated is displayed in percent (%), and the residual mass is also displayed (dried sample mass). The drying process continues for finding the moisture content till the sample is of zero moisture, afterwards the heating bulb is fully shut-off.

In gravimetric method, the equation used for calculating the moisture percentage is:

$$\% \textbf{ Moisture content} = \frac{\textbf{wet mass} - \textbf{dry mass}}{\textbf{wet mass}} \cdot \textbf{100} \tag{3.11}$$

The calculated moisture is wet base, since divided by the wet mass (initial mass before drying). Incase of dividing over the dry mass, then dry base moisture calculation.

Figure 3.6 shows the oven as gravimetric method (old measurement) used for measuring the moisture content. In the research body, a figure of the used moisture analyzer (labeled) is presented.

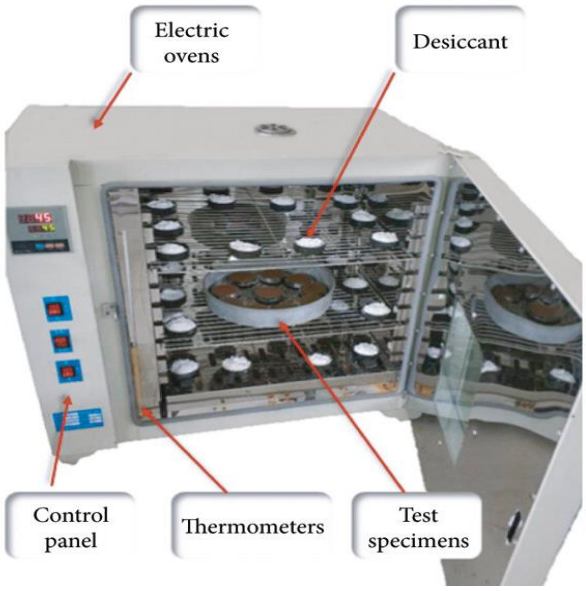

Fig. 3.6. Soil moisture content obtained using an oven (Tao et al., 2021).

3.5 Measuring terrain properties

For characterizing the terrain through identifying its properties, the tests used are divided into to types, tests used for identifying the terrain composition property and the others used for measuring the mechanical properties (Lambe, 1964), (Bishop and Heknel, 1964), (Yong and Warkentin, 1975). The mechanical properties of near surface-materials are measured by the following tests: cone penetrometer, bevameter (plate penetration test and shear test), direct shear test (shearing machine used) and triaxial test (Baladi, 1987). In order to assess a vehicle's mobility, relations describing the terrain response to the vehicle must be recorded (Murakami, 1991), thus for analyzing the terrain response to the vehicle's excitation/s, empirical, analytical, and numerical approaches have been used (Bekker, 1956), (Sela and Ehrlich, 1972), (Baladi and Meier, 1987), (Yong and Fattah, 1981). The cone penetrometer, bevameter and the traditional civil engineering techniques are the mostly used infield techniques for measuring the terrain properties when studying the mobility of a vehicle on a terrain (Wong, 2010). Selecting the particular technique is related to the purpose of the measurement for studying the mobility case. Incase of using the method for the sake of developing and designing new

products in the off-road technology, then the technique is different than the technique used in military operations for taking the go/no-go decision over a terrain (Wong, 2010). Bekker mentioned in his book that there are two major techniques for measuring and characterizing the terrain properties, aiming to evaluate the off-road vehicle mobility in the field, and the two techniques are the cone penetrometer and the bevameter (Wong, 2010).

3.5.1 Cone penetrometer technique

The technique was developed by the Water Ways Station (WES) of the US army corps of engineers in the second wold war period. The aim behind inventing this technique was to provide the army with a simple device that is used infield for assessing vehicle mobility and terrain trafficability, thus taking the go/no-go decision over a terrain. The WES developed the cone penetrometer of 30-degree cone angle and 3.23 cm^2 (0.5 in^2) base area (shown in Figure 3.7). The measured value resulting from the cone penetrometer test in known by the cone index, representing the resistance of the terrain to penetration per unit base area of the cone. The cone index is a number reflecting the shearing and compression characteristics of the terrain, in addition to expressing the adhesion and the friction at the interface between the cone and the terrain. The change in the cone index value relative to the penetration depth is known by the gradient, and forms the base for predicting the performance of an off-road vehicle on fine (clay) and coarse grained (sand) soil terrains (Wong, 2010). Despite finding the index simply using the cone penetrometer, there is still a controversy on the usage of the index, if either to be used in identifying the terrain characteristics resulting from the vehicle mobility or resulting from the terrain trafficability. Reece and Peca (1981) mentioned that even though the cone index may help in identifying the shear strength of remoulded frictionless clay, but is not suitable for characterizing the properties of sand. Turnage (1984) based on reanalyzing obtained experimental results, deduced that additional laboratory tests are required for defining the relationship between the gradient of cone penetration resistance (before tyre pass), relative density, compactability and the distribution of grain size for ending with accuracy in predicting the tyre performance on sand soil of a moisture content.

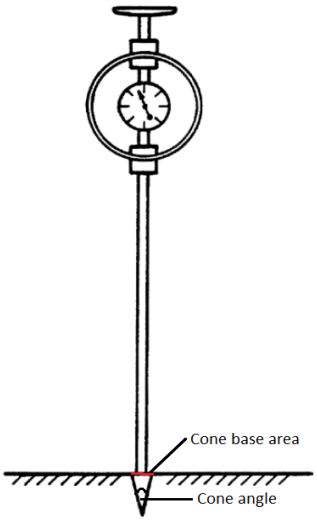

Fig. 3.7. Cone penetrometer basic form (Wong, 2010).

Ralph and Volker (1992) mentioned in their article that the cone penetrometer is widespread adopted technique for characterizing the soil strength in traction prediction equations. Wismer and Luth (1973) used the cone index as a variable reflecting the soil strength in their dimensionless ratio known by the wheel numeric, and this term (wheel numeric) was used in

developed equations for predicting the net and gross traction ratios, also for predicting the motion resistance ratio.

Gee-Clough et al. (1978) used the mobility number in their equations, and is an extension of the wheel numeric obtained by Wismar and Luth. Dwyer et al. (1974) used a shear meter and cone penetrometer both mounted on a tractor for determining strength parameters data. Ralph and Volker (1992) adjusted Wismer and Luth equation aiming to compute the wheel numeric taking into consideration wheel slip, drawbar pull, and the input dynamic loads, where the benefit of this step is determining the cone index continuously on a terrain. Máthé and Kiss (2015) used an empirical model built by Hernanz et al. (2000) which depends on the cone penetration method in determining the rolling losses during vehicle towing. Meirion-Griffith and Spenko (2011) have shown that the cone penetrometer is a method used in determining the bearing capacity, evaluating the quality of cultivation, determining rolling losses of vehicles, and in tyre-terrain interaction investigations.

Ralph and Volker (1992) also mentioned that the majority of the traction prediction equations rely on the cone index as a main value for measuring the soil mechanical properties. Freitag (1965) demonstrated that the cone resistance can be used for defining soils by dimensionless parameters (mobility number and sand number) when dealing with purely frictional or cohesive soils, where these numbers describe the tyre's performance on the soil, and mentioned that in frictional soils the cone index gradient with depth is of importance instead of the absolute cone index value.

American Society of Agricultural Engineers (1969) settled two cone sizes as a standard with the insertion speed, and are 30° cone (angle) of sizes 20.27 and 12.83 mm (diameters) at 30.5 mm/s penetration speed. Cones of different geometries (angle, diameter) have been used, Abeels and Declercq (1977) described a cone of 60 ° angle and 5 mm height, so it is required to state the size of the cone used and the units for expressing the cone resistance. Wismer and Luth (1973) noted that the cone index varies with depth, so the cone index value used for predicting the traction over a terrain is the average of the cone index values recorded along the depth corresponding to the maximum sinkage of the traction element (tyre, track).

The cone index is also used in determining other indices that are important in studying the terrain. The remoulding index RI is the ratio of the cone index CI after remoulding to that before remoulding. The remoulding process depends on the soil grains, incase of fine-grained soils the remoulding is done by 100 blows using 1.135 kg (2.5 lb) hammer dropped from a height 30.5 cm (12 in) on the soil sample (inserted using Hvorslev sampler) in the remoulding cylinder, and in case of having coarse-grained soils with fines the remoulding cylinder with the base having the soil sample inside is dropped 25 times from a height 15.2 cm (6 in) to a firm surface (Mobility and Environmental Systems Laboratory US, 1958), (Meyer and Knight, 1961), (Society of Automotive Engineers, 1967b). When finding remoulding cone index, the cone used for measuring the cone index before and after remoulding is of base area 1.29 cm^2 (not the 3.23 cm^2). Remoulding might strengthen or weaken the terrain (influence the terrain strength), and that depends on the terrain type and its conditions. The rating cone index (RCI) is the product of the remoulding index (RI) and the cone index (CI) before remoulding. The vehicle cone index (VCI) is the minimum cone index in the soil critical layer (layer's depth varies with vehicle's type and weight) allowing the vehicle to make specific number of passes without immobilization. The terrain slope index can be found using the cone penetrometer which is an important soil property (Taghavifar and Mardani, 2017). The RI, RCI and VCI are

indices representing the strength of the terrain under vehicular traffic (terrain trafficability) (Wong, 2010).

3.5.2 Bevameter technique

The bevameter technique is used for measuring the terrain properties under loading conditions that emulate the loading conditions resulting from the mobility of an off-road vehicle over a terrain, and this technique was developed by Bekker as a solution for ending up with suitable terrain properties when it comes to off-road case of study (Wong, 2010). The interaction between the terrain and the vehicle results in normal and shear loads on the terrain, so for emulating the normal and the tangential loads on the terrain, Bekker developed the original bevameter technique, and it embeds two separate tests; the shear and normal test. The first test is the plate penetration test, a plate which is of a suitable size, close or similar, to the contact area of the running gear (tyre or track contact area with the terrain), is pressed using hydraulic force and as a result of the test the pressure-sinkage relationship of the terrain will be measured. The pressure-sinkage relationship will help in predicting the normal pressure distribution on the interface between the vehicle and the terrain. The shear test and is the shearing of a plate (might be with grousers) on the terrain surface, and simulates the shearing between the wheel and the terrain.

The shear test having simultaneoulsy a normal stress (normal load) applied on the shearing plate ends with the soil shear-displacement relationship, thus the shear-displacement relationship at different applied normal loads.

The shear-displacement under an applied normal load provides the required input for predicting the shear stress distribution at the vehicle-terrain interface, the multipass performance of the running gear, the additional vehicle sinkage resulting from slipping, and provides information about the terrain behaviour under repetitive shearing and normal loads. bevameter is an instrument that can be used for insitu measurement, so used in the field. It consists of the normal and the shear testing parts, the normal test will help in measuring the bearing capacity of the soil terrain, and the shear test will end up with the terrain's shear strength (Taghavifar and Mardani, 2017). An annular ring is used as a shearing device mounted at the end of the shaft and is rotated at constant velocity. The torque and displacement measured values are used for calculating the shear strength. The bevameter plate pressing test without shearing is known by the bearing capacity device (plate penetrometer), and this test is processed by forcing a plate (can be of different sizes) into the soil. The penetration forces and the sinkage are recorded and used for measuring the terrain bearing capacity (Taghavifar and Mardani, 2017). The bevameter composed of the two tests (plate pressing and shearing) will end up with the cohesion, angle of internal friction, sinkage moduli, and the sinkage exponent (n) (Meyer et al., 1977). The operational mechanism of the bevameter technique is shown in Figure 3.8.

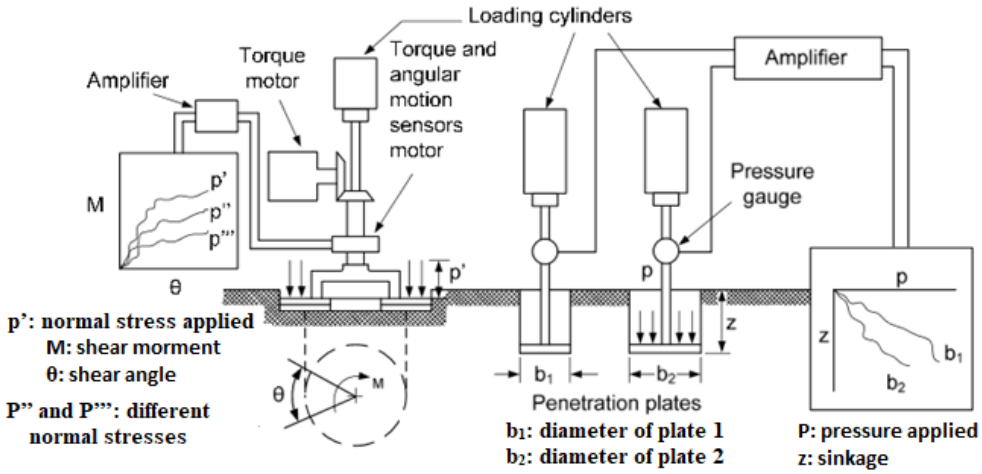

Fig. 3.8. Bevameter schematic diagram (Bekker, 1969).

Petawawa National Forest Institute (PNFI) of Canada developed a bevameter integrated in a single body that is capable of performing both tests (plate press and shear, Figure 3.9) (Golob, 1981). The apparatus is equipped with specially developed hydraulic cylinder incombination with a hydraulic motor. Incase of the pressure-sinkage test, a plate is attached to the bottom of the cylinder rod and the force acting is resulting from the hydraulic pressure acting on the piston.

In the shear test a shear head (ring) is replaced by the plate and a normal load is applied by the hydraulic force. The shear head rotates using the hydraulic motor installed and connected to the top of the cylinder rod by a splined shaft (Wong, 2010).

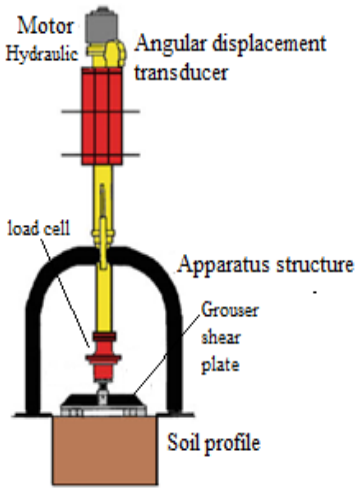

Fig. 3.9. Bevameter and the shear plate with grousers (two tests integrated in one body) (Taghavifar and Mardani, 2017).

3.5.3 Terrain mechanical properties by geo/civil engineering techniques

Civil engineering deals with studying the soil parameters such as shear strength, shear modulus, density, void ratio, etc. In most cases for studying the soil properties, samples are taken from the field inorder to be studied in equipped laboratories. Different machines are used in a laboratory for ending up with the soil properties. The shear strength of the soil is measured

using different methods in the laboratory, usually using the triaxial or direct shear box methods. Measuring the terrain properties infield is much more accurate than in laboratory, and the most advantage behind measuring infield is that soil is undisturbed. The soil sampling process disturbes the soil upon removing the samples from the field, thus infield measurements serve in the undisturbance of soil. Field measurement is less expensive and faster upon the usage of portable data acquisition system. When it comes to studying vehicle mobility over soil, dealing with the soil strength and properties using the civil engineering soil mechanics is not suitable and its usage (the methods) is limited (Wong, 2010).

The cohesion and the internal friction angle are shear strength parameters. These two parameters have formed the base for civil engineering soil mechanics since Coulomb's work (1776). Recently these two parameters are used in vehicle and implement mechanics' studies over soil terrain (Osman, 1964). The studies related to soil-implement mechanics have shown that the cohesion, internal friction angle, and density are the parameters that the analysis of forces and failure modes depends on (Payne, 1956), (Osman, 1964). Even though measuring the cohesion and the internal friction angle is the most important, but it is of high difficulty (Osman, 1964). Regardless of the availability of different methods for measuring the shear strength of soil, there is lack in the information published comparing the results obtained using the different methods, and the reason behind that might be due to the difficulty in obtaining reliable set of values from a single method (Osman, 1964).

Figure 3.10 shows the methods used for measuring the shear strength and their classifications (direct or indirect) (Damian and Dudzinski, 2021).

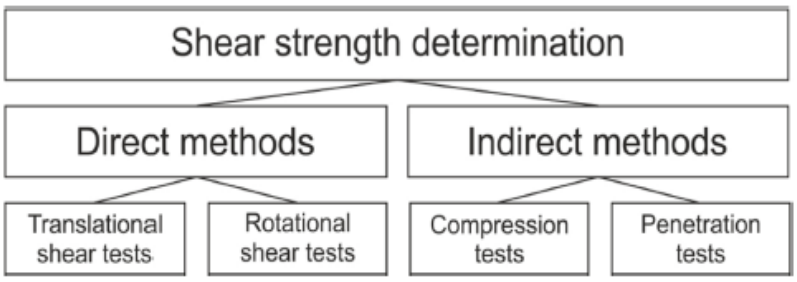

Fig. 3.10. Types of methods used for measuring the soil shear strength (Damian and Dudzinski, 2021).

Among the methods used by civil engineers for measuring the shear strength there are:

a - Translational shear box (direct method - translational shearing)

This method consists of two halves, one of them (the upper half) is free to slide over the lower half (Figure 3.11). The box where the soil is filled is installed in brass container keeping the lower half static (fixed, tighted by screws), while the top half move in longitudinal direction at constant rate applied using geared jack. The upper part (top) deflects till reaching the maximum having a normal load applied on the sample (consolidation load). The shear force applied on the upper half is measured using calibrated proving ring (sensor), and having the shear load divided by the area of the shearing zone, the shear stress is obtained. The maximum shear stress is the shear strength of the soil under the applied normal stress (load over area). Plotting the shear strength against the normal stress will lead to finding the shear strength parameters. The internal friction angle is the angle of the plotting (Mohr-Coulomb failure line) with the

horizantal, and the cohesion is the intercept of the line with the shear strength axis (y-intercept) (Osman, 1964).

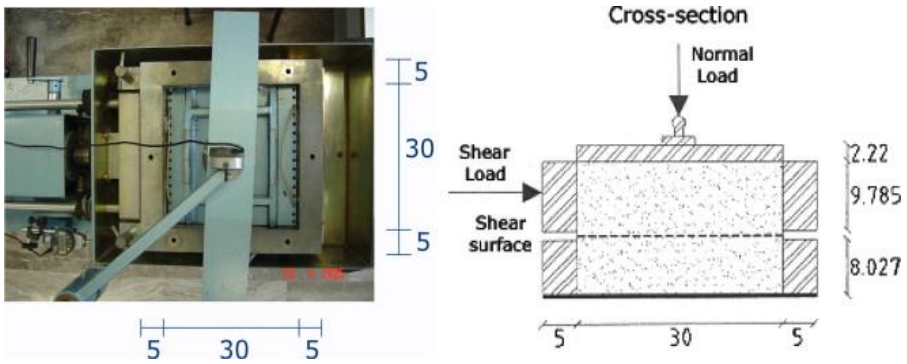

Fig. 3.11. Plan view and cross-section of large direct shear box (dimensions in cm) (Dimitrios et al., 2010).

b - Insitu shear vane test (direct method - rotational shearing)

The insitu shear vane test is an experiment that requires inserting a vane into the soil (borehole), and rotating the inserted vane at slow and constant strain rate (constant angular velocity, approximately six degrees per minute). Figure 3.12 shows how the vane is inserted and rotated (twisted). The surface, upper area, and the lower area of the vane (shown in the figure) interact with the soil, shearing till failure. The torque applied on the vane will be resisted by the soil till failure (failure resistance will be the maximum torque applied by vanes) (Changbin et al., 2018).

The maximum applied torque resisted by the soil directly before failure is obtained by the algebraic equation summing the torque values at the lateral, upper, and lower area of the vane.

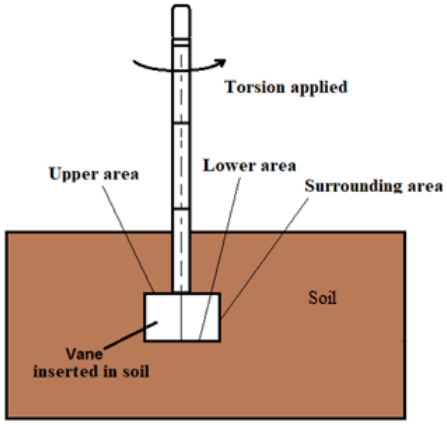

Fig. 3.12. Vane inserted in the soil, with the areas surrounding the vane.

The torque applied by the shear vane is equal:

$$\mathbf{M = M_s + M_{e1} + M_{e2}} \qquad (3.12)$$

$\mathbf{M_s}$ is the torque applied at the surface between the vane and the soil
$\mathbf{M_{e1}}$ is the torque applied at the upper part of the vane.
$\mathbf{M_{e2}}$ is the torque applied at the lower part of the vane

$$M_s = \pi \cdot D \cdot H \cdot \sigma' \cdot R = \frac{\pi}{2} \cdot D^2 \cdot H \cdot \sigma' \quad (3.13)$$

$$M_{e1} = \int_{r_1}^{R} 2\pi \cdot r dr \cdot \sigma' \cdot r = \frac{2}{3}\sigma' \cdot \pi \cdot \left(R^3 - r_1^3\right) = \frac{1}{12}\sigma' \cdot \pi \cdot (D^3 - d^3) \quad (3.14)$$

$$M_{e2} = \int_{0}^{R} 2\pi \cdot r dr \cdot \sigma' \cdot r = \frac{1}{12}\sigma' . \pi . D^3 \quad (3.15)$$

D, R, and H are the diameter, radius, and height of the sheared cylinder, and are similar to the geometry of the vane (diameter, radius, and height).

d and r_1 are the diameter and the radius of the shaft.

σ' (in equations 3.13, 3.14, 3.15) is the yield shear stress (undrained shear strength).

Parameters used in the equations are shown in Figure 3.13.

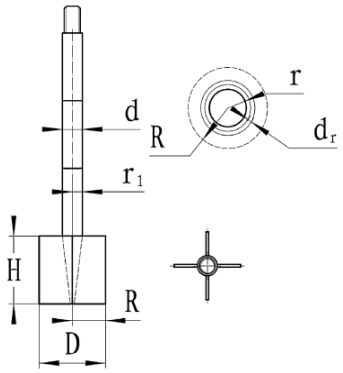

Fig. 3.13. Showing the parameters used in the equations (Changbin et al., 2018).

Assuming that the soil used is homogenous and isotropic, thus the yield stress of the soil is same along all the directions, so the shear strength is evenly distributed in the lateral area and is equal at the upper and lower areas of the vane. Thus, the resulting torque equation is:

$$M = \frac{\pi}{12}\sigma' \cdot (2D^3 + 6D^2H - d^3) \quad (3.16)$$

The shear strength is calculated using Equation 3.16 based on the vane geometry, and is the measured torque value incase of vane shear apparatus. Equation 3.16 indicates that the soil and parameters of vane geometry directly influence the torque.

When dealing with same soil (same properties) the shear strength can be assumed to be the same incase of using another shear vane for measuring the shear strength (different vane diameter having same height and same shaft diameter). Launching from this assumption, a polynomial function results from the above equation M relating the soil failure torque to the diameter of the vane.

Assume the shear strength (σ') is of a value 1 kPa, and having vanes of different diameters (3, 4, 5, 6, 8, and 10 cm) with height and shaft diameter both fixed (d=1.5cm and H=5cm).

Finally, relying on the above assumptions and taking into consideration the different vanes used, a relationship between the failure torque (M) and the diameter of the vane (D) was

derived, with a regression analysis showing that the relationship is of coefficient of determination above 0.999. Thus, the diameter of vane (D) can be used in finding the torque leading to the soil failure resistance (Changbin et al., 2018).

Thus, the simplified following equation is:

$$\mathbf{M} = \boldsymbol{\alpha'} \cdot \mathbf{D}^{\boldsymbol{\beta'}} \tag{3.17}$$

Where α' and β' are parameters having d and H fixed, and are obtained with different shear strengths.

α' and β' are affected by the shear strength, and since the soil shear strength is influenced by density and moisture content as reported by (Zhang et al., 2001), this means that α' and β' are influenced by the soil conditions (Changbin et al., 2018).

The shear strength obtained using the shear vane couldn't be broken down to cohesive and frictional components, and thus used for clay soils (Osman, 1964).

c - Triaxial compression test

The triaxial test is one of the most widely used geotechnical laboratory tests to determine the strength and stiffness of rocks for using the results in engineering designs, and this test closely corresponds to insitu state of stress (Deepak and Ivan, 2017). Wong (2010) mentioned in his book that the triaxial apparatus and the translational shear box are commonly used in soil mechanics studies related to civil engineering.

In the triaxial test a constant hydraulic pressure and known by the confining pressure is applied to the cylindrical surface of the specimen, and at the same time an axial compressing load is applied on the specimen (at its ends). Having the confining pressure applied on the cylindrical surface and of constant value (fixed value), the axial load is increased till the failure of the specimen. The oil used for applying the confining pressure is separated from the soil specimen by a rubber membrane.

The specimen test is carried out in a high pressure cell, shown in Figure 3.14. Tests are made on different samples (same tested geo-material), but with an increase in the applied confining pressure in each test. These tests will lead to drawing the Mohr circles (each Mohr circle passing through major and minor principal stresses on the x-axis), and the envelope passing tangential at the circle's circumferences will end up with the internal friction angle and the cohesion. The shear strength is obtained using these two parameters by the Mohr-Coulomb equation (Equation 3.7) (Bell, 2007).

Where σ'' is substituted instead of σ in Equation 3.7, and is the major principal stress. σ'' is the sum of the applied axial stress and the confining stress.

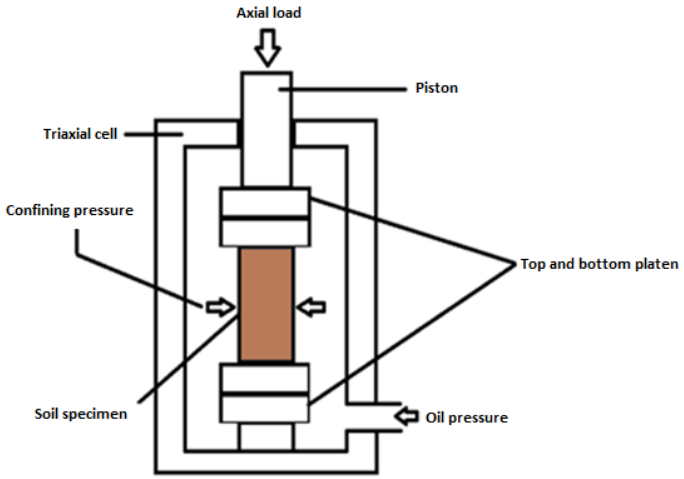

Fig. 3.14. Tri-axial test (front view).

3.6 Soil colour

Determining the colour of the soil might be helpful in specifying the soil organic carbon with saving time and cost (Wills et al., 2007), (Angelopoulou et al., 2020), (Gholizadeh et al., 2020). The description of the soil colour has been used by soil scientists infield to classify the soil, also used in mapping (Soil survey staff, 1999), (Viscarra Rossel et al., 2006). Soils might reflect a wide range of colours, the grey, black, white, reds, browns, yellows, and greens (Brady and Weil, 2008). The resulting colour of a soil is due to different processes and conditions influencing the soil, the minerals present in the soil, and the content of the organic matter (USDA, 2020). The organic matter is what mostly influences the soil colour (Aitkenhead et al., 2013), that is why scientists worked on relating the darkness of the soil colour to its organic matter content (Wills et al., 2007), (Brady and Weil, 2008), (Torrent and Barrón, 1993), (Konen et al., 2003).

The decomposed organic matter in darker soils is higher relative to other soils, and this decomposed matter is known by humus, where this substance is carbon containing polymers and absorbs the most visible wavelength coming from light, thus giving the soils (that are rich in organic matter) the dark brown colour (close to black colour) (Vodyanitskii and Savichev, 2017). The pedologists relied on the Munsell soil colour charts (1975) for more than 60 years in describing the normal range of soil colours, which is a qualitative colour estimation method (Rabenhorst et al., 2015). This method relies on determining the colour visually, and then comparing it to standard chips that are arranged systematically based on their Munsell's notation. In this system, the colour is identified based on three parameters, the Hue which describes the dominant wavelength or basic colour, the Value and is a parameter representing the overall brightness (lightness), and the Chroma parameter reflecting the saturation or intensity of the Hue, as an example of that, the brown soil may be noted as Hue Value/Chroma (10YR 5/2). The newest edition of the Munsell Soil Colour Chart (MSCC) contains 443 colour chips divided on 13 pages. This system was designed by Albert H. Munsell aiming to compare the soils anywhere in the world based on their seen colour (vision), having the illumination provided. Identifying the soil organic carbon requires many observations related to time and space (region), but this method (Munsell) can be used in large-scale citizen science-based approach, so that going over the limitation of conventional soil organic carbon analysis methods (Smith et al., 2019), (Angelopoulou et al., 2020), (Dickinson et al., 2010), (Liu et al., 2017). Not specifying the colour consistently and precisely is forming a challenge infront of

this scheme (Munsell) (Torrent and Barrón, 1993), (Sanchez Maranon et al., 1995, 2005, 2011), (Marques Mateu et al., 2018).

There are different factors that influence the colour of the soil, such as environmental conditions (as the moisture and illumination) (Mouazen et al., 2007), the characteristics of the sample (as roughness and size), difficult statistical analysis (as limited colour chips and cylindrical colour coordinates) (Kirillova et al., 2014), (Stiglitz et al., 2016), and the observer's vision (as colour blindness, subjectivity, poor colour memory, eye fatigue) (Torrent and Barrón, 1993), (Sanchez Maranon et al., 2011), (Mouazen et al., 2007), (Kirillova et al., 2014), (Stiglitz et al., 2016), (Gomez Robledo et al., 2013), (Post et al., 1993). The challenges faced when using this chart means that the scientists have used the colour data descriptively (Soil survey staff, 1999), (Gholizadeh et al., 2020), (IUSS, 2006). Replacing this method by fast instrumental technologies and methods to rely on in specifying the soil colour such as UV VIS spectrophotometry, is leading to precise and quantitative approach in specifying the colour (quality control) (Viscarra Rossel et al., 2006), (Aitkenhead et al., 2013), (Bloch et al., 2021). The spectrophotometer removed some of Munsell's method limitations by using standard values and removing the human judgement (as the observer viewing angle and the lighting conditions) (Wills et al., 2007), (Liles et al., 2013), (Viscarra Rossel et al., 2006), (Rabenhorst et al., 2015), (Doi et al., 2010), (Warr et al., 2015), (Turk and Rebecca, 2020). The usage of the quantitative colour measurement (spectrophotometer) has increased worldwide, and the colour data obtained is being used in different applications (Viscarra Rossel et al., 2006), (Bloch et al., 2021). Even though this measurement is quantitative and its results are precise, but it hasn't been adopted by scientists for different reasons, the cost, speed, lack of portability, adapted and familiar with Munsell method, and its small-scale heterogeneity (Stiglitz et al., 2016).

The soil colour is a useful field property, and beside that, it is an apparent property (Baumgardner et al., 1985). The colour is a chip used for identifying different soil kinds (Soil survey staff, 1999). Researchers related the organic matter content of the soil to its colour (Al-Abbas et al., 1972). Since the colour is a property that also provides information about other soil properties, it has been used as an indicator for assessing the soil drainage and its classification (Franzmeier and Yahner, 1983), (Mokma, 1997). For identifying field conditions, different methods for measuring the soil colour and its reflectance have been widely adopted (Post et al., 1993). In agriculture, the soil spectral data is used for deriving its moisture content (Muller and Decamps, 2001).

The spectrophotometric technology is a quantitative method used for measuring the colour of an object. In optics world there is nothing known by colour, but instead, it is the wavelength of the reflected light wave that our brain decodes to a colour, and thus seeing the object of a specific colour based on the reflected wavelength (Sitkei, 2020).

Technology is using light in variety of measuring techniques, but these techniques rely on the light-matter interaction (such as reflection, refraction, absorbance, etc) (Winters, 1930). The spectrophotometric soil colour results vary with the soil physical conditions, which are influenced by the moisture content (Carter, 1931).

3.6.1 Spectrophotometers

Light is a part of huge electromagnetic spectrum that can be seen by eyes (eyes can detect). The electromagnetic waves range from very high energy, short wavelength gamma rays, to X-

rays, vacuum ultraviolet, ultraviolet, visible, near infrared, infrared, microwaves and radio waves. Each of these waves band is detected by special technology that also measures the spectrum. The light travels in vacuum with a constant speed c_0 of a value 3×10^8 m/s, but when light travels through a substance its speed decreases, thus the refractive index of the substance which is the ratio of the speed of light in vacuum to the speed of light in the substance. If the speed of the light is slower in the substance (compared to other substances), then categorizing the substance as more optically dense and of a higher refractive index compared to another substance (that speed is higher in it). Based on that, glass is more optically dense than air, and air is more optically dense than vacuum. Technology is using light in variety of measuring techniques, but these techniques rely on the light-matter interaction, thus deducing the properties of the substance (matter) based on the interaction. The interaction between the light and the matter might be reflection, refraction, elastic scattering, absorbance, inelastic scattering, emission (Morris, 2015).

-*Reflection :* The boundary between a matter and another is known by interface, such as in a fish tank the boundary between the glass and the water is the interface. When the light energy strikes the interface it might pass to the other material or might be reflected back. The bounce of the energy back is known by reflection, and is reflected at an angle that is similar to the striking angle but opposite to it (relative to the surface perpendicular line). This kind of reflection is called specular, as if reflecting from a mirror. The refractive index of the two substances and the striking light ray angle specify the amount of energy reflected. The energy reflection is minimum when the ray strikes normally the surface, and is proportional to the angle (increases with angle increase) till reaching 100% reflection at critical angle (Morris, 2015).

-*Refraction :* The passage of the light ray to a new medium changes its speed. If the light is striking the medium (at the interface) perpendicularly, it will continue its path normally. If striking the interface at an angle not perpendicular, then the ray will change its direction (refract) when propagating in the other medium. If the other medium is optically dense, then the ray tilts its path towards the normal, and if the material is less optically dense, it tilts the ray away from the normal (Morris, 2015).

The refraction and reflection phenomenons occur when light strikes flat and well-defined interfaces (Morris, 2015).

-*Elastic scattering :* Light travels in vacuum straight at constant speed, and that lasts forever. The passage of light across a substance in a straight path means that the substance would be perfectly transparent. Upon the ray striking a particle (for example light ray striking water droplet in the air), the ray might be elastically scattered, and it is the change in the light path, but the wavelength remains the same (Morris, 2015).

-*Absorbance :* The capture of light energy by molecules when getting in contact with photons is known by absorbance, and this energy may be re-emitted as light or converted to heat. The wavelength of the re-emitted light is what specifies the amount of the absorbed energy, and based on the wavelength the concentration of the absorbing molecules is measured in a sample. This technique is known by spectrophotometry. Light is absorbed when the wavelength (or frequency) of the light is similar to the natural frequency of molecular vibrations, or it might be due to the differences of electrons on the energy levels when emitting energies (Morris, 2015).

-*Inelastic scattering :* This scattering changes both the direction and the wavelength of the light, and is used in Raman spectroscopy to identify the molecular bonding (Morris, 2015).

-*Emission :* Light might be emitted by a substance upon having the molecules of the substance excited, and this light is known by luminesce. The energy provided as mechanical, chemical, nuclear, electrical, or optical energy simulates the substance, thus the input energy is converted to photons that are emitted. If the wavelength of the exciting light is of high energy photon (short wavelength) and the excited molecule emits lower energy photon (longer wavelength), then the luminescence is fluorescence and used to quantify the substance's concentration (Morris, 2015).

Spectrophotometers (instruments) have been in laboratories, educational, and industrial fields for more than 70 years. Many designs and models are available, but all of them operate relying on few basic principles. Some spectrophotometers are presented as black box (closed and hidden components from sight, its operation isn't clear), and its operation is limited to one measurement kind as the Spectronic 200 used to measure the absorbance of liquids at few wavelengths in the visible spectra portion (360 to 1000 nm) (Morris, 2015).

Other spectrophotometer kinds are composed of modular parts. Some manufacturers (Ocean optics) provide products that use optical fibers to connect the various components to functional systems, thus having the components seen and controlled (specified and selected) by the user (Morris, 2015).

The traditional kind used to depend on white light source that is spreaded into a spectra, and one wavelength at time is selected which is entering to the sample and is detected by the detector. The advantage of this design is that the sample is receiving less light energy and the disadvantage is that just one wavelength is analyzed at a time (Morris, 2015).

The usage of microelectronic detector arrays has settled new spectrophotometer architecture. Broad band light (white) is directed through a sample, and then spreading into spectrum ending up at array of simultaneous detectors. As an example, the Flame-S (optics ocean) spectrum strikes a line of 2058 detectors. Each detector detects one light wavelength and is of 14 μm wide. With these detectors (arrays) the entire spectra is collected in milliseconds, and the wavelengths are captured in the time interval (Morris, 2015).

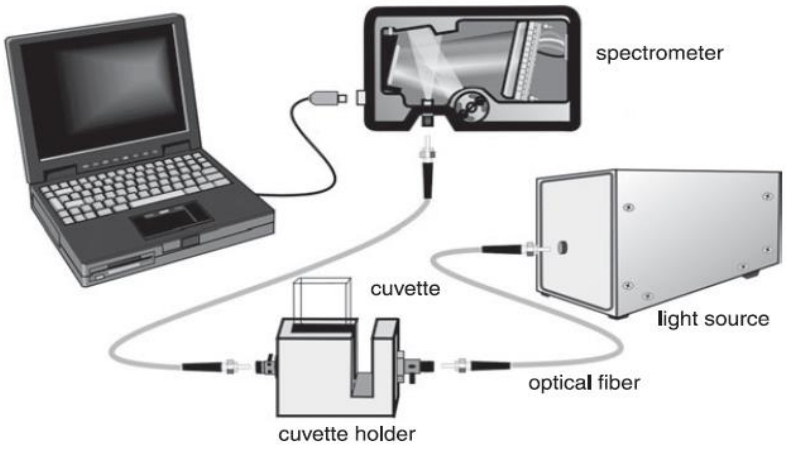

Fig. 3.15. Typical post-dispersive spectrometer with its components (Morris, 2015).

The absorbance spectrophotometer components are shown in Figure 3.15. The optical fiber carries the light to the cuvette, and on most modern spectrophotometer systems the user's interface is provided through a computer (Morris, 2015).

3.7 Soil bearing capacity and its shearing strength

The land locomotion laboratory was founded by Bekker in 1954 (Liston, 1965). Bekker's researchers realized that the soil under a rigid wheel is subjected to two loads, the compressive load resulting from the weight of the vehicle and the shearing load due to the moment resulting from the rotation of the wheel (Laib, 1995).

a - Soil bearing capacity

Upon the passage of a vehicle on the soil, the ability of the soil to withstand or fail in the face of the static surface loads (ideal study) resulting from the vehicle is judged by the behaviour of the terrain during the passage of the tractive element. The plate sinkage test facilitated studying the soil behaviour under a vehicle normal load, and in predicting trafficability. The size and the shape of the plate influence the obtained results, also the magnitude, duration, and rate of the applied stress affect the results. Pressure-sinkage relationships may result in fluctuations with sinkage, meaning that different modes of failure are interacting (Soane et al., 1980 /1981). Deriving basic sinkage parameters from the plate sinkage test for describing the soil behaviour (Bekker, 1969) did not receive universal acceptance due to assuming that the applied pressure on the plate contact area is uniform, and also due to not taking into consideration shearing components in this test (Karafiath and Nowatzki, 1978).

When using the plate sinkage test in emulating the tractor tire on the terrain, the case becomes difficult, since the contact area of the tractor tyre is of huger size (also higher pressure applied). Even though there were different attempts for relating the plate sinkage test to the behaviour of the wheel (tractor case), it is not pratical to use plates that are of sizes similar to such tyre/s contact area having same applied pressure (Dwyer et al., 1974), (Soane et al., 1980/1981). In the plate sinkage test, two or more diameters are used and are of sizes 200 mm and 250 mm, and by the plate sinkage test, the sinkage modulus and exponent (k, n) will be evaluated (Soane et al., 1980/1981). Wills (1966) based on plate sinkage technique, and depending on results obtained from rectangular plates tests of sizes 0.016 to 0.394 m^2 (area, square meter), ended up with an empirical pressure-sinkage equation that he claimed to be the most appropriate when compared to others. Gee-Clough (1976, 1978) modified the sinkage parameter approach of Bekker by considering the wheel width effect, skidding, sinkage depth, and the rolling resistance (rigid wheel). Bekker analysis was used by Perdok (1978) showing that pneumatic tyre that is undriven can be treated similar to a rigid tyre of large diameter. Perdok used full size rigid wheel aiming to apply real loading to the soil surface, and as a result of his work he ended up with the sinkage modulus (k) and exponent (n) values obtained by measuring the rolling resistance under different loads.

The sinkage and the rolling resistance of vehicles on soft soils are predicted using plate pressure test (often used), having the plate pressing the soil in a quasi-static and of small size. In reality when a vehicle moves on soft soil, the load applied by the wheel on the terrain is not a quasi-static load, but in fact it is a dynamic load (load impact depends on rolling speed). Grahn (1991) carried out tests for studying the influence of the penetration velocity on the pressure-sinkage relationship, and modified the analytical formulation and the results of dynamic pressure plate test (Grahn, 1989) used for rigid wheel of dynamic vertical pressure.

Sinkage and rolling resistance based on rolling speed are predicted from Bekker's pressure-sinkage relationship (Bekker, 1956, 1969).

When studying the pressure-sinkage relationship, the vertical component (ż) of the velocity resulting on a peripherial point of the wheel (point contact with ground) must be considered (Grahn, 1991).

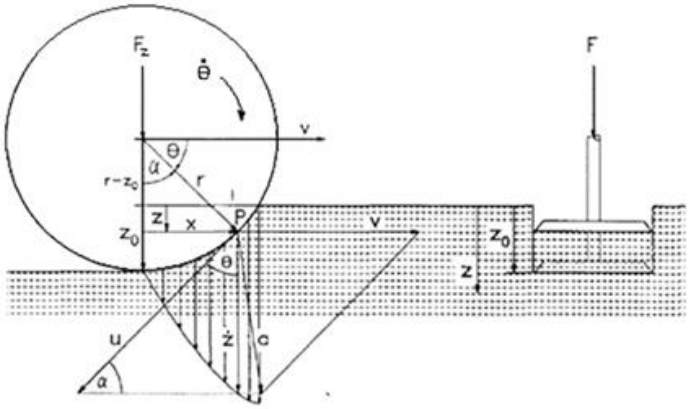

Fig. 3.16. Rolling rigid wheel analogous to penetration plate (Grahn, 1991).

In Figure 3.16 analogy, comparing the penetration of the wheel to that of the plate shows that the penetration velocity ż when entering the soil (z = 0) is at maximum, whereas at maximum sinkage (z_0) it is equal to zero (Grahn, 1991).

The vertical speed of the peripheral point depends on the driving speed v (including slip s), and on the angle of contact with soil (α) (shown in figure 3.16 on the wheel). The contact angle α of a point P on the circumference of the wheel depends on the certain sinkage z (at P level), maximum sinkage z_0, and the radius of the wheel r.

Thus, the sinkage velocity for the wheel (at P) is (Grahn, 1991):

$$\dot{z} = \frac{\mathbf{v}}{\mathbf{1-s}} \cdot \mathbf{sin}\left[\mathbf{arccos}\left(\mathbf{1} - \frac{\mathbf{z_0 - z}}{\mathbf{r}}\right)\right] \tag{3.18}$$

Figure 3.17 shows the curves of the vertical velocity as function of the sinkage ratio of a rigid wheel (without slip) at different driving speeds (Grahn, 1991).

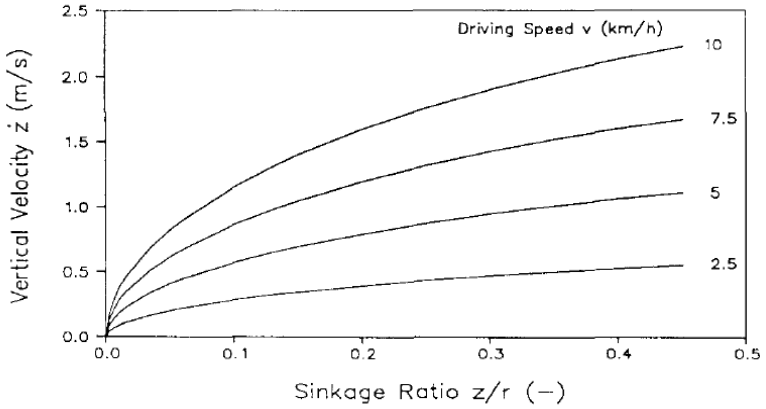

Fig. 3.17. Vertical velocity as function of sinkage ratio at different driving speeds (Grahn, 1991).

Based on Goriatchkin (1937) pressure-sinkage relationship (was later investigated and modified by Bekker using the bevameter method).

$$\mathbf{p = k \cdot z^n} \tag{3.19}$$

Since prepared plate pressure-sinkage tests (check reference if required) at different speeds are showing curves parallel to each other (as in figure 3.18), thus the sinkage component n is constant for all penetration velocities, and the modulus of soil deformation k depends only on the penetration velocity and is expressed by the exponential function.

$$\mathbf{k = k_0 \cdot \dot{z}^m} \tag{3.20}$$

k_0 is the static modulus of the soil deformation and m is the exponent of the penetration velocity.

Substituting k in the pressure-sinkage relationship (Equation 3.19), thus the pressure equation:

$$\mathbf{p = k_0 \cdot \dot{z}^m z^n} \tag{3.21}$$

The above equation 3.21 (a dynamic equation) is not valid for penetration velocities below 1cm/s (the static condition).

Inserting the penetration velocity ż of a rigid wheel in Equation 3.21, ends with the resulting pressure-sinkage as function of the driving speed:

$$\mathbf{p = k_0 \cdot z^n \cdot \left[\frac{v}{1-s} \sin\left[\arccos\left(1 - \frac{z_0 - z}{r}\right)\right]\right]^m} \tag{3.22}$$

The dynamic vertical pressure curves (under a wheel having slip s=0) as function of sinkage ratio at different driving speeds, with Bekker's quasi-static curve of penetration velocity 2 cm/s, are shown in Figure 3.18 (cases compared at a fixed sinkage ratio) (Grahn, 1991).

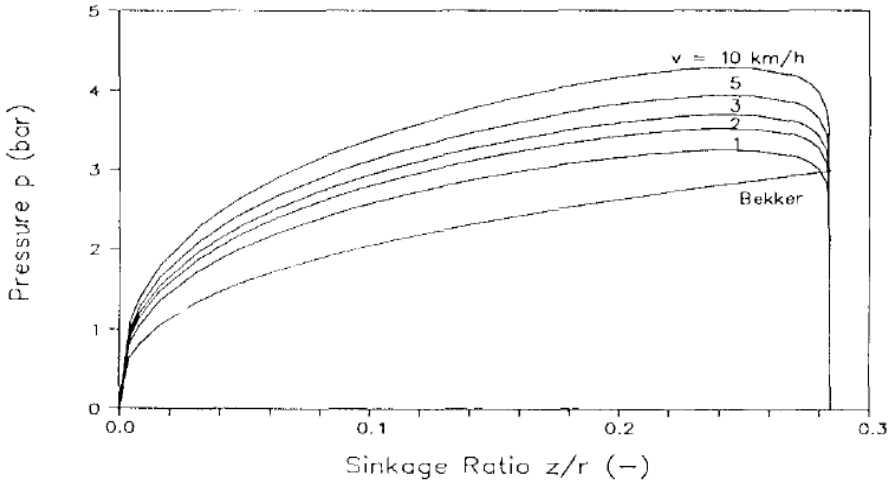

Fig. 3.18. Dynamic vertical pressure with sinkage ratio at different driving speeds of a rigid wheel, with the curves compared to the quasi-static Bekker's curve at a constant sinkage (Grahn, 1991).

It is shown in Figure 3.18 that for a constant sinkage the soil resists higher pressure at higher driving speed, thus at higher driving speed the wheel exerts higher load, and that is also recognized in Figure 3.19 (Grahn, 1991).

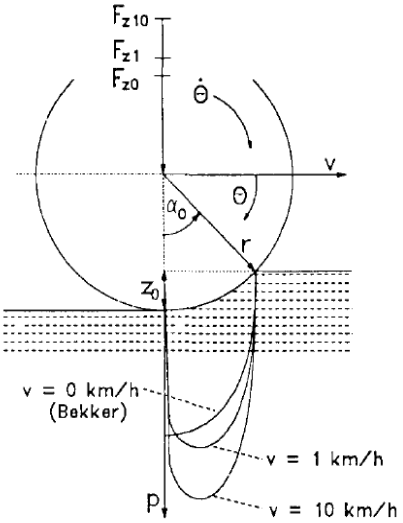

Fig. 3.19. Pressure under a rigid wheel (without slip) at different driving speeds having the sinkage constant, also shows the quasi-static Bekker's pressure (Grahn, 1991).

b - Soil shearing strength

The soil shear strength is obtained either from laboratory tests or field tests, but different results appear from different tests (result based on the test), where these differences are resulting from the different stress conditions in the different tests (Wroth, 1984), and because of interpreting the results differently (Atkinson and Lau, 1990). In vehicle mobility studies, the soil strength has been measured using many methods (Shoop, 1993a). Soil samples that are cored were tested using triaxial compression aiming to study the soil condition for mobility (Chamberlain et al., 1988), (Blaisdell et al, 1987). Shear strength results were obtained using different tests (vane shear and direct shear), and it appeared that each test gives considerably different result (Kogure et al., 1988). The direct shear test emulates most closely the failure mechanism under a tire on soil terrain, thus in 1950 a field instrument was invented and is known by the bevameter (Bekker, 1969). The bevameter was designed to load the soil till failure in a behaviour similar to that resulting from a vehicle, so relying on this method, the measured properties would be reliable to depend on in studying vehicle performance (Shoop, 1993). The shear strength depends on many factors, such as the soil density and its degree of saturation, it should also be taken into consideration the inhomogeneity and anisotropy of the soil (Dudzinski and Damian, 2019).

The failure mode and shear strength of a uniform soil sample depends on the stress distribution. Since the soil is a material that behaves in a complicated way, and the need for understanding how the soil behaves when dealing with mobility study case, it is much simple to study the mobility problem by dublicating the soil loading conditions resulting from a vehicle over the soil, thus simplifying terrain behaviour equations (Shoop, 1993). The bevameter technique solved this problem, even if not perfectly. Some researchers worked on using instruments that emulate similarly the wheel of the vehicle on the terrain, thus duplicating exactly the loading conditions, as the CRREL Instrumented Vehicle (CIV) (more about this test in Shoop, 1993), thus the strength parameters results obtained from the technique mobility test will be

implemented for studying the performace of other vehicles (Shoop, 1993). The cohesion and the internal friction angle are soil properties chosen for characterizing the soil strength, and there are two reasons behind that: first, they are determined using simple and well known tests and analysis techniques taking into consideration that the Mohr failure envelope is linear or partially linear, and the second reason is that these two parameters have physical meaning (physical structure of soil) reflecting the internal friction (depends on the normal stress) of the soil and its material cohesion.

Dudzinski and Damian (2019) published an article about his direct shear machine, the device has been patented and was built in the laboratory of the department of off-road machine and vehicle engineering at Wroclaw University of Science and Technology. Their device is able to measure in a wide range of shearing speed, starting from a low speed 1 mm/s that is used in civil engineering to speed corresponding to shearing speed between the wheel/track and the soil and is equal to 5 m/s (dynamic shearing strength). There are other factors that were taken into consideration in this device and these factors are the scale effect, the wall effect, and the shear kinematics.

When it comes to the scale effect, the size of the instrument used for measuring the strength properties influence the output result (Dudzinski and Damian, 2019). The small size instrument (hand held, as the shear vane) allows for fast and easy measurement, but the results are dispersed, and that makes interpreting the results much difficult (Kolk et al., 1988). The large instruments provide much more precise results, but such instruments require longer preparation and measuring time, also its cost is higher. Large instruments serve in decreasing the scale effect of the measurement, since the size of the measuring instrument influence the measured parameters, and this occurs in both measurements, the shear strength and the load bearing capacity (Dudzinski and Damian, 2019). There are many results obtained by researchers that confirm the influence of the instrument size on the measured properties (Zhou et al., 2009), (Chew et al., 2011), (Hu et al., 2011).

A second factor influencing the measured results is the wall effect when measuring in soil bins. The wall effect changes the measured parameters due to the transfer of some loads from the walls of the bin (action-reaction principle), and this effect was considered by researchers (Song and Malla, 2010), (Agui et al., 2013). When designing a container, stresses at the walls should be considered using Steinbrenner's theory (Das, 1999).

Shear kinematics is also a factor influencing the measured parameters. The anisotropy of the soil leads to different parameters in different loading directions. Selecting the direction of loading relative to the direction of the consolidation, influences the shear strength (Kogure et al., 1988). Many infield direct shear tests lead to what is known by the bulldozing effect (as shear grouser) (Bekker, 1956), and it is the push of soil layer at the front of the measuring instrument leading to pushing forces at the lugs. So, when choosing a measuring instrument it is important to choose the instrument with no bulldozing effect and generating only shearing action.

Dudzinski and Damian (2019) in their device they have met the requirements of a precise measuring instrument allowing for easy measurements using different shearing speeds, ranging from mm/min to m/s, also of a shearing surface of at least 300 cm^2 to avoid the scale-effect, and of linear shear kinematics generating only shearing motion to avoid bulldozing.

This device allows for both laboratory and in-situ tests, shown in Figure 3.20.

Incase of laboratory test, relying on the Steinbrenner's theory, the soil bin is of dimensions 45×45×70 cm (height×length×width), thus reducing the stresses at the walls to 15% of the normal load generated by the device.

Fig. 3.20. The new device used for measuring quasi-static and dynamic shearing strength of the soil (Dudzinski and Damian, 2019).

3.7.1 Normal stress distribution at the wheel-soil interface

Understanding the stresses resulting from the vertical and traction loads at the contact zone between the tyre and the soil, could improve our knowledge about soil behaviour upon having a dynamic load applied, thus facilitates tackling soil dynamics problems (Wanjii et al., 1997).

A model is used to evaluate the normal stress distribution and is the three-element Maxwell model. The three-element Maxwell model is used in describing the relation between the stress and the deformation of soil, since it represents elastic after-effect and stress relaxation behaviour. Vertical stress and displacement (sinkage) are used in defining this model (Wanjii et al., 1997).

Figure 3.21 shows the model implementation on a rigid wheel travelling on soil.

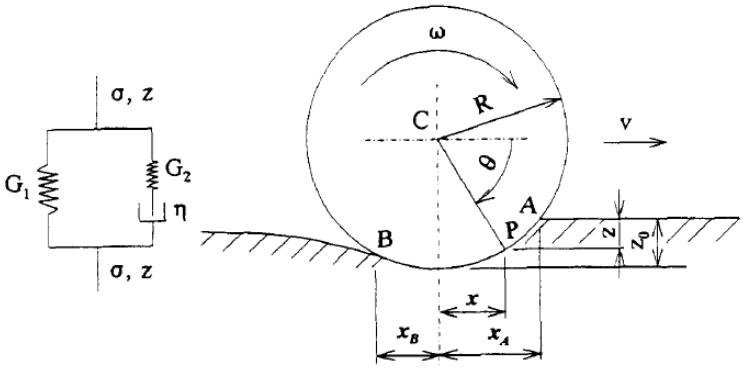

Fig. 3.21. Three element Maxwell model implemented on rigid wheel travelling on soil (Wanjii et al., 1997).

G_1(MPa/m) and G_2(MPa/m) are the elastic moduli and ɳ (MPa.s/m) is the coefficient of viscosity. Having σ and z to be the normal stress and vertical deformation (sinkage), the following equations represent the change in the stress and sinkage as function of time:

$$\frac{d\sigma}{dt} + \frac{G_2}{\eta} \cdot \sigma = (G_1 + G_2) \cdot \frac{dz}{dt} + \frac{G_1 \cdot G_2}{\eta} \cdot z \tag{3.23}$$

Having $T_r = \frac{\eta}{G_2}$ the relaxation time,

$$\frac{d\sigma}{dt} + \frac{\sigma}{T_r} = (G_1 + G_2) \cdot \frac{dz}{dt} + \frac{G_1}{T_r} \cdot z \tag{3.24}$$

With deformation at constant velocity at $t \geq 0$, $z = v_Z \cdot t$; $\frac{dz}{dt} = v_Z$ (constant)

And by integrating equation $\frac{d\sigma}{dt}$ from t=0 to time t

$$\sigma = e^{-\frac{t}{T_r}} \cdot \int_0^t \left((G_1 + G_2) \cdot v_Z + \frac{G_1}{T_r} \cdot v_Z \cdot t \right) dt$$

$$= G_1 \cdot v_Z \cdot t + G_2 \cdot v_Z \cdot T_r \left(1 - e^{-\frac{t}{T_r}}\right) \tag{3.25}$$

With $z = v_Z \cdot t$

$$\sigma = G_1 \cdot z + G_2 \cdot v_Z \cdot T_r \left(1 - e^{-\frac{z}{v_Z \cdot T_r}}\right) \tag{3.26}$$

Obtaining the parameters is achieved with plate penetration test at constant penetration speed. The constant speed value is fulfilled using a plate penetration test, and from the test G_1, G_2, and T_r are found, and are influenced by plate or wheel width (Hiroma and Ota, 1990).

If removing the penetration plate from the deformed soil at a speed higher than the speed of the soil rebound, the soil will be able to return to its previous level form.

Considering the soil is always in contact with the plate, will help in analyzing the normal stress under the plate during loading and unloading (visco-elastic behaviour of soil).

In analyzing the normal and tangential stresses under the wheel-soil contact, the following assumptions based on Bekker's method should be taken into account:

a- consider the soil surface deforms vertically when analyzing the vertical stress.
b- the normal stress is purely radial and equal to the normal pressure beneath a horizontal plate at the same depth of same deformation history (approximately same initial stress condition in soil).
c- the normal stress doesn't influence the tangential deformation and the stress resulting from slipping.

In the above Figure (3.21), the rigid wheel is rolling on soft soil at a constant speed and of sinkage z_0. Every point on the circumference starts the contact with the soil at A and exits at point B (Wanjii et al., 1997).

Based on the assumption that soil deforms vertically only, then the point P on the wheel surface can be expressed as: (Wanjii et al., 1997)

$$\mathbf{x^2 = (2R - (z_0 - z)\,)\cdot(z_0 - z)} \tag{3.27}$$

$(z_0 - z)^2$ is smaller compared to R so can be neglected.

$$\mathbf{x^2 = 2R \cdot (z_0 - z)} \tag{3.28}$$

Point P from point A takes time t,

$$\mathbf{t = \frac{x_A - x}{v}} \tag{3.29}$$

Thus, $x = x_A - v \cdot t$

At point A, z = 0 and $x = x_A$; substitute in Equation 3.28

$$\mathbf{x^2 = 2R \cdot (z_0 - z)}$$

$$\mathbf{z_0 = \frac{x_A^2}{2R}} \tag{3.30}$$

Substituting the time t and z_0 in the Equation 3.28,

$$\mathbf{z = \frac{v \cdot (2x_A \cdot t - v \cdot t^2)}{2R}} \tag{3.31}$$

The change in z as function of time,

$$\mathbf{\frac{dz}{dt} = \frac{v \cdot (v_A - v \cdot t)}{R}} \tag{3.32}$$

Substituting $\frac{dz}{dt}$ in the main normal stress equation:

$$\mathbf{\frac{d\sigma}{dt} + \frac{\sigma}{T_r} = (G_1 + G_2) \cdot \frac{v}{R}(x_A - v \cdot t) + G_1 \cdot \frac{v}{RT_r} \cdot (x_A - \frac{1}{2} v \cdot t) \cdot t} \tag{3.33}$$

When $t \leq 0$, $\sigma = 0$, thus solution of (3.33) is,

$$\mathbf{\sigma = \frac{G_1}{2R} \cdot (x_A^2 - x^2) + \frac{G_2 \cdot v \cdot T_r}{R}\left((x_A + v \cdot T_r\,)\left(1 - e^{-\frac{x_A - x}{v \cdot T_r}}\right) - x_A + x\right)} \tag{3.34}$$

3.7.2 Tangential (shear) stress distribution at the wheel-soil interface

The traction equation of the tractive element (tyre/track) is determined using the shear strength of the terrain and the contact area. Based on shear-displacement test results, and relying on the multiple regression analysis that gives the best model for τ_{max} as function of σ, the model used for calculating the maximum shear strength is:

$$\mathbf{\tau = c + \sigma \cdot \tan \phi} \tag{3.35}$$

The shear stress is related to the shear displacement, having the displacement value ranging from zero at the wheel-soil initial contact point, to the maximum value at the rear of the contact area (point entering with less displacement and exiting with maximum displacement). From

the analytical diagram of a rigid wheel moving on soft terrain, the shear displacement velocity v_j is obtained using the following equation (Wanjii et al., 1997).

$$\mathbf{v_j = R \cdot \omega - v \cdot \cos\left(\frac{\pi}{2} - \theta\right) = R \cdot \omega - R \cdot \omega \cdot (1 - s)\sin\theta} \\ \mathbf{= R \cdot \omega \cdot [1 - (1 - s)\sin\theta]} \tag{3.36}$$

At the element level (element shear displacement), the diplacement is,

$$\mathbf{d_j = v_j \cdot dt} \tag{3.37}$$

Integrating dj from t=0 to t=t or from angle θ_A to θ,

$$\mathbf{j = \int_0^t v_j\, dt = \int_{\theta_A}^{\theta} R \cdot [1 - (1 - s)\sin\theta]\, d\theta}$$

$$\mathbf{j = R \cdot [(\theta - \theta_A) + (1 - s)(\cos\theta - \cos\theta_A)]} \tag{3.38}$$

Since the soil (tested) exhibits smooth shear stress displacement characteristic, then Janosi and Hanamoto proposed equation (Bekker, 1969), (Janosi and Hanamoto, 1961) may be used for expressing the shear stress displacement relationship.

$$\mathbf{\tau' = \tau \cdot \left(1 - e^{-\frac{j}{k}}\right) = (c + \sigma \cdot \tan\phi) \cdot \left(1 - e^{-\frac{j}{k}}\right)} \tag{3.39}$$

The predicted values using the above equation 3.39 comply and fit with the curves resulting from the shear-displacement experimental test (check reference for data). Thus, the new shear stress equation expresses the stress as function of wheel parameters, soil parameters, wheel slip, and normal stress. The cohesion c, internal friction angle ϕ, and the deformation modulus k result from the shear displacement test.

Substituting j in τ will lead to the following equation:

$$\mathbf{\tau' = (c + \sigma \cdot \tan\phi) \cdot \left(1 - e^{-\frac{R}{k}[\theta - \theta_A + (1 - s)\cdot(\cos\theta - \cos\theta_A)]}\right)} \tag{3.40}$$

The gross traction,

$$\mathbf{F_g = \frac{wheel\ input\ torque}{radius}} \tag{3.41}$$

The gross traction F_{gh} horizantal component of an arbitrary point p (at the interface) having shear stress τ is:

$$\mathbf{F_{gh} = b \cdot R \int_{\theta_A}^{\theta_B} \tau' \cdot \sin\theta\, d\theta} \tag{3.42}$$

$$\mathbf{F_{gh} = b \cdot R \int_{\theta_A}^{\theta_B} (c + \sigma \cdot \tan\phi) \cdot \left(1 - e^{-\frac{R}{k}[\theta - \theta_A + (1 - s)\cdot(\cos\theta - \cos\theta_A)]}\right) \sin\theta d\theta} \tag{3.43}$$

The net traction force F_n (net wheel thrust) acts parallel to the terrain surface and with the travel direction.

Taking into consideration that the shear force has vertical component supporting the vertical load, and by resolving vertically and horizantally, leads to the following equilibrium equations.

$$\mathbf{W = b \cdot R \int_{\theta_A}^{\theta_B} (\sigma \cdot \sin\theta + \tau' \cdot \cos\theta) d\theta} \tag{3.44}$$

$$\mathbf{F_n = b \cdot R \int_{\theta_A}^{\theta_B} (\tau' \cdot \sin\theta - \sigma \cdot \cos\theta) d\theta} \tag{3.45}$$

Substitute with,

$$\mathbf{\sigma = \frac{G_1}{2R} \cdot (x_A^2 - x^2) + \frac{G_2 \cdot v \cdot T_r}{R} \left((x_A + v \cdot T_r) \left(1 - e^{-\frac{x_A - x}{v \cdot T_r}}\right) - x_A + x \right)}$$

And,

$$\mathbf{\tau' = (c + \sigma \cdot \tan\phi) \cdot \left(1 - e^{-\frac{R}{k}[\theta - \theta_A + (1-s)\cdot(\cos\theta - \cos\theta_A)]}\right)}$$

The rolling resistance is obtained by the equation:

$$\mathbf{R_c = F_{gh} - F_n} \tag{3.46}$$

$$\mathbf{R_c = b \cdot R \int_{\theta_A}^{\theta_B} \sigma \cdot \cos\theta \, d\theta} \tag{3.47}$$

In order to solve the above equations (from-to), θ_A, θ_B, x_A, and x_B are needed. To solve for x_A and x_B, boundary conditions are considered at B, and are $x=x_B$ and $\sigma=0$. Substituting these two boundary conditions in σ equation with the term $\delta = \frac{v \cdot T_r}{x_A}$, we end up with the following expression in terms of x_A and x_B (the unkown values).

$$\mathbf{\exp\left(-\frac{x_A - x_B}{\delta x_A}\right) = 1 + \left(\frac{x_A - x_B}{x_A}\right) \cdot \left(\frac{\frac{G_1}{G_2}\left(\frac{x_A + x_B}{x_A}\right) - 2\delta}{2\delta(1+\delta)}\right)} \tag{3.48}$$

To solve for x_A and x_B, another equation is required. Assuming the vertical shear stress component is neglected in Equation 3.44, that $\tau' \cdot \cos\theta = 0$, thus:

$$\mathbf{W = b \int_{\theta_B}^{\theta_A} \sigma \cdot R \cdot \sin\theta \, d\theta = b \int_{x_B}^{x_A} \sigma \, dx} \tag{3.49}$$

Inserting σ in W equation :

$$\mathbf{W = b \int_{x_B}^{x_A} [\frac{G_1}{2R}(x_A^2 - x^2) + \frac{G_2 \cdot v \cdot T_r}{R}\left((x_A + vT_r) \left(1 - e^{-\frac{x_A - x}{vT_r}}\right) - x_A + c \right)] dx} \tag{3.50}$$

Integrating (3.50) will give W as function x_A and x_B:

$$W = \frac{b \cdot G_1 \cdot x_A^3}{6R}\left(2 - 3\frac{x_B}{x_A} + \left(\frac{x_B}{x_A}\right)^3\right) + \frac{b \cdot G_2 \cdot v \cdot T_r \cdot x_A^2}{2R} \cdot \left(\frac{G_1}{G_2} + 1\right) \cdot \left(1 - \left(\frac{x_A}{x_B}\right)^2\right) \quad (3.51)$$

The two equations 3.48 and 3.51 are solved using a value W_0 as a vertical load used in the first iteration to get the values x_A and x_B. The obtained x_A and x_B values are substituted in Equation 3.44 to solve for finding W_1 taking into consideration the vertical component of τ (angles can be obtained geometrically from x_A and x_B). Repeat the iteration by having the W value obtained from the equation $W_1 = W_0 \cdot W/W_1$, then the new W_0 is substituted by W, and the process is repeated for calculating x_A and x_B. Iterations are repeated until the x_A and x_B values when substituted in equations 3.44 and 3.51 give the same W value, or until $|W_1 - W_0| <$ error. Finding x_A from the iteration process and substituting it in Equation 3.30 will end up with the sinkage z_0. The above equations are solved by numerical calculations (Kantaris, 1987), through substituting the load W, angular velocity ω, and the slippage s for determining the sinkage z_0, x_A, and x_B values. The normal stress distribution at the wheel-soil interface is calculated using v (travelling speed), x_A, and x_B in Equation 3.34, with $v = R\omega(1 - s)$, and the shear stress distribution is obtained by substituting the calculated normal stress in Equation 3.40. Figure 3.22 shows the flow chart of the calculation process (Wanjii et al., 1997).

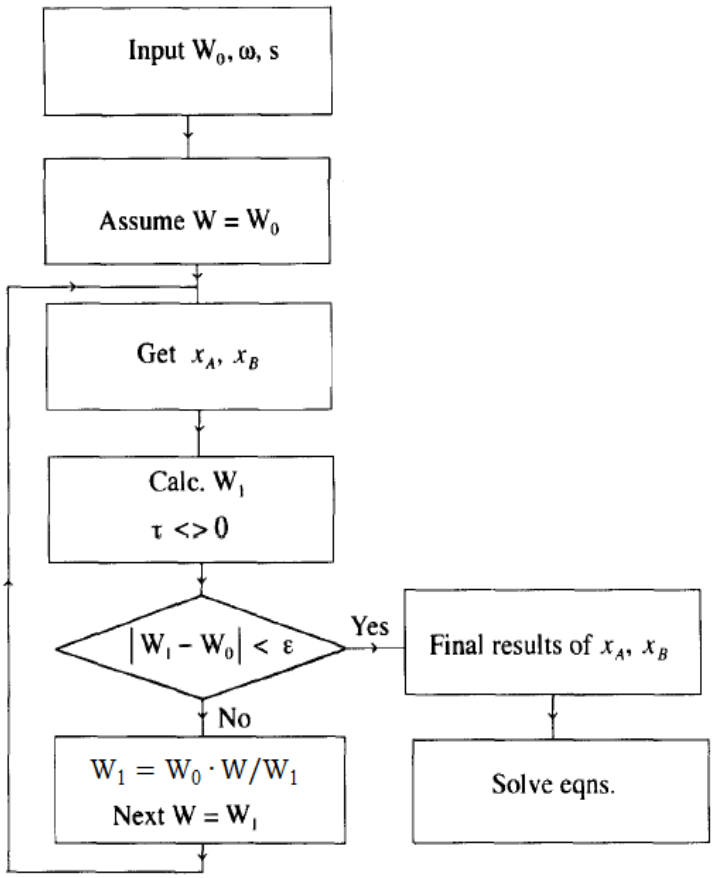

Fig. 3.22. Flow chart for finding the distribution of stresses and the traction at the wheel-soil interface (Wanjii et al., 1997).

3.8 Numerical methods for studying terrain response

Terrain responses have been analysed using empirical and (Bekker, 1956) analytical relationships (Sela and Ehrlich, 1972), (Baladi and Meier, 1987), also using numerical approaches such as finite element analysis (Yong and Fattah, 1981). The experimental or empirical analysis occurs through analyzing the plate or the tractive element displacement and/or velocity relative to the force that soil applies to resist the exerted load, where the analysis is based on experimental results.

Data resulting from experimental tests is useful infield, but its application is limited to the data base obtained from the experiments. Analytical methods are built based on using the experimental or analytical obtained stress, strain, velocity, and displacement at the contact surface (Sela and Ehrlich, 1972). When dealing with numerical approach, lagrangrian finite element codes have been used for describing the soil behaviour through 3-dimensional plastic or viscoplastic models (Hallquist, 1981, 1983). Using Lagrangian in numerical approaches, and due to large strains and having new failure surfaces near the contact zones, the finite elements have become inside out (not in the boundary), leading to the stop of the computation. Since the frequent manual remeshing and creating new surface/s are very costly operations, using Eulerian finite element codes may be a solution for solving the vehicle-soil interaction cases (Hallquist, 1983). The analytical models for soil-tool interaction might be of limited use since not all the variables involved are available, so Finite Element Method/Analysis (FEM/FEA) has been used for analyzing the soil-tool interaction (Upadhyaya et al., 2002), (Mootaz et al., 2004), (Hemmat et al., 2012), (Bentaher et al., 2013). Discrete Element Method (DEM) is among the newest numerical methods for modeling and simulating soil-tool interaction (Mak et al., 2012). Finite and discrete element methods are useful for simulating soil resulting stresses and its flow when displaced. Discrete element method has gained popularity in studies of rigid wheels especially on granular particulate soils, such as Mars rovers having the wheels equipped with grousers. Discrete element method requires a consistent method for specifying the parameters' quantities of the model, so representing realistic infield terrain properties (Taghavifar and Mardani, 2017). The attempt for adopting numerical based computational methods, such as the finite element method, did not succeed since certain deterministic characteristics to be attributed to the finite element parameters are not available, and since the assumption that soil is always behaving as a continuum medium is not real, failing to model discontinued soil deformations (Taghavifar and Mardani, 2017). By the help of the improved computer technology and the commercial computer codes, the FEM and DEM have been used to analyse vehicle-terrain interaction (Wong, 2010). Liu and Wong (1996) and Seta et al. (2003) have shown that tyre performance studies based on these methods ended with results that comply with experimental data on certain terrains. Both methods are still in the nascent stage when relied on in studying vehicle-terrain interaction, thus before relying on them as useful tool in designing and evaluating off-road vehicles, there are some computational challenging issues that should be treated (Wong, 2010). Kim et al. (2024) studied the influence of the wheel design parameters and the slip ratio on the terrain response using DEM simulations. Lan et al. (2024) studied the wheel-terrain interaction using discrete element method, where a method was proposed, and it has shown efficiency in dealing with granular medium fields (with boundaries).

Regardless of mentioning in the literature a section that deals with studying the vehicle mobility relying on numerical methods, the research deals purely with empirical work for finding the colour (apparent physical property) and the strength (shear strength in my study) of the soil aiming to reach the correlation between them, so no numerical methods (simulations)

were used to solve system-soil interaction study cases, just laboratory physical experiments were carried out. All measurements were carried out at approximately the same surrounding conditions (measuring environment), such as same humidity and same room temperature (around 20 °Celsius).

3.9 Conclusion of the literature review

Measuring the terrain physical and mechanical properties is a major step for studying the behaviour of the terrain. The load bearing capacity and the shear strength of the soil are influenced by the moisture content present in the soil. Even though there are different techniques (standard and prototypes) used for measuring the soil shear strength, each technique (machine or instrument) ends up with different shear strength result. As mentioned in the literature review that the direct shear test is a test that closely emulates the shearing mechanism beneath the wheel or track on the soil. The shear vane helps in finding the shear strength of the soil in field (shear strength result approximates the cohesion). These two geotechnical measuring methods are used by geotechnical and civil engineers.

When studying the performance of a vehicle on a terrain, the most important step is to understand how the terrain responds to the normal, tangential, and lateral excitations resulting from the wheel/track on the terrain. The response of a terrain (to excitation/s) is studied through knowing its physical properties such as, the density and the moisture content, in addition to its mechanical properties as the shear strength. Relating soil physical properties and its shear strength to the tractive load (the traction) resulting from the rotation of the tractive element (wheel/track), will serve in ending up with traction equations that are beneficial in studying the traction performance, also relating the vehicle normal applied load at the interaction zone to the bearing capacity (with physical properties) of the terrain, will help in ending up with equations leading to predicting the expected sinkage of the wheel/track into the terain. Upon moving on an unprepared terrain, the vehile is faced by two major locomotion challenges, and are the sinkage and slippage (the increase in slippage might increase the sinkage). As a main step before studying the performance of a vehicle over unprepared terrain is to find the required physical (such as density and moisture content) and mechanical properties of the terrain, thus dealing with the terrain as a separate excited body. Among the machines and instruments used for measuring the soil shear strength there are, the direct shear test, insitu shear vane, and the triaxial test. The direct shear test is a simple test, since it doesn't require big efforts and costs, where the shear load and the displacement records are measured by sensors. The insitu shear vane is an infield instrument that is instersted into the soil (terrain), and then a torque is applied to turn the vane till the failure of the soil (rotational shearing), and the record of the shear strength can be read from the instrument measuring scale. The insitu tests end with the strength of undisturbed soil (as the vane, despite the result difference from a spot to another). When sampling the soil to be tested in the laboratory (direct shear test or triaxial test), the soil will get disturbed, and that might not lead to precise measured results (results with disturbance errors).

The most well known methods used for measuring the shear strength of the soil were mentioned, and among them the direct shear test, the test that will be used in the research. The gravimetric method, mentioned in the literature, will be used for measuring the soil moisture content using the moisture analyzer. Findings related to the role of the soil colour in predicting soil characteristics and properties were mentioned. Many attempts and researches were considered by scientists for finding the soil moisture content from the colour, but there isn't till now a reliable (precise) quantitative method to deal with for estimating the moisture content

from the colour. The research work is restricted to the usage of the visible range spectrophotometer for finding the soil reflectance, thus ending with estimating the moisture content from the colour reflectance.

The most important part in the literature which is tangibly related to the research, is the explanation given on the machines/instruments used in the terramechanics field for finding the soil shear strength, and among them the direct shear test. The conventional method for finding the soil colour is also presented (Munsell's charts), in addition to giving an explanation about the spectrophotometric technology. The research is a new topic, and based on the scientific database, there isn't any researcher that has dealt with this study before. With using machines/instruments for finding the shear strength and the colour (both empirical work), a correlation between the colour and the shear strength will be reached. Despite which machine/instrument is used for measuring the shear strength, and the same for the colour, upon carrying out the measurements using other machines/instruments, the reached correlation methodology (process) can be followed (implemented).

4. Determining the soil moisture content from its colour reflectance

Most of the agricultural machinery or vehicles are of heavy weights, a reason that might put these machines at the risk of getting immobilized when performing their work on soil terrain. The soil at higher moisture content becomes of different mechanical properties, when compared to having it at low moisture content.

Adjusting the contact zone area of the tractive element on the terrain leads to controlling the applied normal and shearing stresses. Changing the size of the contact area can be achieved by adjusting the track dimensions in case of tracked vehicles, and by adjusting the air pressure in case of pneumatic tires. This will help in reaching a normal stress value that the soil can withstand, also in reaching a tangential stress less than the shear strength of the soil, the case that prevents the soil layer from peeling.

If the shearing stress cannot be decreased by changing the area, it is possible to decrease the torque applied from the wheel or track, thus the colour idea (soil strength related to colour) is also important in adjusting the output driving torque (off-road drive). Incase both ideas cannot be fulfilled, at least the machine can avoid moving on the soil zone.

In another chapter (chapter 5), the mechanical properties (shear strength) of different soils will be linked to the moisture content, and this will be achieved through laboratory work using laboratory measuring methods that comply with the case of study (as vertical deformation or shear-displacement). The moisture content is a factor that influences the colour of the soil. In most of the soils, with the increase in the moisture content, the soil becomes darker.

4.1 Importance of measuring the soil colour reflectance

The main target from this section is reaching the ability of estimating the moisture content from the colour of the soil as a preliminary step for linking the colour to the shear strength values. Reaching convincing results (after validating field measurements) will help in predicting the performance of a vehicle on soil terrain based on the colour of the soil, upon having the moisture content provided to strength equation.

There is a gap in the soil colour measurement work, it is that the measurement is restricted to the usage of a spectrophotometer measuring the colour in the visible band (400-700 nm). Choosing this range, is due to its compliance with the human vision. Initially the spot of high moisture content is recognized by the human vision (or a normal camera on a drone infield), then the moisture content is predicted by the spectrophotometer.

4.2 Spectrophotometer for measuring the soil colour reflectance

The spectrophotometer is a modern technology used for measuring the colour of a body (material). The working principle of the used type is by sending light wave which is in the visible band, spectrum (400-700 nm), and based on the collected reflected wavelengths, the colour of the soil is identified. The colour of the soil is described by the reflected wavelengths, which are digital values (quantitative). It is difficult to specify the colour of the soil based on the vision as in Munsell charts, since it is a qualitative method. Despite the errors that might result from the traditional Munsell charts method, such as human errors (vision), using this method in the case of moist soil becomes complicated. In most of the soils, the increase in the moisture content of the soil makes the soil darker, but, even though not being able to see the change in the colour by the eye's vision, the spectrophotometer is able to decode the colour of the soil to a digital value.

The colour of the soil was measured using a visible range spectrophotometer (Konica Minolta CM-700d), see Figure 4.1. The visible range spectrophotometer measures the colour of the object by sending light wave, and the colour is represented by the reflected wavelengths.

The spectrophotometer was used for measuring the colour reflectance of the soils at different moisture contents. The soil is a particulate matter, so the reflectance will not be exactly the same upon repeating the measurement (on same soil at the same moisture content). For this reason, three data records were taken per each measurement (at a moisture content), and the average of the colour reflectance was taken into account.

The technical usage of the spectrophotometer and the compaction of the soil (either by the instrument lens, or if having the soil already compacted) influence the colour reflectance. The lens of the instrument is applied perpendicularly to the soil surface, so that the lens is touching the soil at equal smooth compaction, having it totally covering the surface. The records are saved in the spectrophotometer and then imported to a computer. The reflectance results (of each soil sample at a moisture content) at the light wavelengths (from 400 to 700 nm with an increment 10 nm) are recorded.

Fig. 4.1. Spectrophotometer CM-700d.

The spectrophotometer CM-700d is used for measuring the colour of an object. It is a handheld instrument that ergonomically provides the user with comfort while usage. A pulsed Xenon lamp (with UV cut filter) is used as a light source. The size of the integrating sphere is of a diameter 40 mm. Diffraction grating is used as spectral separation device. Dual 36-element Silicon photodiode array is used as detector (multichannel) for detecting the wavelengths (of the light source). Wavelength range (spectrum) is 400-700nm, with 10 nm wavelength pitch. The measuring time is approximately 1 second (reflectance record). Despite the different colour spaces that can be used in this spectrophotometer, the XYZ was considered as the colour space in the research. Among its wide range of illuminants, the D50 illuminant was selected in the measurements. 2 or 10 degrees observer angle can be chosen, where the 10 degrees angle was considered. The standard deviation of the spectral reflectance repeatability is 0.1 %. Measurement area selector can be set to either MAV (large aperture size) or SAV (small aperture size), dependent on the size of the measuring area, with changing the target mask (Spectrophotometer user manual, 2008).

4.3 Colour reflectance results of the tested soil textures

The lens of the spectrophotometer is placed directly on the soil sample, covering all the lens, thus the reflected light is captured by the sensor without losses or any external light noise affecting the measurement.

The records are imported from the instrument to the computer. X, Y, and Z are the tristimulus values, are also shown among the results, beside that the view angle is 10 degrees.

Following the manual instructions for using the spectrophotometer, before every measurement the measuring port was checked that there is no dirt or dust covering it. The measurements were carried out in the same surrounding environment, besides that, the spectrophotometer was calibrated regularly using its white calibration head to avoid any deviations in the results (Spectrophotometer user manual, 2008).

For identifying the brightness colour reflectance of the spectrophotometer, colour measurements were carried out on pure white (white body) and pure black colour (black body). For each colour, three records were taken. The records show that the reflectance of the dark colour is low (records' average of black at 700 nm is 5.40), while the reflectance of the bright colour is high (average of white at 700 nm is 73.52). The absorbency of the black colour (or dark colour in general) is high when compared to a bright colour, leading to low reflectance.

What differentiates a soil from another is its texture, the mechanical composition. For the colour reflectance measurements, five different textures were tested. The below figures show the colour reflectance results (collected from the spectrophotometer) of the tested soil textures, each tested at different moisture contents. The reflectance (in percentage) of the sent light wave at each wavelength across the visible range spectrum is shown in the figures below (Figures 4.4 to 4.8, each figure is of a soil texture).

The soil textures used in the research for the colour reflectance measurements are marked on the texture triangle below (Figure 4.2), also among them the textures used in the shear strength measurements chapter (chapter 5). The textures in details, the percentage of each mineral, are in the Table 4.1. Soils were sieved before carrying out the measurements on them (physical status: loose soil).

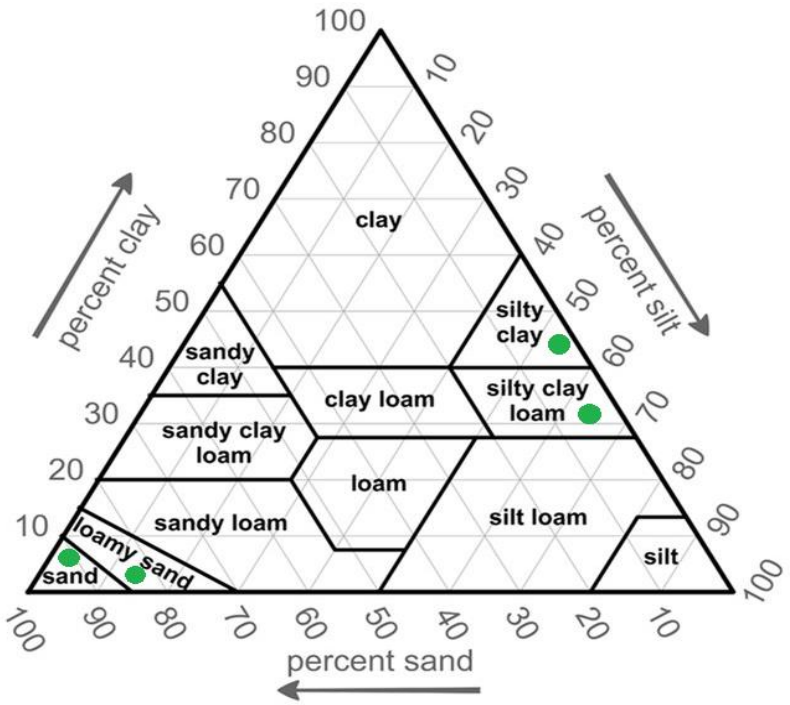

Fig. 4.2. Soil texture triangle, marked on it the textures used in the research.

Table 4.1. Textures used, with their minerals percentages (Institute for Soil Sciences TAKI).

Soil texture	Sand (%)	Silt (%)	Clay (%)
Sand	94.53	4.78	0.69
Silty clay loam	14.07	47.46	38.47
Loam sand	90.50	3.20	6.30
Sand	95.68	2.12	2.21
Silty clay	3.34	52.05	44.61

The reason behind choosing these textures is that they are common soils in Hungary, in addition to the difference in their types (for example, sandy soil the coarse particles soil, and silty clay the fine particles soil). The change in physical and mechanical properties of a soil with moistening is dependent on its texture, a reason behind choosing different soil textures (texture affects type).

The moistening process of each soil was by adding water and then stirring till becoming of uniform colour. The moisture content in the soil was measured using the moisture analyzer (HE 53), a gravimetric measurement, operates based on the drying principle (Figure 4.3). Halogen bulb is installed on the top cover of the analyzer for drying the soil sample. The sample is totally dried, and the remaining mass is recorded by the analyzer. The analyzer calculates the moisture percentage by deducting the remaining mass from the initial mass (wet mass), and the value is divided by the initial mass (wet base moisture calculation).

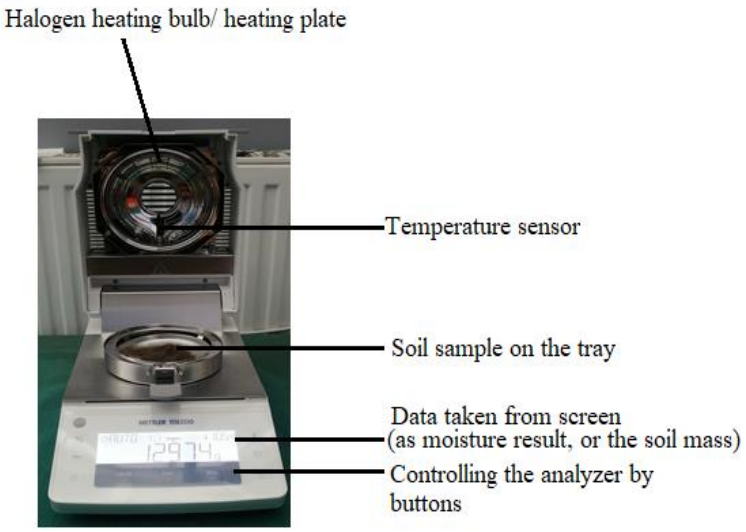

Fig. 4.3. Soil prepared on the moisture analyzer tray before closing the cover (HE 53 moisture analyzer).

HE 53 (230 Volt) Halogen moisture analyzer is initially tared (zeroed), with having the upper cover (lid) closed, as an initial calibration before starting the measurement. A soil sample is placed on the tray, then the cover is closed and the analyzer is operated. The halogen bulb/heating plate heats the soil sample on the tray (maximum capacity 54 grams), till reaching unchanged mass. Both soil masses (before and after heating) are recorded by the scale on which the tray is placed. Using the two masses, the percentage of the moisture content is obtained on wet basis. On the screen, input and output data is displayed, as the set heating temperature (50-160 ˚C as input, but 105 ˚C is used for soil), and as showing the moisture result and the two

masses with the time consumed to dry the sample (output). The HE 53 switches off automatically with the completion of the drying process. Standard and rapid drying programs can be used in this analyzer. The readability of the moisture content is 0.01 %. The repeatability (standard deviation) with 10 grams sample is 0.05 % (HE 53 user manual, 2021).

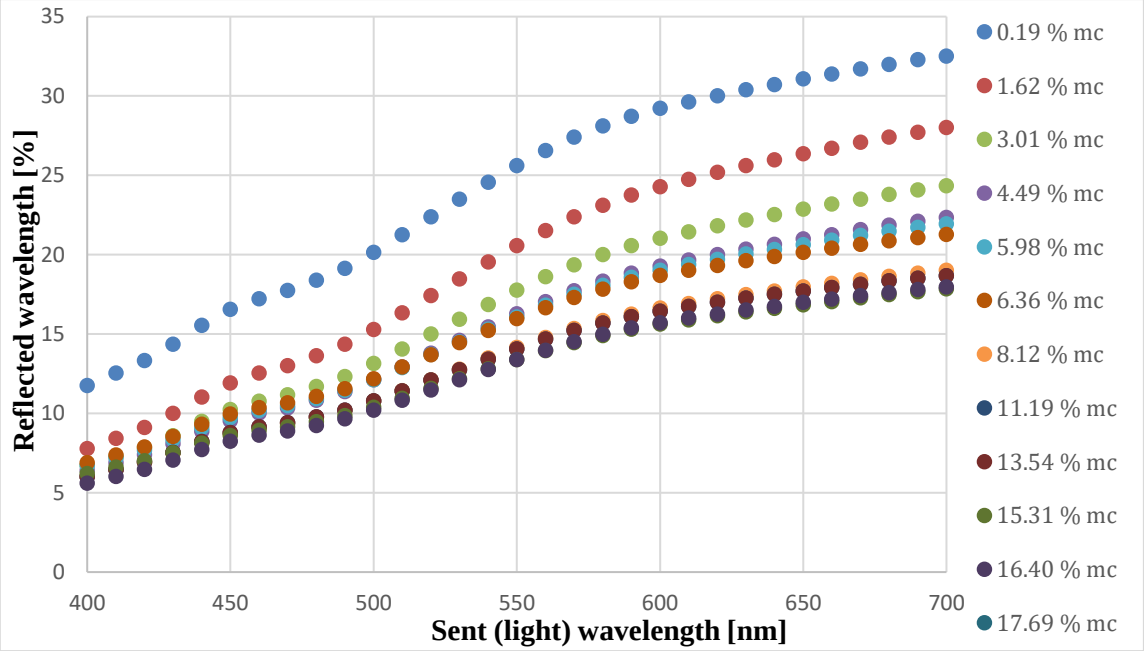

Fig. 4.4. Sand soil (94.53 % sand, 4.78 % silt, 0.69 % clay) spectral reflectance at different moisture contents.

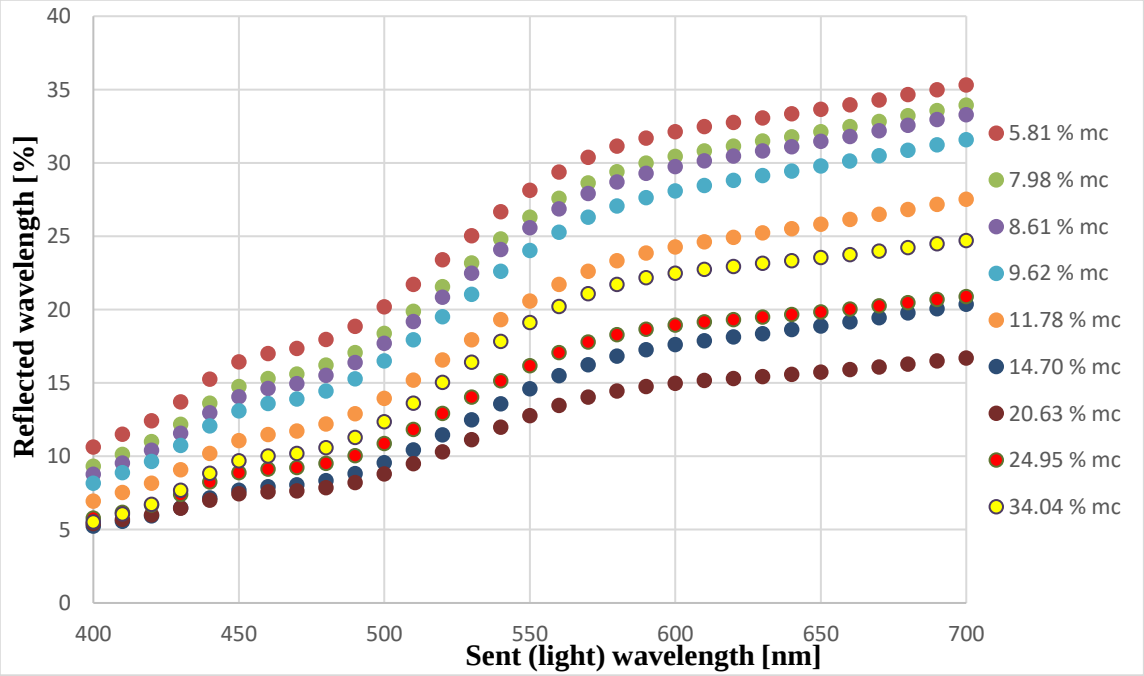

Fig. 4.5. Silty clay loam (14.07 % sand, 47.46 % silt, 38.47 % clay) spectral reflectance at different moisture contents.

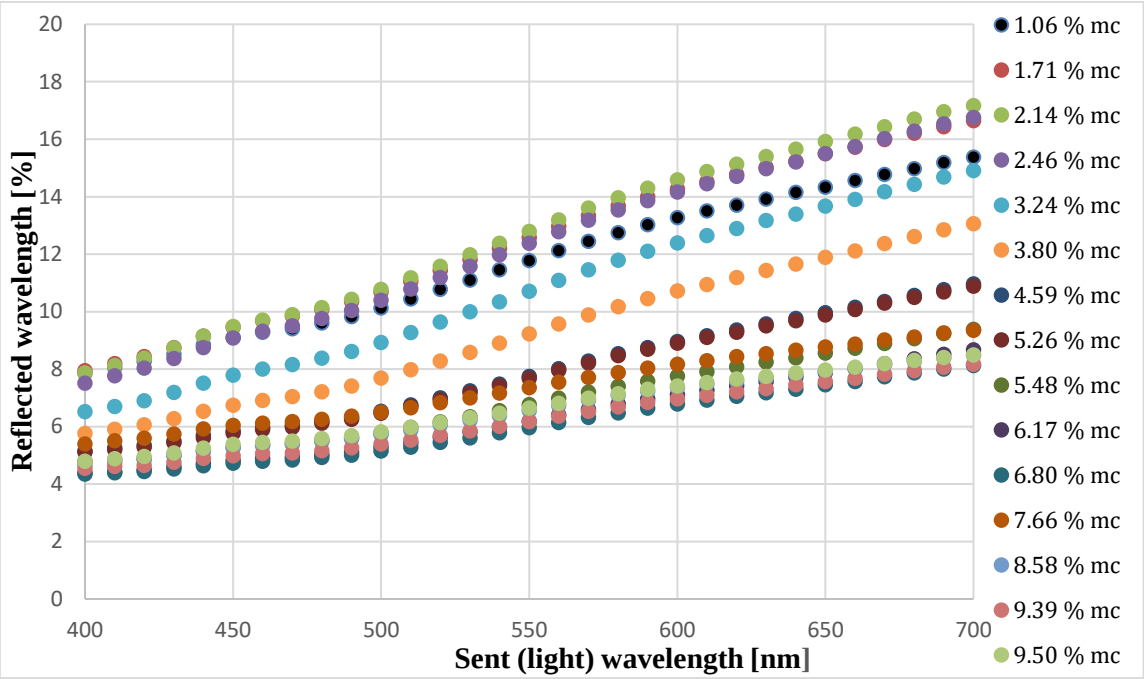

Fig. 4.6. Loam sand soil (90.50 % sand, 3.20 % silt, 6.30 % clay) spectral reflectance at different moisture contents.

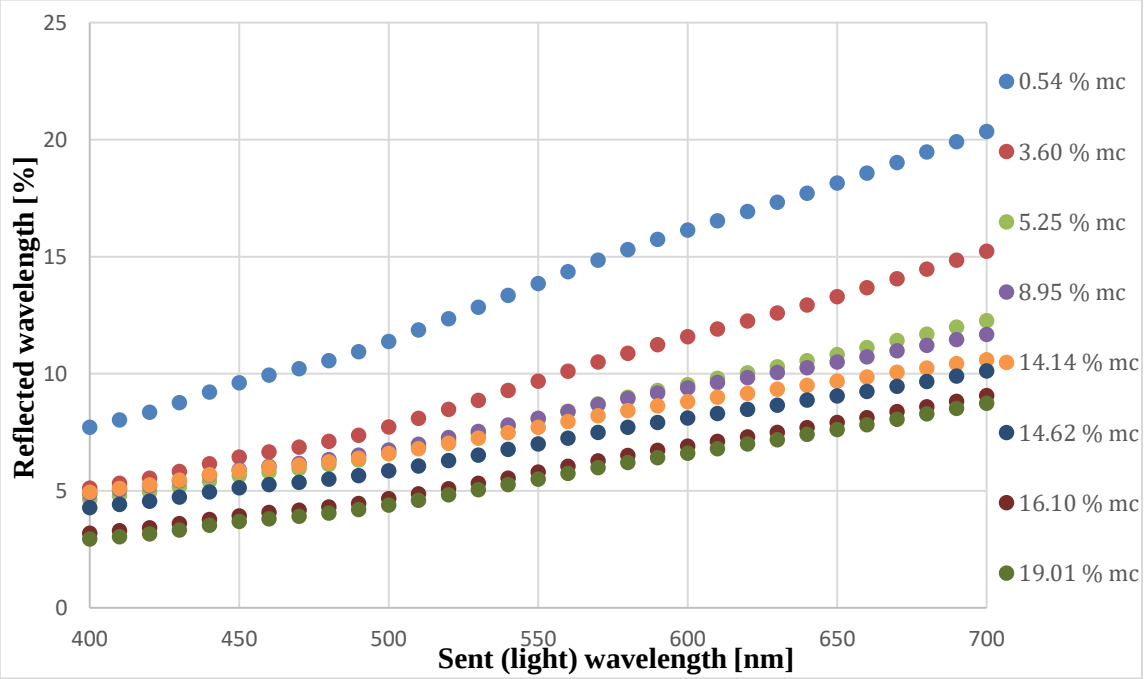

Fig. 4.7. Sand soil (95.68 % sand, 2.12 % silt, 2.21 % clay) spectral reflectance at different moisture contents.

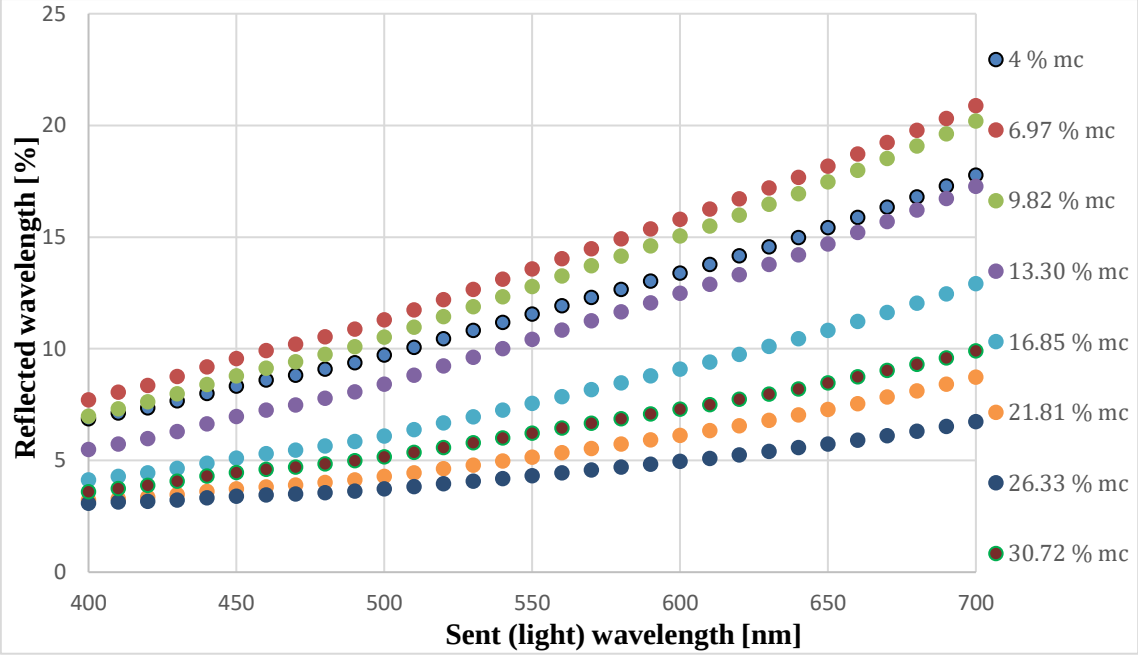

Fig. 4.8. Silty clay soil (3.34 % sand, 52.05 % silt, 44.61 % clay) spectral reflectance at different moisture contents.

In most of the soils, the increase in the moisture content leads to dimming (darkening) its colour, and that can be recognized in the measurements, not only visually by seeing how the colour of the tested soils is changing, but also by the spectrophotometric results.

In all the tested soil textures (Figures 4.4 to 4.8), the colour reflectance is increasing with the increase in the wavelength (from 400 to 700 nm), which can be recognized in the increasing curve path of the colour reflectance with the increase in the wavelength at a moisture content. This means that in the visible band (400-700 nm), the higher the wavelength is, the higher the reflectance will be. Usually, the curve from 400 to 700 nm has a positive slope that differs markedly from a soil type to another (Torrent and Barrón, 1993).

The sand soil (94.53 % sand, 4.78 % silt, 0.69 % clay) reflectance at 700 nm shows that from 0.19% the reflectance is decreasing, applicable till reaching the moisture content 8.12 %. Beyond 8.12 %, the colour reflectance starts to overlap in a colour reflectance range (as shown in Figure 4.4, but will be clarified in the discussion).

For the silty clay loam (14.07 % sand, 47.46 % silt, 38.47 % clay), at 700nm, starting from 5.81 %, with the increase in the moisture content, the colour decreases, till reaching 20.63 %. Beyond the value 20.63 % (the minimum soil reflectance reached), with the increase in the moisture content, the reflectance starts to increase (slight increase), and that is clear at the moisture values 24.95 % and 34.04 % (Figure 4.5).

For loam sand soil (90.50 % sand, 3.20 % silt, 6.30 % clay), at a fixed wavelength (considering 700 nm), with the increase in the moisture content, the colour reflectance decreases (on average). Starting with the moisture 1.06 %, with increasing the moisture content, the reflectance starts to decrease till reaching 5.48 % (in reality it is different and will be clarified in the discussion, but that is seen in Figure 4.6). Beyond this value, with the increase in the moisture content, the colour reflectance starts to overlap in a reflectance range, applicable till reaching the maximum moisture content used. The mentioned tendency is the general curve

tendency, but a slight increase in the reflectance can be recognized in the beginning of the moisture range (at the starting moisture values), from 1.06 % to 2.14 % mc. The increase in the tendency is clear in 700 nm reflectance-moisture curve below (Figure 4.16), and a solution will be given regarding dealing with the curve peak (will be discussed in section 4.5).

The sand soil (95.68 % sand, 2.12 % silt, 2.21 % clay) shows that from 0.54 % mc the reflectance at 700 nm is decreasing, applicable till reaching the moisture content 19.01 %.

For the silty clay soil (3.34 % sand, 52.05 % silt, 44.61 % clay), at 700 nm, with the increase in the moisture content from 4 % the reflectance decreases reaching a minimum point at 26.33 % (reflectance is decreasing on average, despite the slight increase from 4 % to 6.97 %). Beyond the minimum point reached at 26.33 % mc, with the increase in the moisture content, the reflectance slightly increases (clarification will be given in section 4.5).

The soil colour under moist conditions is different than when having it in dry conditions (IUSS, 2015), (Kirillova et al., 2021). The behaviour of the soil spectral reflectance as function of moisture content complies with researchers' findings. In a research work it is mentioned that the reflectance at all wavelengths in the range 0.4-2.5 micrometer decreases with the increase in the moisture content (Hoffer and Johannsen, 1969). With increasing the moisture content, the soil colour becomes darker due to the reduced reflectance (Bhadra and Bhavanarayana, 1997). Soils become darker with the increase in the moisture content, which is the reason behind decreasing their spectral reflectance (Zanetti et al., 2015), (Bowers and Hanks, 1965).

4.4 Discussion on the colour reflectance results

Dealing with the records taken from the spectrophotometer to end up with the ability to find the moisture content from the colour by plotting different curves (reflectance parameters curves) as function of moisture content, such as the averaging of the reflectance from 400 to 500 nm and 400 to 700 nm, also plotting the reflectance at the lowest and the highest wavelengths (at each, 400 and 700 nm), in addition to plotting the Z tristimulus value (spectrophotometric reflectance measuring parameter); Also, by plotting the area below each curve (energy method, in each figure, 4.4 to 4.8, at each moisture content) as function of moisture content. All the mentioned paths were used for reaching a way to determine the moisture content from the colour reflectance, and among all these trials, it appeared that using the reflectance at a one wavelength will serve in decreasing the error in the estimated moisture content. Comparing the predicted moisture obtained from plotting the 700 nm reflectance to the moisture obtained using the 500 nm reflectance, has shown that the 700 nm is ending with better estimated moisture content. The Figures below, 4.9 to 4.13, show plotted reflectance parameters as function of moisture content.

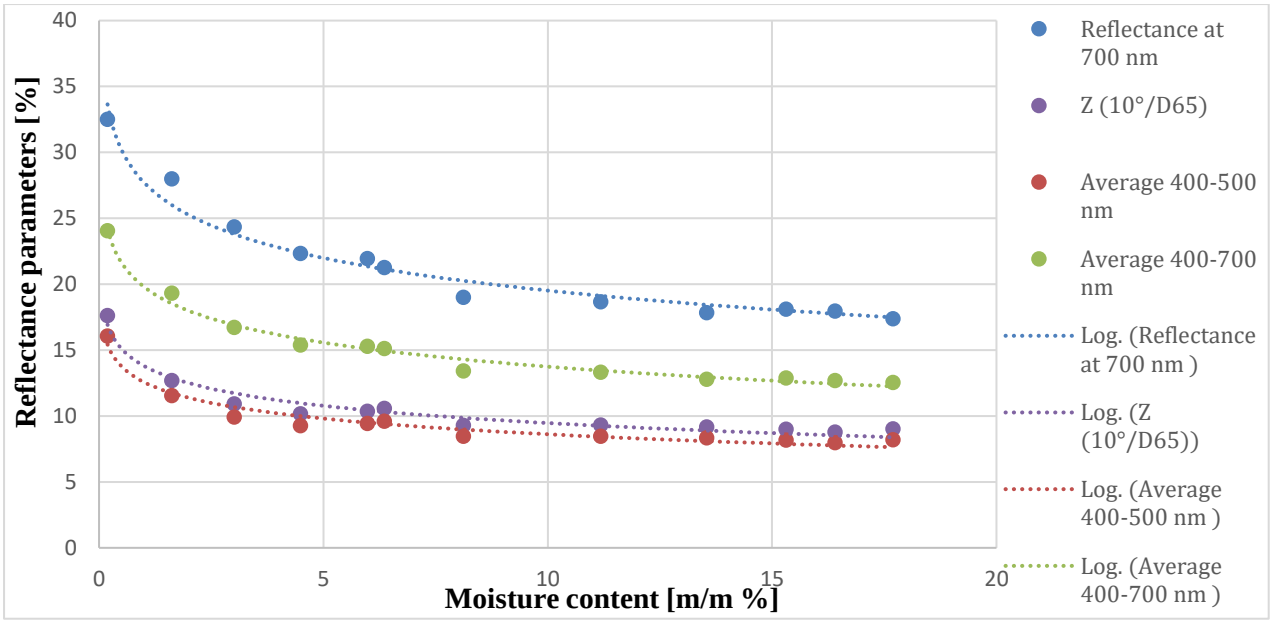

Fig. 4.9. Sand soil (94.53 % sand, 4.78 % silt, 0.69 % clay) colour reflectance parameters as function of moisture content.

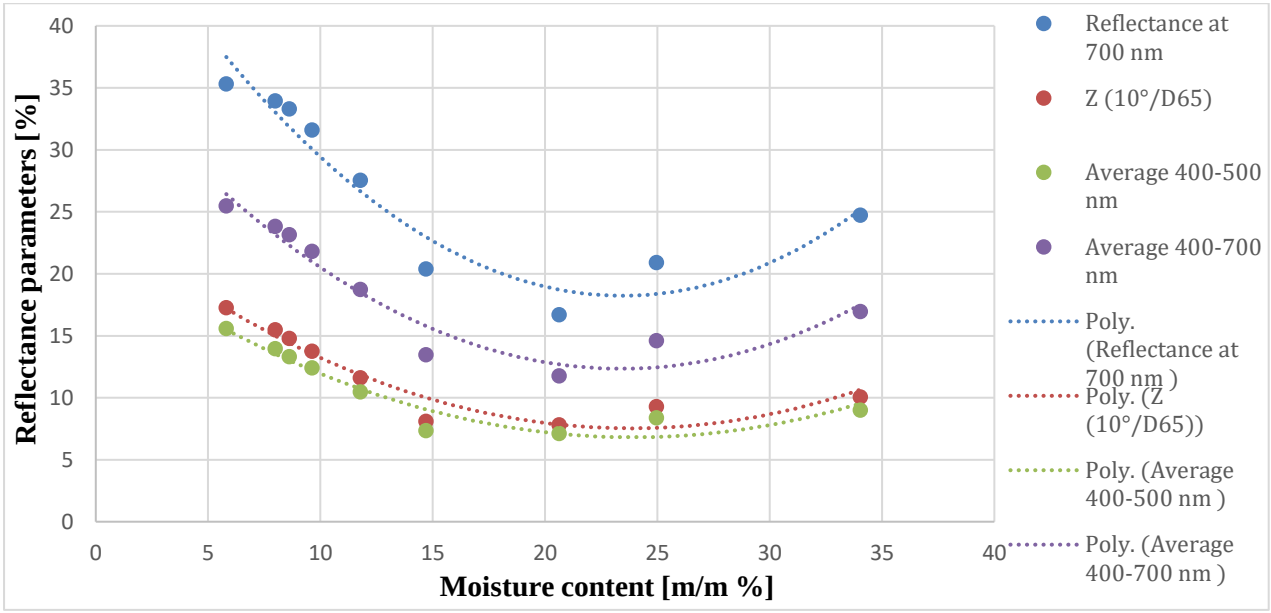

Fig. 4.10. Silty clay loam (14.07 % sand, 47.46 % silt, 38.47 % clay) colour reflectance parameters as function of moisture content.

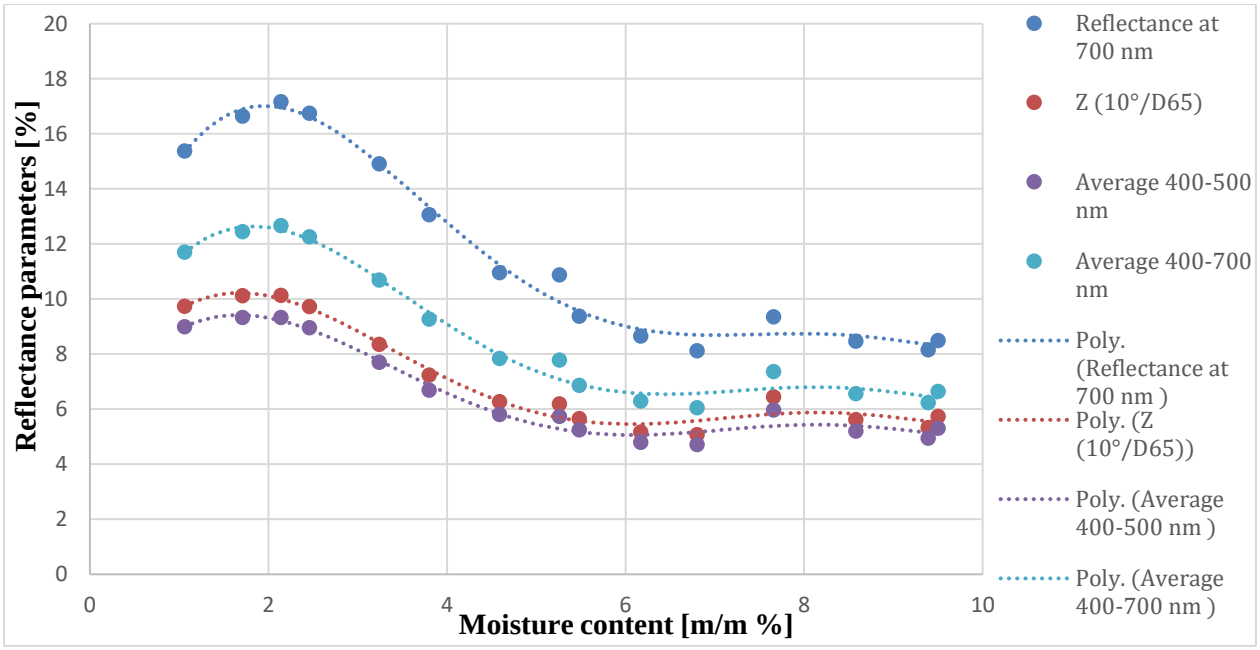

Fig. 4.11. Loam sand soil (90.50 % sand, 3.20 % silt, 6.30 % clay) colour reflectance parameters as function of moisture content.

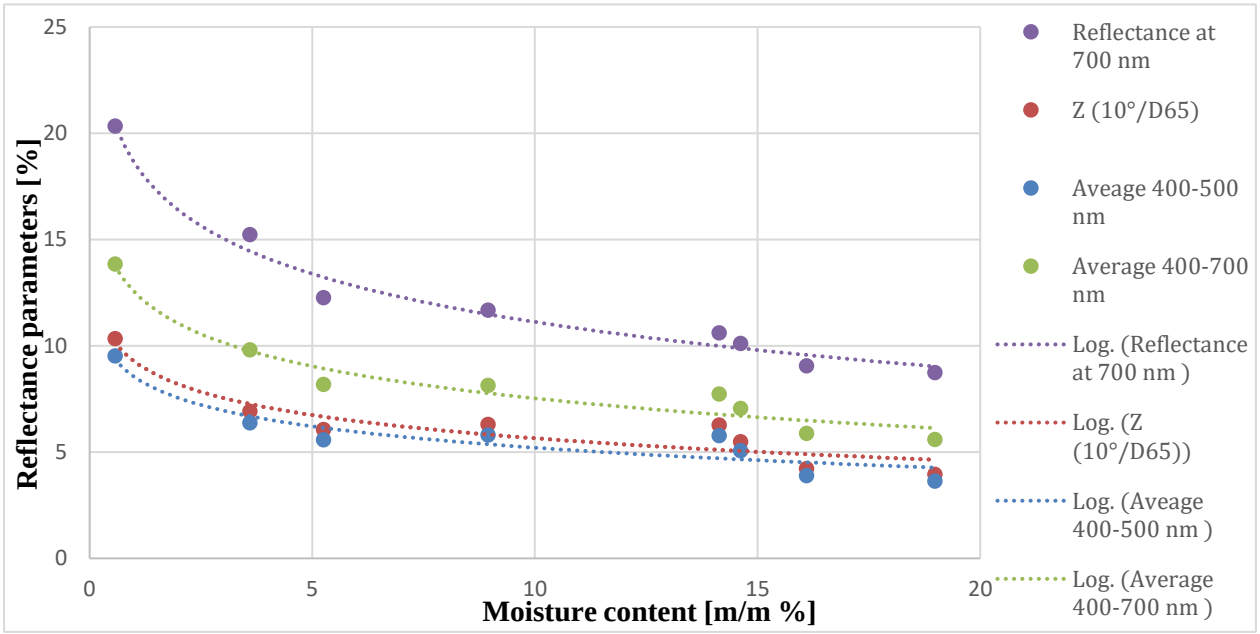

Fig. 4.12. Sand soil (95.68 % sand, 2.12 % silt, 2.21 % clay) colour reflectance parameters as function of moisture content.

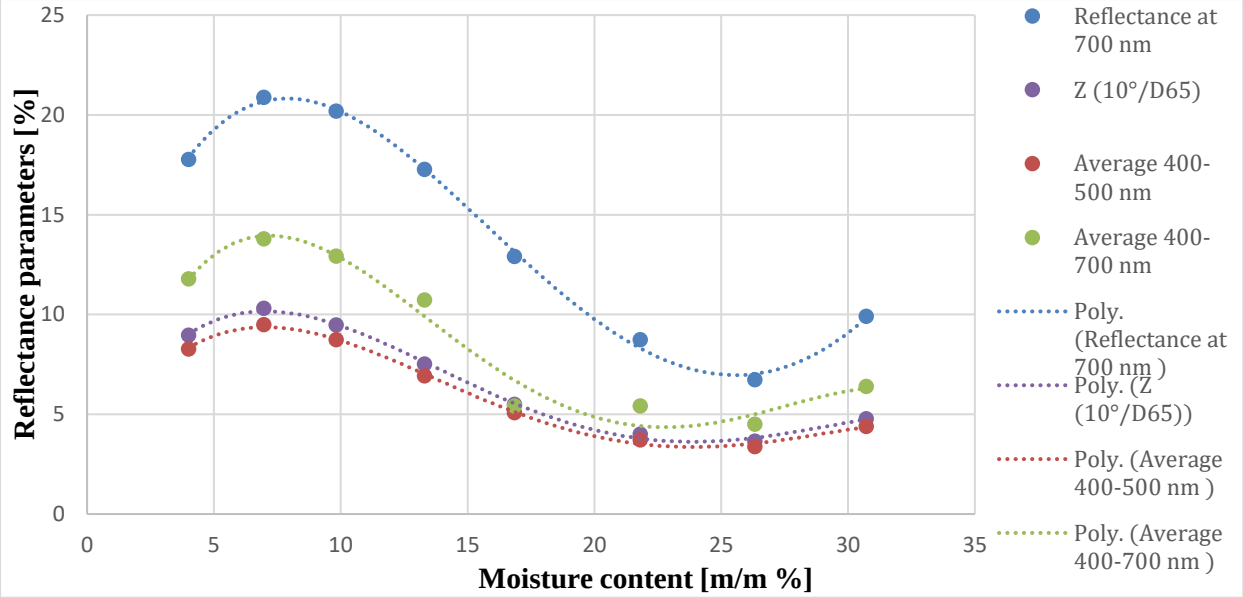

Fig. 4.13. Silty clay soil (3.34 % sand, 52.05 % silt, 44.61 % clay) colour reflectance parameters as function of moisture content.

Dealing with the original curves shown in Figures 4.4 to 4.8 using the area under each curve (energy method) at each moisture content, by plotting the area result as function of moisture content, did not lead to good results. Considering the reflectance results at one point (at one wavelength or one tristimulus value) to be plotted as function of moisture content, will decrease the error in the estimated moisture content.

Taking into consideration averaging of the reflectance results (400-500 nm and 400-700 nm) or finding the area under a curve will result in the averaging or integration of errors at the wavelengths.

Empirically and mathematically, the validity of the curves' equations of each soil (mentioned in the above text, some are shown in Figures 4.9 to 4.13) was checked by substituting each reflectance value (Z, the averaging, and at 700 nm; obtained from a new measurement at a moisture content) in its equation. The closest estimated moisture value is at the reflectance 700 nm, where the points are mostly dispersed (check figures 4.4 to 4.8). Upon substituting a new colour reflectance record at 700 nm in the already obtained curve equation (for each soil, 700 nm reflectance results as function of moisture content), the closest moisture value is obtained (relative to the value measured by the moisture analyzer).

Due to the difference in the reflectance upon repeating the measurement (taking a new record), the difference in the results (at each wavelength) is considered as error, so dealing with the reflectance on large wavelength scale (as averaging or area) might increase the error, resulting in inaccurate estimated moisture content.

By plotting the reflectance at 700 nm as function of moisture content, upon fitting a curve into the plotted points and obtaining its equation, the resulting equation is reliable to be used for estimating the moisture value (at a colour reflectance). With this curve, the colour-moisture relation is built, and the term estimation is a relative term. When measuring the moisture content using the analyzer (gravimetric method), the measuring process is approximately deterministic with repetition. Even though there isn't a fixed percentage error calculated

relative to the moisture content measured by the analyzer, but the value estimated from the colour is approximate to the analyzer result.

The colour-moisture equation of a soil texture can be generalized equation for this texture, but when finding the best fitting curve equation from a new measurement, the resulting equation will not be exactly the same, since the soil is a particulate matter and there are factors that might lead to deviation in the reflectance results (thus another equation), such as the compaction resulting from placing the spectrophotometer on the soil while measuring and the density change at different soil spots (density change from spot to another). Also, with finding the curve equation, it is better to deal with more plots (more moisture content points), since decreasing the plots will lead to a recognized change in the fitting curve.

The below section focuses on dealing with the reliable curve (each tested soil texture, at 700 nm) for estimating the moisture content.

4.5 Reflectance curve at 700 nm (moisture content estimated from the colour reflectance)

Soil colour records were taken (three records at each moisture content for averaging them) and simultaneously a sample was placed in the analyzer for the validity of the work. Starting with each soil at ambient conditions (moisture is due to the surrounding atmosphere), the water was added to the soil in an increment way.

Dealing with the reflectance results at 700 nm, as mentioned in the above text, since the 700 nm reflectance-moisture curve is ending with best estimated moisture value compared to using the reflectance parameters (shown in the curves above). Each of the below curves shows the reflectance results at 700 nm plotted as function of moisture content of a tested soil texture.

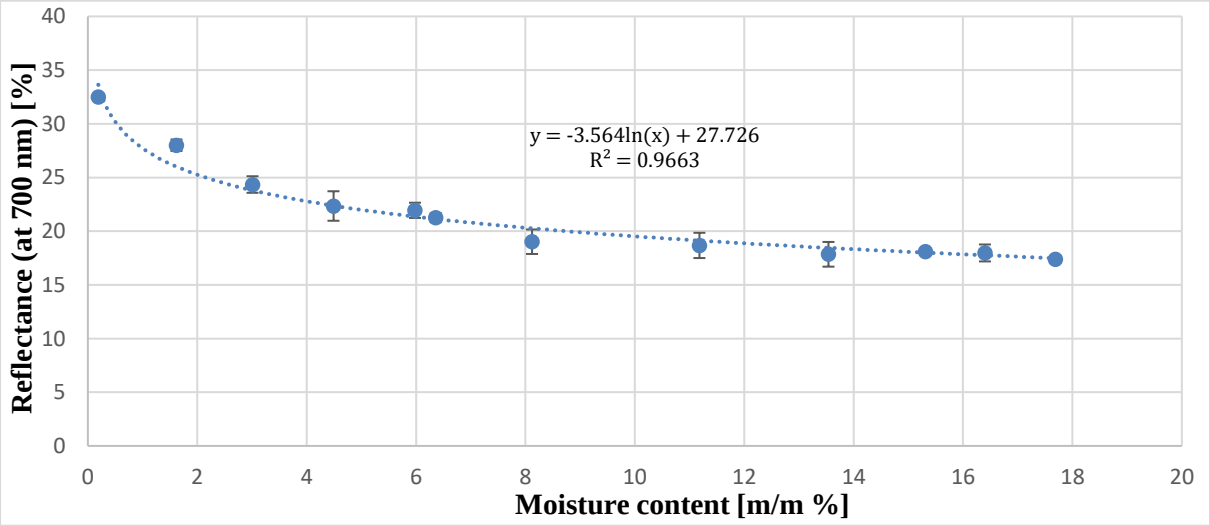

Fig. 4.14. Colour reflectance (at 700 nm) as function of moisture content, sand soil (94.53 % sand, 4.78 % silt, 0.69 % clay).

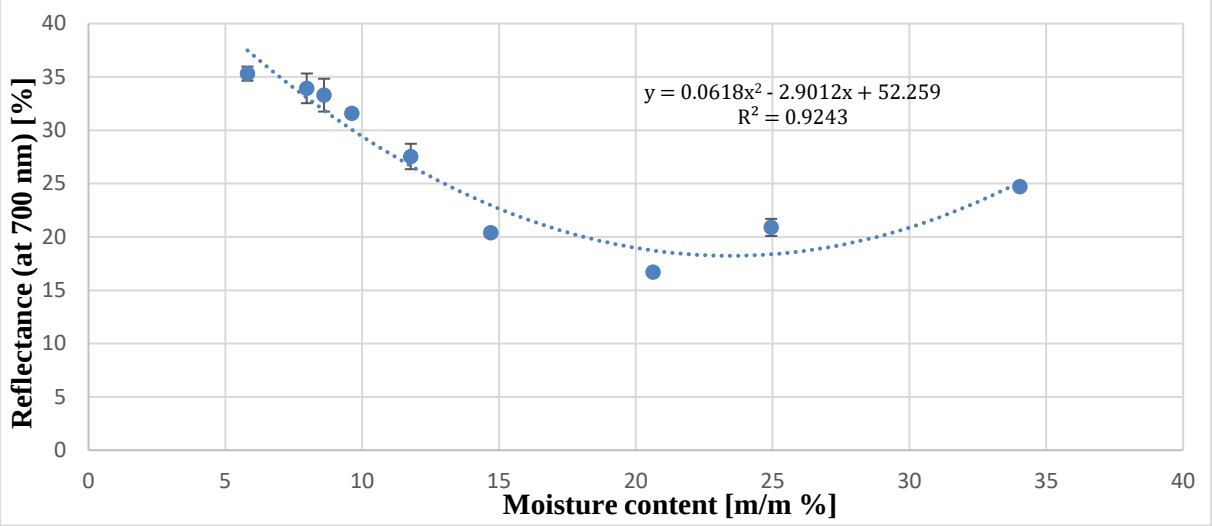

Fig. 4.15. Colour reflectance (at 700 nm) as function of moisture content, silty clay loam (14.07 % sand, 47.46 % silt, 38.47 % clay).

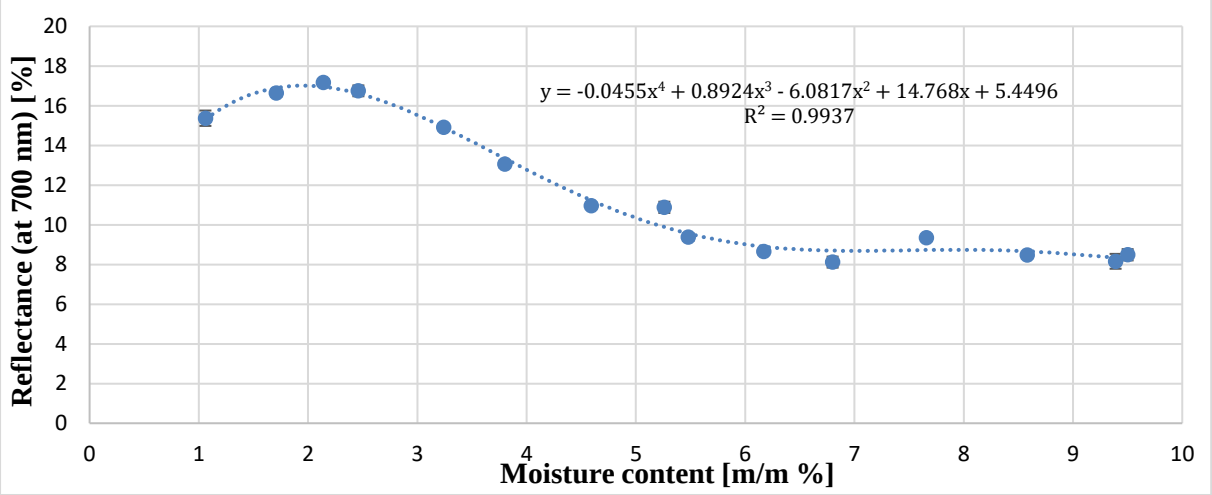

Fig. 4.16. Colour reflectance (at 700 nm) as function of moisture content, loam sand soil (90.50 % sand, 3.20 % silt, 6.30 % clay).

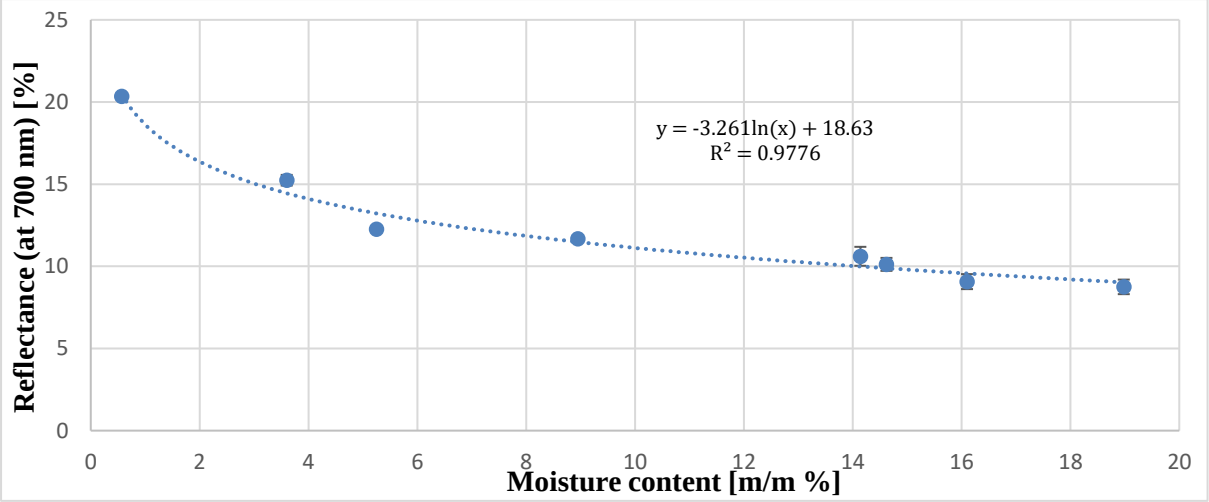

Fig. 4.17. Colour reflectance (at 700 nm) as function of moisture content, sand soil (95.68 % sand, 2.12 % silt, 2.21 % clay).

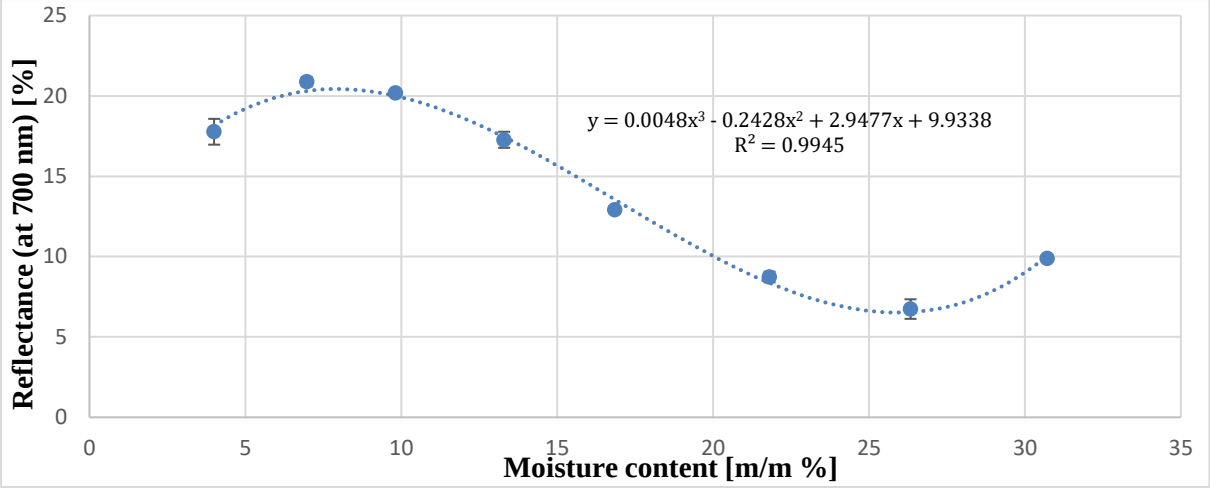

Fig. 4.18. Colour reflectance (at 700 nm) as function of moisture content, silty clay soil (3.34 % sand, 52.05 % silt, 44.61 % clay).

In Figures 4.14 till 4.18, it is clear that with the increase in the moisture content, the reflectance is decreasing (on average). Based on the above results, it can be considered as a general rule which was also mentioned (confirmed) by researchers (Zanetti et al., 2015), (Bowers and Hanks, 1965), that on most of the soils with the increase in the moisture content the colour becomes darker, thus leading to decreasing the spectrophotometric reflectance value.

Looking at the loam sand soil curve (Figure 4.16) and at the curve of the silty clay soil (Figure 4.18), the curve tendency falling in the low moisture range shows an increase to a peak value making a hump on the curve. Upon repeating the measurement on the tested soils, the curves are showing the same tendency in a certain low range (range can be checked on the figure of each soil). The reason behind this hump tendency might be due to the initial phase of the bonding formation (soil from dry to wet status), leading to a slight increase in the reflectance by the bonds counteracting the spectrophotometric sent light wave (hump formation is dependent on the soil). Beyond the peak reached, the reflectance will be dominated by the change in the colour. The hump falling in the moisture range of each of these soils might lead to results' conflict when predicting the moisture result from the curve tendency equation, since for the same input colour value two accepted results should be in this range (of each soil). The exact solution for this case might be by relying on the soil electrical resistivity or conductivity at the moisture content where having the maximum point reached.

For example, having the electrical resistivity at the peak value (at its moisture content) already found in the laboratory, the remote sensor compares the real-time measured value (electrical resistivity) to the value at the peak (already prepared), then chooses the correct moisture content (when having conflict). A higher measured resistivity compared to the one at peak, means the low moisture value in the range, and a lower resistivity means the higher moisture value.

Resistivity and conductivity of the soils are not measured in our work, this work should be carried out by experienced persons in this measurement (resistivity and conductivity), in addition to using an accurate instrument following a standardized procedure applicable on the tested soil type/s. The research colour measurement only focuses on results obtained using a visible range spectrophotometer on different soil textures. The mentioned suggestion is for solving the hump case obtained on the curves, thus not ending with conflicts in the results. The curve tendency, having a soil curve with a hump, requires further investigation after obtaining the resistivity or conductivity value at the peak moisture content, in addition to validating the

work through another separate measurements (new input colour results in the obtained soil curve equation, having the conductivity or resistivity measured, for estimating the actual moisture content). The hump in the silty clay soil will be treated following the same process.

In the soil textures that contain high clay and silt portions (mostly clay, particles of high cohesion), the silty clay loam and the silty clay, after reaching the minimum point in the curve at a moisture value, beyond the minimum point the tendency shows a slight increase in the reflectance. The reason behind this behaviour is that at a moisture content that is close to the minimum point moisture content, the colour reaches an approximately constant level and what is dominating the spectral reflectance at this stage is the behaviour of the soil. With the presence of silt and clay, mainly clay, at high moisture content these fine particle change the soil matter from a particulate matter to a one body bonded paste. Thus, having the sent light wave reaching the soil, the sent wave is no more scattered and absorbed at the particles' level (maybe a small portion), leading to increasing the reflectance. When having the soil as powder (granulated), the specularly reflected wave is a small fraction of the incident light, and the rest part of the incident light penetrates into the soil mass encountering surfaces of minerals and organic particles (Torrent and Barrón, 1993). The material behaviour of the soil at this stage (a moisture range in each of the two soil textures) is a paste like material. In real-time terramechanics case, vehicles move on soil as particulate matter, thus a reason behind cancelling this part of the curve tendency and not considering it when accounting the curve tendency.

The Figures 4.19 and 4.20 below show the behaviour of the two tested silty clay soil textures.

In Figure 4.19, at high moisture contents, the colour shows unrecognized change with moistening, but the change in the soil behaviour is clear. The soil has changed to a one face paste like material (at moisture values 24% and 34 %). Thus, approximately the colour is no more darkening for decreasing the reflectance, and the physical behaviour of the soil (bonding) is leading to a slight increase in the reflectance.

The same principle is applicable on the silty clay, at 30.72 % moisture content, the soil is no more a separate particulate matter, particles bond due to polarity forming the one body material, leading to a slight increase in the reflectance.

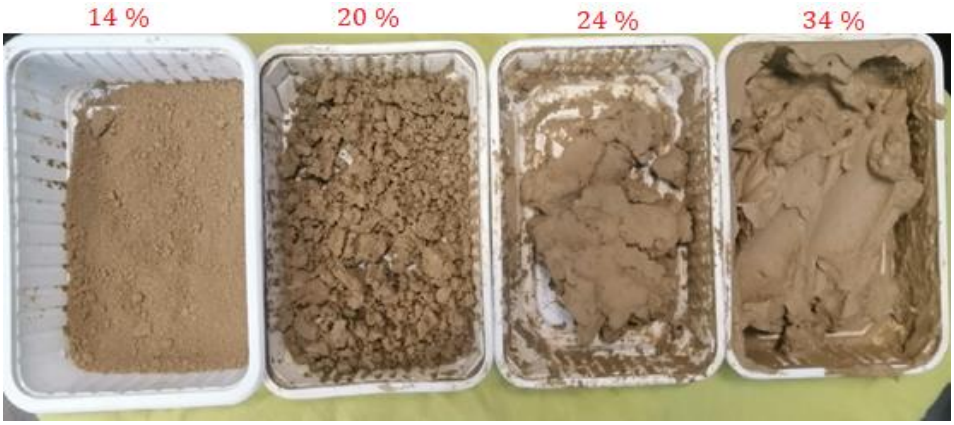

Fig. 4.19. Soil colour and physical behaviour changing with the change in the moisture content, silty clay loam (14.07 % sand, 47.46 % silt, 38.47 % clay).

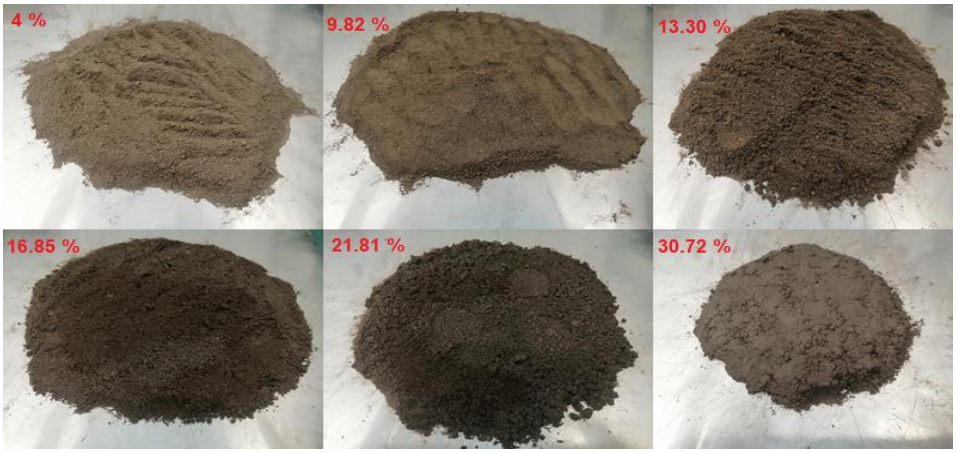

Fig. 4.20. Soil colour and physical behaviour changing with the change in the moisture content, silty clay (3.34 % sand, 52.05 % silt, 44.61 % clay).

4.6 Validity of the colour-moisture curve equation at 700 nm (of each soil texture)

The work focuses on dealing with the reliable curve (each tested soil texture, at 700 nm) for estimating the moisture content. Fitting a curve across the plotted points (at 700 nm) with having small incrementation in the moisture content, leads to the curve with the best regression analysis emulating the change in the colour tendency.

Choosing one wavelength value from the visible range for analyzing the reflectance results at different moisture contents, is a solution to know how the colour is varying with moisture content. The chosen wavelength value is the one where the points are dispersed, and as recognized in the section 4.3 graphs, that at 700 nm the reflectance points are separated, except for the high moisture range where the results start to overlap or show a slight increase.

Relying on the graphs in the above section (4.5), the graphs showing the change in the colour reflectance at 700 nm with the increase in the moisture amount (of each soil):

For the sand soil (94.53 % sand, 4.78 % silt, 0.69 % clay), the curve fitting the plotted points with the best regression analysis is of logarithmic equation (shown in figure 4.14), of regression analysis 0.9663. In the analysis of figure 4.4, it is mentioned that the reflectance reaches an overlapping level, but in figure 4.14 it is clear that the reflectance is still decreasing (slight decrease at high moisture contents).

Giving an example about calculating the moisture content of this sand soil having the colour reflectance. Input to be to substituted by y in Equation 4.1, solving for x.

$$\mathbf{y = -3.564 \ln(x) + 27.726} \qquad (4.1)$$

The colour reflectance at 700 nm (of new sample) is measured by the spectrophotometer, of a value $\mathbf{y = 20.81}$. Substituting y will result in $\mathbf{x = 6.96}$. Measuring the moisture content using the analyzer, the obtained result is 6.40 %, which is approximate to the predicted value, the 6.96 (8.04 % difference in the results relative to the highest value), and the difference between them has an explanation. The moisture measured by the analyzer is the precise value (gravimetric measurement), while the result obtained from the colour equation is predicted (estimated) and not the actual (from the masses).

The reason behind having this difference is in the colour reflectance of the soil between a measurement and another. Since the soil is a particulate material, the colour result differs with measurement repetition on the same spot or on other spot, so using each of the different reflectance records as an input in the equation, will lead to another moisture result.

For the silty clay loam (Figure 4.15), the colour reflectance behaviour is split into two ranges, the first range, which is the part where the reflectance is decreasing with the increase in the moisture content (till 20.63 %), and the second part is beyond this moisture content. The explanation for this behaviour is that at high moisture content the clay behaves like a paste and it is no more broken particulate material, thus leading to increasing the reflectance of the sent light wave (less absorption and scatter of the wave at the particles' level). The performance of vehicle is studied on soil terrain and not on a paste like material. From this point, the first moisture content range is the range that will be taken into account, considering studying the vehicle performance on soil as particulate material. Dealing with the first range and fitting a curve into the plotted colour reflectance, will result in a curve equation that can be used for predicting the moisture content of the soil. The equation of the curve fitting the plotted points is shown in Figure 4.21 with regression analysis 0.9572.

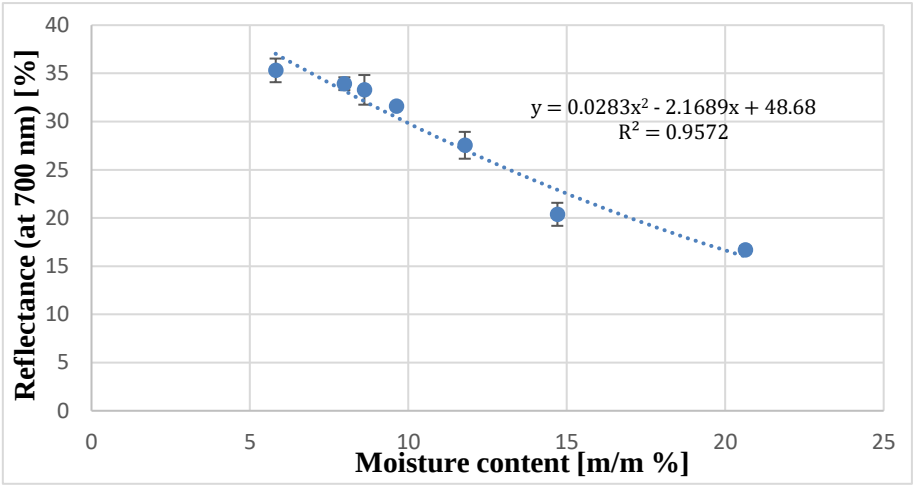

Fig. 4.21. Silty clay loam soil colour reflectance (at 700 nm) change with moisture content; moisture ranging from 5.81 % to 20.63 %.

Solving Equation 4.2 for an input colour value, will result in two solutions.

$$\mathbf{y = 0.0283x^2 - 2.1689x + 48.68} \quad (4.2)$$

For the input colour reflectance value $\mathbf{y = 32.35}$ at 700 nm, measured by the spectrophotometer, the output results are $\mathbf{x_1 = 68.17}$ and $\mathbf{x_2 = 8.46}$. The first value does not fall in the moisture range, thus a rejected result, while the second belongs to the moisture range (5.81 % - 20.63 %). Measuring the moisture content of the same soil sample using the moisture analyzer, resulted in a value equal to 8.61 %. The two results (8.46 and 8.61) are close values (1.74 % difference).

In Figure 4.16, the colour reflectance initially slightly increases with moistening reaching a peak, and beyond this point with the increase in the moisture content, the reflectance decreases till reaching the moisture value 6.80 %. Exceeding this moisture value, the colour reflectance values start to move in approximately a straight path. In the first moisture content range, a curve fitting the plotted reflectance can be drawn, which can be used for predicting the moisture content with having an input colour reflectance value (at 700 nm). In the second range, the

stability in the reflectance shows (till saturation level, around 23 % moisture content, but in the graph the moisture content is stopped at 9.50 %), that either the colour is no more changing despite the amount of water added for moistening the soil, or the visible range spectrophotometer is unable to provide precise colour reflectance results at this stage.

In the first range, the curve fitting the plotted points is given by the equation shown on the graph (Figure 4.22) with regression analysis 0.9937.

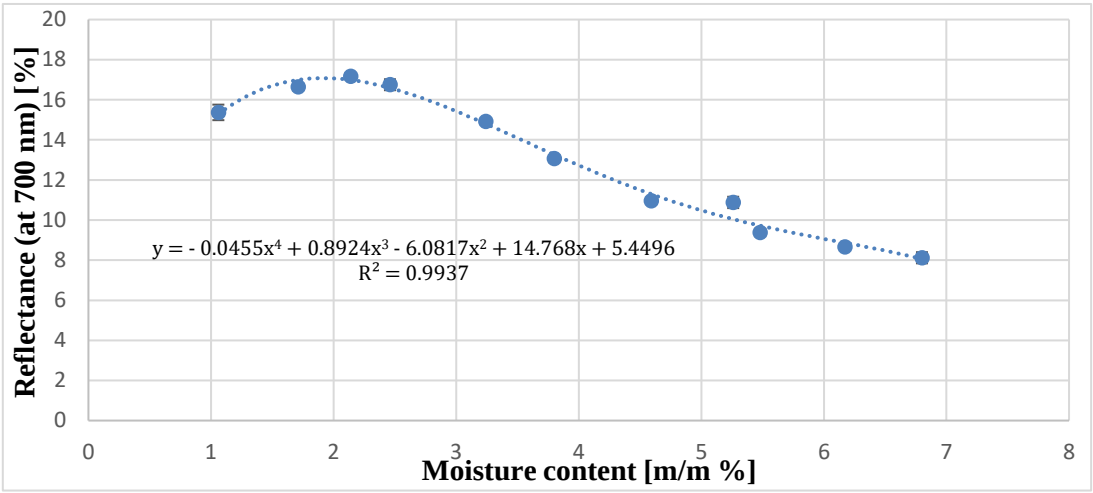

Fig. 4.22. Loam sand soil colour reflectance (at 700 nm) change with moisture content; moisture ranging from 1.06 % to 6.80 % (before results constancy).

Giving an example about using the colour equation (of the curve passing through the plotted points in the moisture range 1.06 % to 6.80 %) for calculating the moisture content, a random soil sample (but already knowing that its moisture content is in the equation range) was measured by the spectrophotometer, and the record at 700 nm was substituted in Equation 4.3.

$$\mathbf{y = -0.0455x^4 + 0.8924x^3 - 6.0817x^2 + 14.768x + 5.4496} \quad (4.3)$$

Solving this equation for an input colour value $\mathbf{y = 10.24}$ gives four solutions. The results are, $\mathbf{x_1 = 5.07 + 2.08i}$, $\mathbf{x_2 = 7.07 - 2.08i}$, $\mathbf{x_3 = 5.07}$, and $\mathbf{x_4 = 0.38}$. The correct value is the one that falls in the moisture content range and sure not a complex number, thus the result 5.07 is the one accepted as a moisture value. The moisture content of the random sample was measured using the moisture analyzer, and the result is 4.9 %. The results are close to each other (with 3.35 % difference).

For the sand soil (95.68 % sand, 2.12 % silt, 2.21 % clay), the curve fitting the plotted points with the best regression analysis is of logarithmic equation (shown in Figure 4.17), of 0.9776 regression analysis. In Figure 4.17, it is clear that the reflectance keeps on decreasing (slight decrease at high moisture values), complies with Figure 4.7 analysis.

Giving an example about calculating the moisture content of this sand soil having the colour reflectance. Input to be to substituted by y in Equation 4.4 solving for x.

$$\mathbf{y = -3.261\ln(x) + 18.63} \quad (4.4)$$

The colour reflectance at 700 nm (of new sample) is measured by the spectrophotometer, of a value $\mathbf{y = 11.71}$. Substituting y, results in $\mathbf{x = 8.35}$. Measuring the moisture content using the analyzer, the obtained result is 8.62 %, which is approximate to the predicted value (3.13 % difference).

For the silty clay soil (3.34 % sand, 52.05 % silt, 44.61 % clay), skipping the high moisture range because of the paste like material physical behaviour, similar to the silty clay loam case explained above, and taking into account the first moisture portion. Fitting a curve into the plots, the equation of the resulting curve is shown in the Figure 4.23.

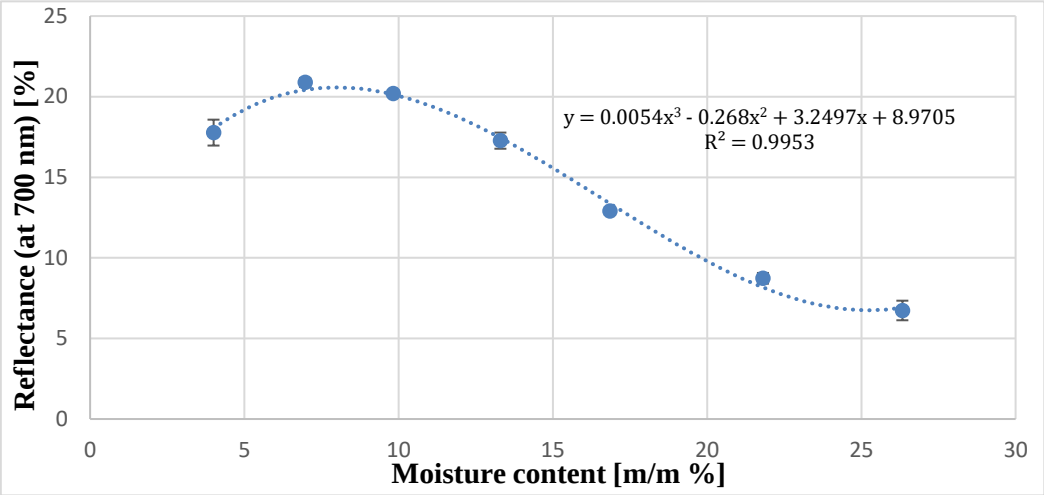

Fig. 4.23. Silty clay soil colour reflectance (at 700 nm) change with moisture content; moisture ranging from 4 % to 26.33 %.

Using the equation in the above figure (4.23) and substituting a colour reflectance instead of y.

$$\mathbf{y = 0.0054x^3 - 0.268x^2 + 3.2497x + 8.9705} \quad (4.5)$$

For the input colour reflectance value $\mathbf{y = 15.65}$ at 700 nm, measured by the spectrophotometer, the output results are $\mathbf{x_1 = 32.06}$, $\mathbf{x_2 = 14.99}$, and, $\mathbf{x_3 = 2.57}$. The first and the third values do not fall in the moisture range, thus rejected results, while the second belongs to the range (4 % - 26.33 %). Measuring the moisture content of the same soil sample using the analyzer, resulted in a value equal to 14.36 %. The two results (14.36 and 14.99) are close values of 4.20 % difference.

Some researchers also confirmed that finding the moisture content from the colour is an estimation method, meaning that the resulting value is not precise as when obtained using the gravimetric measurement. Since the change in the colour shade represents a change in its moisture content, then a quantitative value representing the colour of the soil can be used for estimating the water content of the soil (Persson, 2005), (Torrent and Barrón, 1993).

Summary of the new approach in the chapter

Listing the scientific findings in this section (detailed in the scientific findings chapter):

1- Determining the correlation between the spectrophotometric colour reflectance and the moisture content of the soil, by plotting the reflectance colour records at the wavelength 700 nm as function of moisture content.

2- The soil texture (mainly the type which is based on texture) plays an important role in the colour-moisture curve tendency.

3- In the loam sand soil, the tendency of the curve has shown a decrease in the reflectance (on average) with the increase in the moisture content, and this is applicable till a certain moisture range (around 6 % moisture content), and beyond this range the reflectance becomes constant.

4- In silty clay soils (based on the tested textures), at high moisture content, the reflectance shows a slight increase.

5- In sand soils (tested soils), with the increase in the moisture content, the reflectance keeps on decreasing despite the moisture content reached (close to saturation level).

In addition to providing a solution for dealing with the hump in a curve (if present), avoiding conflict in the results and for accuracy in the estimation (requires further investigation).

5. Mohr-Coulomb principle for finding the soil shear strength and its parameters

The soil texture or its mechanical composition is the identity of the soil. Each component portion in the texture has influence on the soil strength. The size of the soil particles affects the void ratio and the porosity inside the soil, thus affecting the permeability. Loam sand soil of mechanical composition sand, silt, and clay, is a soil type that is of both cohesion and internal friction (when undisturbed). The change in the soil water content influences its load bearing capacity and shear strength (Salman and Kiss, 2018), (Pillinger et al., 2018), (Ahmed et al., 2023), (El Hariri et al., 2023a). The clay soil (sieved soil, no initial bonding) shows an increase in the cohesion with moistening, meaning that the clay particles become stickier with the increase in the moisture content, leading to strong cohesive bonding among the particles forming a one face paste like material at high moisture contents (El Hariri and Kiss, 2023b). Studying how sand soil is behaving with moisture content would be beneficial to different sectors, such as the geotechnical, civil, and off-road engineering. In off-road engineering, the vehicle might face the case of moving on sand soil terrains, as on a desert terrain or on the sea shore. If the sand strength is not strong enough to resist the normal and the shear stresses applied on it, the vehicle will face difficulties in its mobility (despite additional drags, such as the bulldozing effect).

The loam sand soil is of mechanical composition, sand, silt, and clay (90.50 % sand, 3.20 % silt, and 6.30 % clay). When it comes to identifying the cohesion and the friction coefficient of this soil, the mechanical composition makes this soil type of a moderate cohesion and internal friction when having it dry (compared to cohesive and frictional soils). The silty clay and the silty clay loam soils embed high portion of fine particles (the clay), highly cohesive, which makes all the particles bond strongly and accumulate on each other at high moisture values. The sand soil type is a frictional soil, the size of the particle is of bigger diameter (coarse particle) when compared to fine particles, and having the sand particles sliding on each other will lead to the friction at the particles' level (material friction and particles' interlocking). The different soil characteristics regarding the cohesion and the internal friction is what led to choosing these kinds of soils to be tested.

The cohesion of the soil shows its consistency and has two connotations: in physics, soil cohesion reflects the cohesive bonding between the soil particles, but in soil mechanics (from mechanics perspective), the shear cohesion is the shear strength of the soil when the applied normal stress on the surface is equal to zero (Yokoi, 1968). The internal friction angle is a parameter reflecting the internal resistance of the soil to shearing, resulting from the friction on the particles' level. While shearing the soil, the cohesion strength parameter is a stress-independent parameter, while the internal friction angle depends on the applied stress.

The soil thrust which results from the shearing of the terrain by the tractive element (wheel/track) is calculated using the shear strength of the soil. In soil mechanics, the soil thrust is a property that contributes to the propelling of a vehicle (Kogure and Sugiyama, 1975). There are different methods used for measuring the shear strength of soil, but none of these methods are standardised, so choosing the suitable method for measuring the shear strength is decided based on the case of study. For studying land locomotion cases, it is important to choose the shear test that closely emulates the interaction between the tractive element (wheel/track) and the terrain. In the direct shear test, the soil is shearing along a predetermined plane (Sallberg, 1965), thus simplifying the case of the shear failure for measuring the displacement as a

function of the applied shear stress, which is hard to study infield where the failure plane is unidentified or difficult to obtain.

5.1 Importance of finding the shear strength and its parameters

The soil response to an exerted load differs from a texture to another. The soil shear strength is directly affected by its cohesion and the internal friction angle under a normal stress. This chapter illustrates the shear strength values of different soil textures at different moisture contents obtained using the direct shear test. The shear strength values of three soil textures were obtained (from the textures used above in the colour measurement section) using the geo-civil engineering method, parameters determined by drawing the Mohr-Coulomb line, but in undrained condition (higher shearing speed), the case that complies with a terramechanics study case.

Having the curve's tendency equation of each soil shear strength value (cohesion, internal friction, and shear strength) as function of moisture content prepared, will serve in knowing the safety limit of the tested soil at a moisture value, that beyond it the soil fails.

5.2 Shear strength measurement (direct shear test)

The shear strength measurements were carried out on the tested soil textures at different moisture contents, for ending up with equations relating the shear strength to the moisture content (shear strength as function of moisture content). The change in the soil moisture content influences its behaviour by affecting its physical and mechanical properties (load-bearing capacity and shear strength). Ahmed et al. (2021) has shown experimentally in his article the change in load-bearing capacity of the sandy loam soil with the change in the moisture content. In a clay soil (sieved, separated particles), the cohesion increases with the increase in the moisture content, resulting in increasing the bonding strength between the particles, while the internal friction angle decreases (Salman and Kiss, 2018). The soil's physical composition, dampness (water content), density, and initial compression state affect the soil deformation resulting from the passage of a vehicle (Pillinger et al., 2018).

The shear strength values (shear cohesion, internal friction, and shear strength) of three soil textures, Table 5.1, were obtained at different moisture contents. Refer to the texture triangle, chapter 4, if required. Results are obtained based on averaging, since dealing with a particulate matter does not end up with deterministic values. The soils tested in this section were also tested (but other samples) for finding their colour reflectance (colour tests, chapter 4).

Table 5.1. Soil textures used for the shear strength measurements.

Soil texture	Sand (%)	Silt (%)	Clay (%)
Loam sand	90.50	3.20	6.30
Sand	95.68	2.12	2.21
Silty clay	3.34	52.05	44.61

For ending up with convincing cohesion and internal friction results using the Mohr-Coulomb line, there is standardized method to rely on, thus ending with realistic results. The results obtained following the standardized method might not easily solve a terramechanics study case, or might be limited to solving some cases. When it comes to studying vehicle mobility over soil, dealing with the soil strength and properties using the civil engineering soil mechanics is not suitable and its usage (using the methods) is limited (Wong, 2010).

The ASTM (American society for testing and materials) direct shear test method (ASTM D3080/D3080M-23) is a standard method for finding the soil strength parameters. This method deals with a soil as a drained material, thus shearing the soil at very low shearing rate (less than 1 mm/min). This method requires carrying out the measurement in a professional way, thus demanding experienced persons in this test from geotechnical or civil engineering fields (relying on references in the measurement) (ASTM, 2023).

When dealing with the shear strength of a soil and not its parameters at a moisture content using the direct shear test, the machine will yield convincing shear strength results, even if the sample is undrained (high shearing speed). Using these shear strength results for fitting the Mohr-Coulomb line, might not yield the actual and convincing strength parameters (cohesion and internal friction angle).

The soil will be tested at 9 mm/min shearing speed (maximum speed in the machine), the case that might lead to unconvincing cohesion and internal friction angle results.

The difference between shearing the soil in drained and undrained conditions, is that the very low shearing speed in the drained condition leads to squeezing the water outside the soil sample (from the sample shear box pores) under the consolidation stress while shearing. This case decreases the plasticity in the material, thus breaking the cohesive bonds with less plasticity, also decreasing the influence of plasticity on friction at the shearing zone. In the undrained condition, the sample is sheared at higher speed, thus approximately preserving the same moisture amount in the soil from the beginning till the end of shearing.

Finding the shear strength parameters using the Mohr-Coulomb line at a speed higher than the drained condition speed, might lead to unaccepted results (such as negative cohesion, or low cohesion relative to the soil physically recognized cohesion). Based on the empirical work carried out using the direct shear test, a conclusion was deduced, and is that before applying the masses that will be used for drawing the Mohr-Coulomb line, the soil samples (each) should be subjected to a mass that is higher than the maximum mass that will be used in drawing the Mohr-Coulomb line. In the below measurements, 30, 40, 50, and 60 kg (95.86, 127.81, 159.77, 191.72 kPa) masses were used for drawing the Mohr-Coulomb line, thus 70 kg (223.68 kPa) was chosen as a preloading mass to compact the soil before applying each of the four masses.

Applying an initial mass that is higher than the maximum mass used for drawing the Mohr-Coulomb line, is setting the soil sample in overconsolidation ratio above 1, where this ratio is the maximum stress (normal stress) that soil has experienced in the past over the current stress (used while shearing). The usage of the higher mass, to set the soil in overconsolidation ratio above 1, is for obtaining accepted shear strength parameters. The used higher mass is considered as a factor leading to the appearance of the cohesion that is resulting in the measuring normal stress range (on the loose soil). The soil shear strength (only the shear strength result and not the parameters) can be found in any initial stress status (initial condition), where the result will be recorded by the machine, but for reliable shear strength results to draw the Mohr-Coulomb line, the shear strength results leading to accepted shear strength parameters are obtained when having the soil experiencing initially higher mass relative to the maximum mass among the masses used to draw the Mohr-Coulomb line. The 70 kg was chosen as random value higher than the 60 kg that will be used in drawing the Mohr-Coulomb line, so a value that is slightly higher than the 60 kg to avoid the big difference or gap. 30, 40, 50, and 60 kg masses were considered for drawing the Mohr-Coulomb line, since in vehicle mobility the tractive element (in the majority of normal size/weight vehicles, not

huge/heavy machines) applies a ground pressure value (for example, around 2 bar, might be less or more) that falls in the pressure range resulting from the used masses; pressures (in bar) from the used masses (30, 40, 50, and 60 kg) are 0.95, 1.27, 1.59, 1.91 bar, and the 2.23 bar is resulting from the 70 kg.

In each of the sections below (5.3, 5.4, 5.5), each for a soil texture, the procedure followed for measuring the shear strength values of the tested texture is presented. The sections embed shear strength results with analysis.

The direct shear test machine used (ELE 26-2112/01), Figure 5.1, is connected to a computer, and through a software, the applied shear stress and the resulting shearing displacement are recorded relying on the sensors installed on the machine (shear force and displacement sensors).

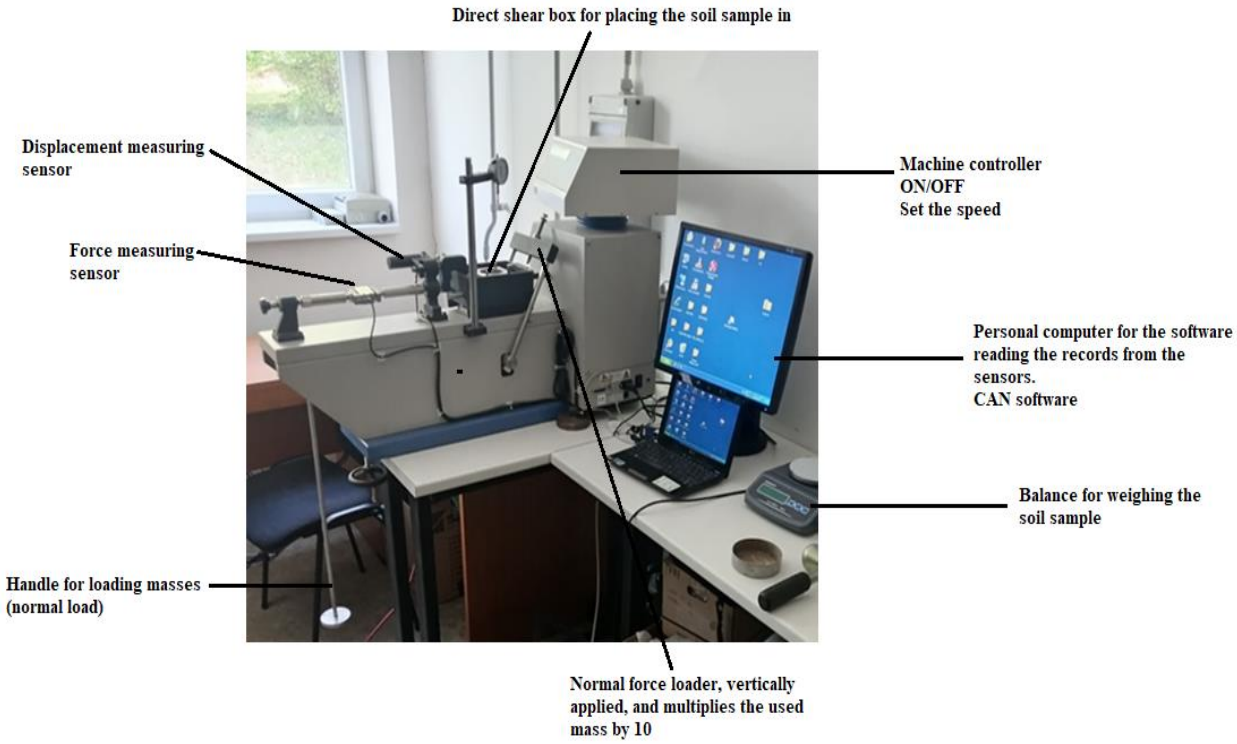

Fig. 5.1. Direct shear test (ELE 26-2112/01).

The used direct shear test contains a microprocessor control that adds to the machine features, as pausing and speed reset during test. Of an LCD screen display with a sensitive keyboard. Speed range, 0.00001 to 9.99999 mm/min. Set of weights (summing 50 kg) comes with the machine, used on the loading system. Maximum vertical load is 10 kN, applied using 10:1 lever ratio. Maximum shear force is 2.3 kN. Maximum shear displacement is 10 mm. Height of the shear box filling space is 36.8 mm (measured by the researcher using Vernier caliper). Diameter of the shearing box is 63.3 mm (measured by the researcher). Diameter of the shear box covering plate is 62.6 mm (measured by the researcher).

5.3 Loam sand soil shear strength (with parameters) measuring procedure

In measurements on loam sand soil samples at different moisture contents, the cohesion and the internal friction angle were obtained relying on the Mohr-Coulomb line. Even though the shear strength can be obtained under a consolidation stress at a shearing speed (relatively higher

speed), but when it comes to using shear strength results (under different normal stresses) for drawing the Mohr-Coulomb line, wrong (unrealistic) strength parameters might be obtained. Based on empirical work and with many trials, convincing results were obtained, achieved by consolidating the soil in direct shear box for few seconds using a mass that is higher than the maximum load (stress) used for fitting the Mohr-Coulomb line, thus making the loose soil with an OCR value above 1. The soil was consolidated with a high mass, maximum mass to be used in the measurement is 60 kg, thus a 70 kg was used for initial consolidation. The cohesion is built up under the 70 kg, and is of a value close to the cohesion that is built up under the lower masses (used for Mohr-Coulomb linearity). The masses 30, 40, 50 and 60 kg were used for drawing the Mohr-Coulomb line.

The initial status of the soil per each measurement was fixed by fixing its soil mass and marking its initial height in the shear box (initial volume is fixed before applying the initial 70 kg mass). For each shear measurement carried out on a sample (at a moisture content), the soil mass and its initial thickness were fixed in the direct shear box to 110 g and 2.38 cm, thus soil of initial density 1.46 g/cm^3; density before normal consolidation. The 70 kg mass is applied for few seconds, and then replaced by the shearing mass, applied during shearing the soil (each, 30, 40, 50 and 60 kg). The obtained results of the cohesion and the internal friction angle, both have ended up with logical tendency as function of moisture content. For the tested soil, the internal friction angle is decreasing with the increase in the moisture content, while the cohesion is increasing with moistening. Figures 5.3, 5.5 and 5.6 show the shear strength values as function of moisture content. Measurements were carried out on the tested soil at moisture contents 1.05, 3.07, 6.91, 9.02 and 12.52 % mc. For the completely dry soil sample, no water added, instead of 70 kg being used, a 100 kg (319.54 kPa) was initially used for compacting the soil for 7 minutes (chosen time) before running the machine.

Sieved dry soil is supposed to be of zero cohesion, since the particles are separted. For ending with accepted cohesion result (close to zero) on this soil, it was compacted initially by higher mass for a longer compaction period (just in dry soil case).

The initial status of the soil before moistening is sieved soil (loose), then moistened reaching a required moisture content by stirring till becoming of uniform face.

5.3.1 Loam sand soil shear strength (with parameters) results

Results recorded by the sensors installed on the machine are imported to the computer. For simplifying reaching the maximum force recorded by the sensor when shearing the soil, which based on it the shear strength can be calculated, the shear force-displacement curves of the tested samples (different moisture contents) were drawn.

Figure 5.2 shows the shear force-displacement curves of the tested loam sand soil at different moisture contents having the same shearing speed applied. The curves shown at a moisture content (at one moisture value) in Figure 5.2 are the shear force-displacement curves under different consolidation stresses (normal stresses). The consolidation masses/stresses used at a moisture content (new soil sample for each applied stress; stress is the applied load (N) divided by the area of the shear box covering plate, of area 0.00307 m^2) are shown in the legend.

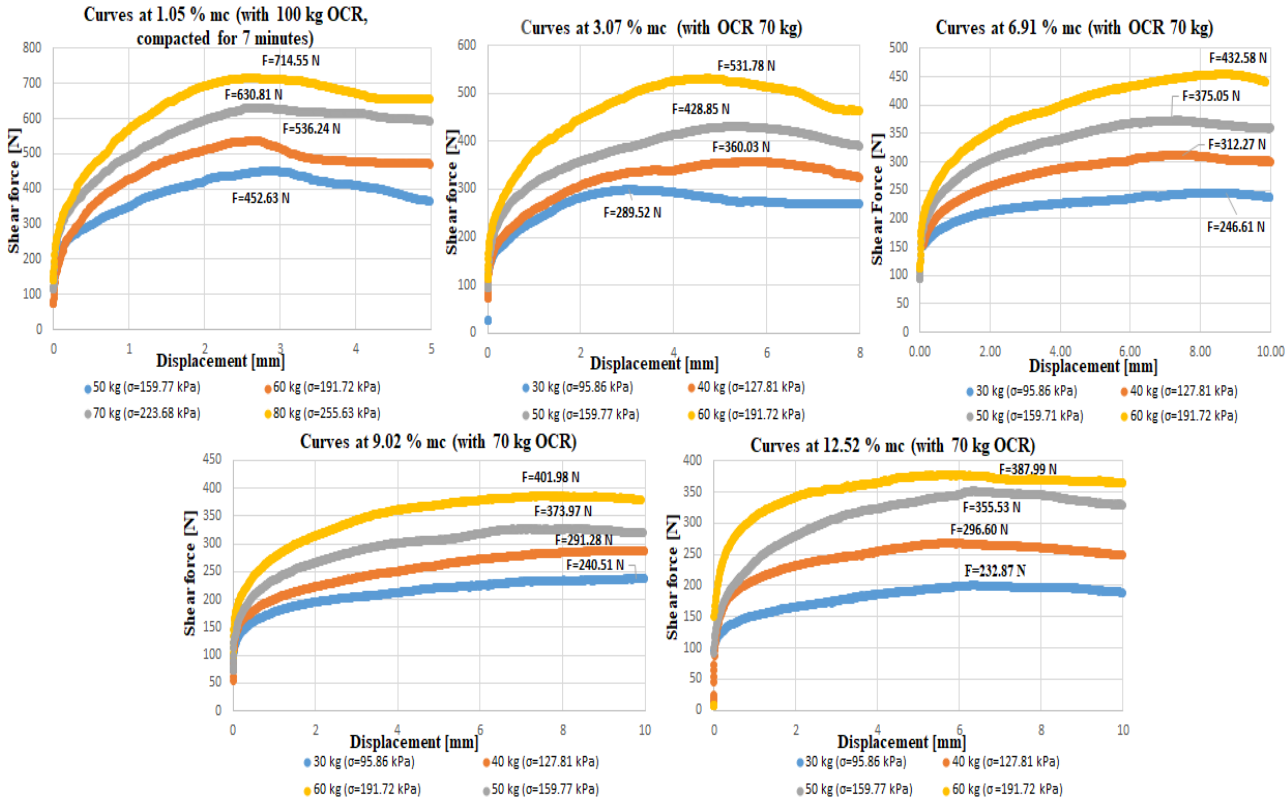

Fig. 5.2. Shear force-displacement curves of the tested loam sand soil under different consolidation stresses, at different moisture contents.

At each of the above moisture contents, it is clear that with the increase in the applied normal stress value, the peak shear force increases. For example, at 1.05 % mc, under 50 kg (159.77 kPa) applied mass the shear force is 452.63 N, while the shear force under 80 kg (255.63 kPa) is 714.55 N.

In Figure 5.2, it is recognized that heavier masses were used when having the soil dry compared to the rest, and also a heavier mass (100 kg) was applied for achieving the OCR.

In order to understand what is happening to the shear strength with the increase in the moisture content, the peak force was converted to shear strength (divided by area) and plotted as function of moisture content, considering the 30 kg consolidation mass (taking one mass as an example). New measurement was carried out on the soil when dry under 30 kg (with 70 kg applied initially), so that all plotted results will be consistent (under 30 kg). Figure 5.3 shows the shear strength results as function of moisture content. Same initial condition in this plot, and is that the soil experienced a compaction load 70 kg (for few seconds) before setting the 30 kg load (applied while shearing). The soil was tested at the following moisture contents, 1.05, 3.07, 6.91, 9.02 and 12.52 % mc.

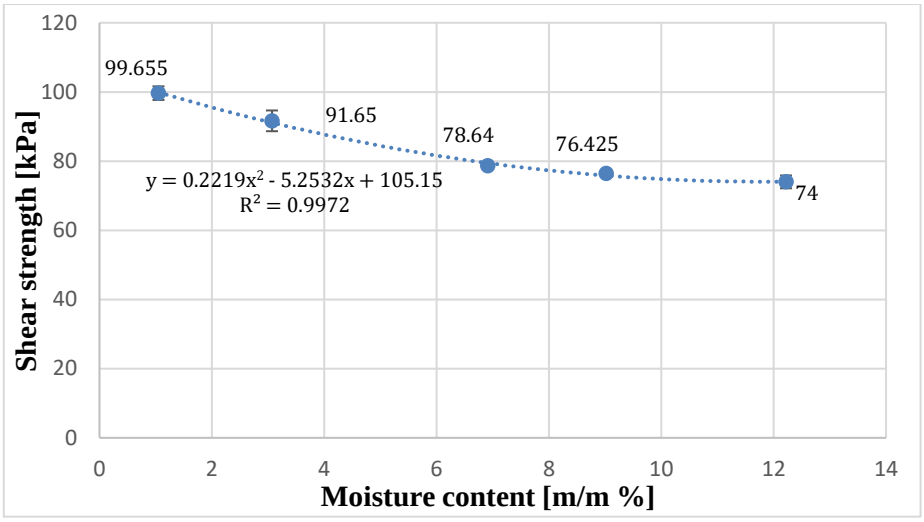

Fig. 5.3. Loam sand soil shear strength as function of moisture content (70 kg/223.68 kPa initially applied load/stress, and 30 kg/95.86 kPa is used with shearing).

Knowing that this soil is neither frictional nor cohesive, and that it embeds both sand (coarse) and clay (fine) particles, with moistening, physically cohesion is built up, with friction at the particles' level (contact friction and interlocking).

The shear strength parameters are required as inputs in terramechanics models used for vehicle mobility study case/s, where most of these models are basically built based on the Mohr-Coulomb model.

The tested soil Mohr-Coulomb line results are shown in Figure 5.4 (moisture contents, are mentioned on the graphs), and the shear strength parameters' results are shown in Figure 5.5 and 5.6. The consolidation stresses considered for drawing the Mohr-Coulomb line are from the masses, 30, 40, 50, 60 kg. For having the soil dry, heavy masses were used with 100 kg initial compaction, and the masses used are 50, 60, 70 and 80 kg (check masses in Figure 5.2).

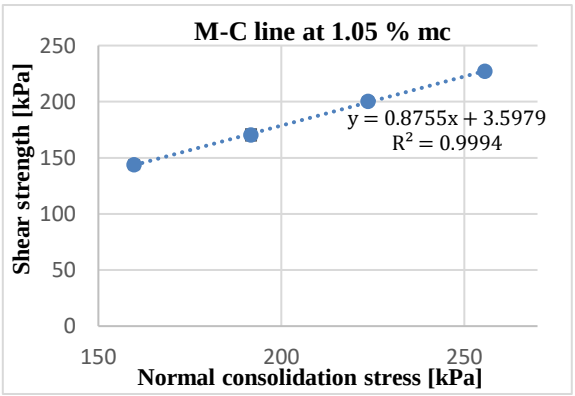

(a)

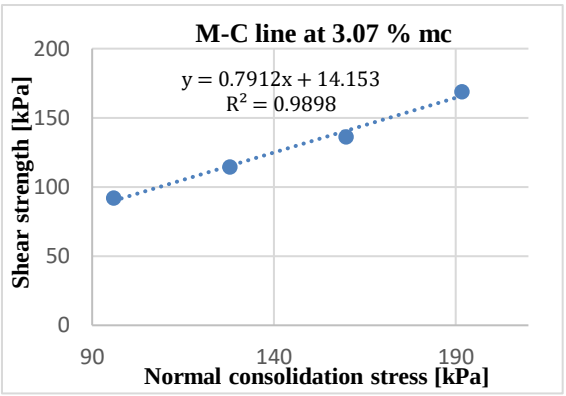

(b)

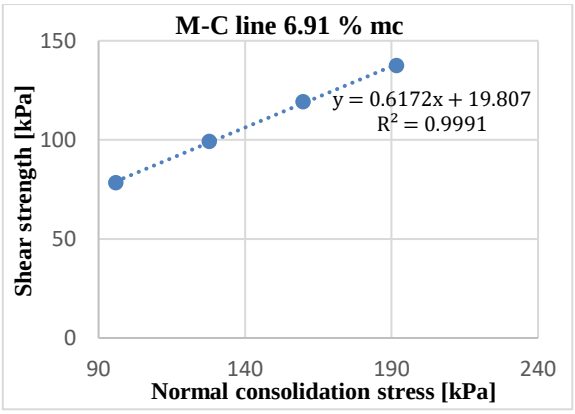

(c)

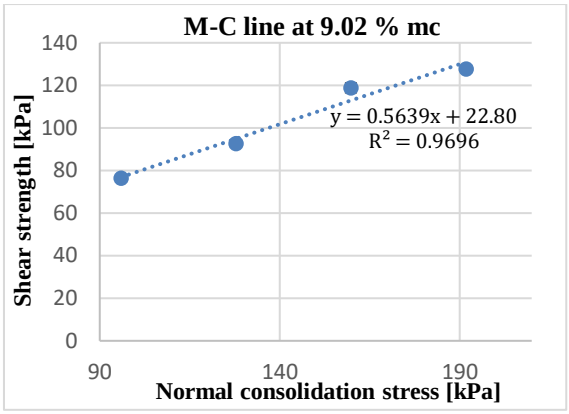

(d)

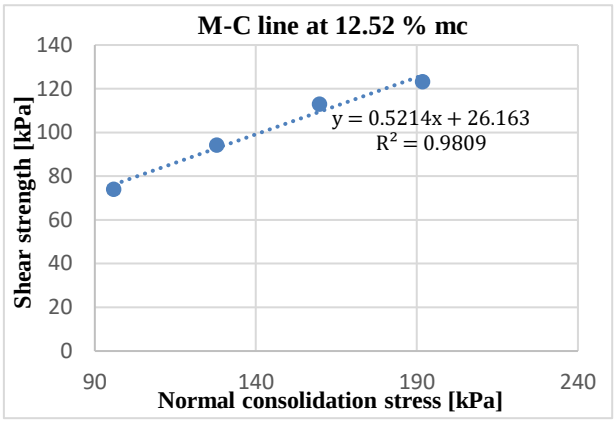

(e)

Fig. 5.4. Tested loam sand soil Mohr-Coulomb (M-C) line at different moisture contents (for the dry soil, at 1.05 % mc, the initial load/stress used is 100kg/319.54 kPa, and at the other moisture contents, the initial load/stress used is 70kg/223.68 kPa).

In Figure 5.4, (a) shows that the shear cohesion of the soil when dry is equal to 3.59 kPa. Fitting a line into the shear strength results having the soil dry is not so accurate, since the soil particles are separated (move freely while shearing), the reason behind choosing the best results for fitting a line with approximately zero cohesion. Trying to end up with precisely same shear strength results having the soil dry with measurement repetition, is not easily achieved (unbonded particles pile over each other in different manners), the reason for choosing higher masses on dry soil samples (more consolidation while shearing).

The cohesion obtained from the Mohr-Coulomb line is not the real physical cohesion of the soil which reflects the cohesive physical status. The physical cohesion is obtained using the cohesion wedge test. The cohesion that is obtained from the shear test is known by the shear cohesion and is in direct connection with the physical cohesion. When it comes to soil shearing, the actual cohesion (physical cohesion) forms the initial stress (compressive stress) acting on the shearing cohesion (Yokoi, 1968). In terramechanics science, scientists rely on the shear cohesion value to be substituted in mobility proposed models. As mentioned before, that most of the vehicle locomotion models are built based on the Mohr-Coulomb equation, which embeds the cohesion as shear cohesion term. Since the physical cohesion forms the initial stress acting on the shear cohesion, then the increase in the shear cohesion (with increasing the moisture content) shows that there is increase in the initial stress acting on the shear cohesion, which is increase in the soil physical cohesion. The shear cohesion and the internal friction

angle results of the tested soil are shown in Figures 5.5 and 5.6, plotted as function of moisture content.

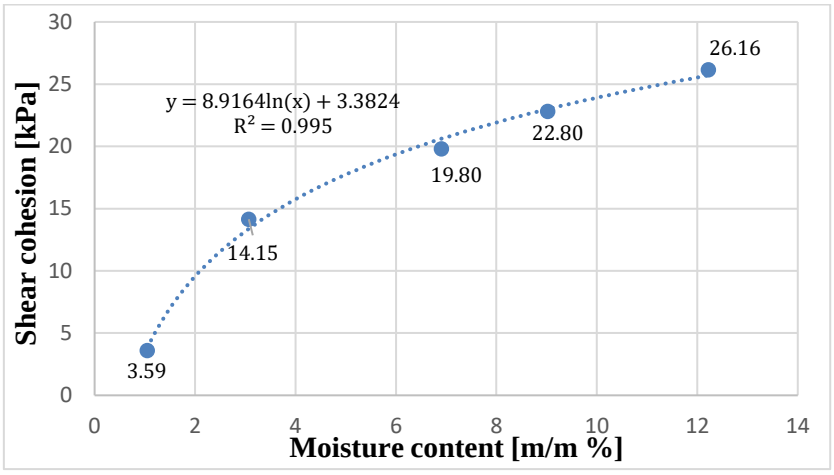

Fig. 5.5. Loam sand soil shear cohesion as function of moisture content.

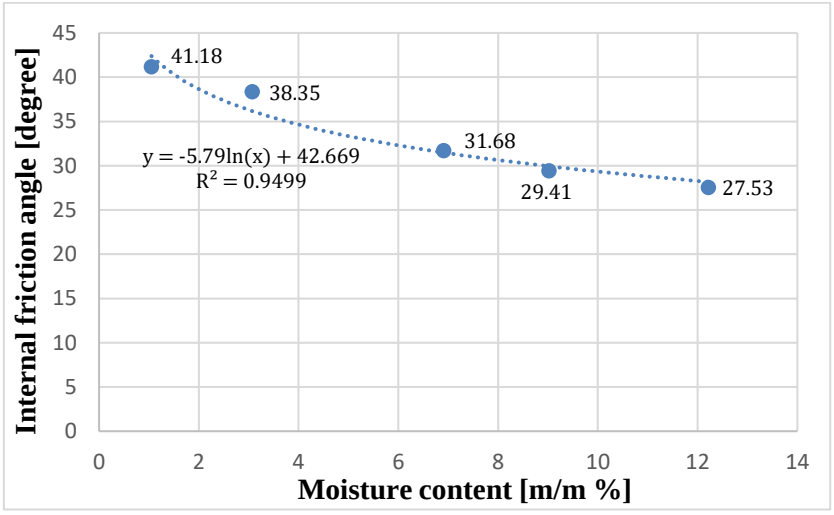

Fig. 5.6. Loam sand soil internal friction angle as function of moisture content.

5.3.2 Discussion on the loam sand soil shear strength (with parameters) results

In Figure 5.3, the shear strength under 30 kg mass as function of moisture content, the curve shows that with the increase in the moisture content, the shear strength is decreasing. The shear strength is weakening with the increase in the moisture content.

For the shear strength parameters, with the increase in the moisture content, the shear cohesion is increasing reaching a peak at the maximum moisture value reached. This result complies with how the soil is changing physically with the increase in the moisture. Initially the soil is dry and sieved with approximately neglected cohesion value (particles' dismantled), physically with moistening the soil it is showing cohesive behaviour, the case that complies with the numerical cohesive results (the increasing tendency).

For the internal friction angle, the angle is decreasing with the increase in the moisture content, these results comply with the physical behaviour of the soil. Having the soil dry, the particles are of weak bonding, besides that the particles are not hydrated. The unhydrated particles will increase the friction when the particles' surfaces contact each other, also the weak bonding will

lead to the movement of the particles in excessive way compared to when bonded, the case that will lead to the particles interlocking each other. With moistening, particles get hydrated, thus decreasing the contact friction, also particles bond to each other leading to decreasing its movement.

In the tested loam sand soil and sand soil (section 5.4) textures, the maximum reached moisture content is around 12 % moisture content, considering that till this moisture content, the soil is still holding a strength to resist the shearing, since at high moisture values the soil becomes of weak strength (entering the weak stage beyond a critical moisture content that depends on the texture). Beyond a critical moisture content, the water starts acting as a lubricant weakening the friction term, in addition to that the water film breaks the bonding between the particles. When it comes to vehicle mobility study case, the range till 12 % moisture content (in the loam sand and sand soil measurements) is considerable range for studying the strength values. In the silty clay soil (section 5.5), the moisture range is wider due to the strong cohesion of the soil, and the reached value in the measurements is around 17 % mc.

5.4 Sand soil shear strength (with parameters) measuring procedure

The tested soil is of sand type, of mechanical composition (2.21 % clay, 2.12 % silt, 95.68 % sand). The shear strength values were obtained at different moisture contents. Starting with the soil at ambient conditions, the moisture is due to the surrounding humidity, and by adding water, the soil was moistened. For each shear measurement carried out on a sample (at a moisture content), the soil mass and its initial thickness were fixed in the direct shear box (110 g and 2.38 cm, thus of initial density 1.46 g/cm^3; density before normal consolidation).

After placing a sample in the box, the soil was compacted by initial compaction load (mass used 70 kg, but not on dry samples) for few seconds, and then the required measuring load was applied (removal of 70 kg and applying the normal load required during shearing). The shear strength results of the soil at a moisture content were obtained at different consolidation stresses (new sample for each consolidation stress).

The masses used for changing the consolidation stresses are 30, 40, 50 and 60 kg. Drawing the Mohr-Coulomb line relying on the obtained shear strength results at the different consolidation stresses, will lead to obtaining the shear strength parameters.

5.4.1 Sand soil shear strength (with parameters) results

Figure 5.7 shows the shear force-displacement curves of the tested sand soil at different moisture contents having the same shearing speed applied. The curves shown at a moisture content (at one moisture content) are the shear force-displacement curves under different consolidation stresses. The consolidation masses/stresses used at a moisture content (new soil sample for each stress applied) are shown in the legend.

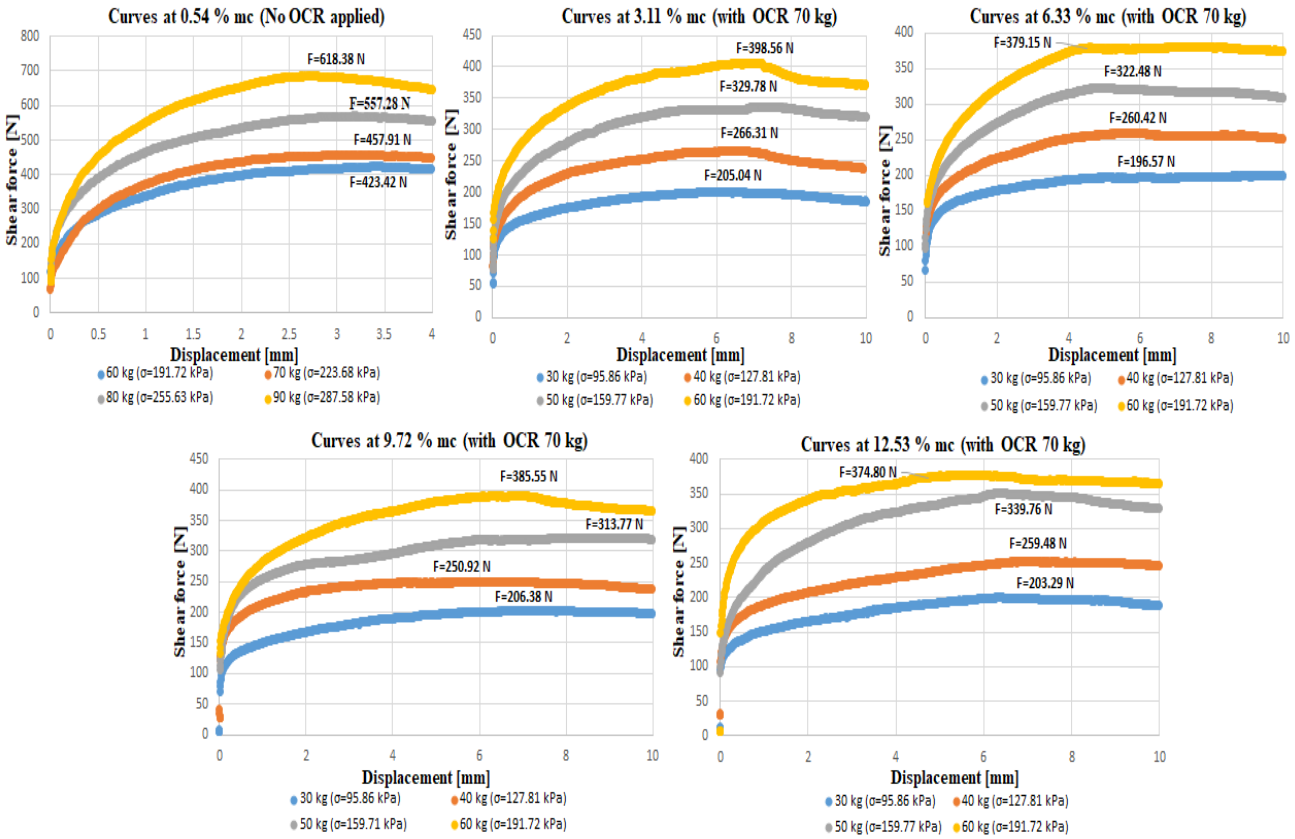

Fig. 5.7. Shear force-displacement curves of the tested sand soil under different consolidation stresses, at different moisture contents.

At each of the above moisture contents, it is clear that with the increase in the applied stress value, the shear force increases. For example, at 0.54 % mc, under 60 kg applied mass (191.72 kPa), the shear force is 432.42 N, while the shear force under 90 kg applied mass (287.58 kPa) is 618.38 N.

In Figure 5.7, it is recognized that heavier masses were used when having the soil dry compared to the rest, and also no heavy mass is applied initially for achieving an OCR value above 1 (that is why, no OCR applied - based on empirical work, is mentioned above the dry curves, but in fact it is equal to 1, since the mass applied initially is similar to the used while shearing). For the rest moisture contents, a 70 kg was used for achieving the OCR above 1.

Dealing with a soil (loose particles) when dry for finding its shear strength parameters, is dependent on its texture, that is why there is difference in the initial mass for the overconsolidation ratio when comparing the sand soil to the loam sand soil (in the previous chapter, 5.3). The method is reached based on empirical work for ending with a cohesion of low value, a realistic value that complies with the physical status of the soil, loose soil.

In order to understand what is happening to the shear strength with the increase in moisture content, the shear force was converted to strength, divided by the shear area, and plotted as function of moisture content (under 30 kg consolidation mass).

Figure 5.8 shows the shear strength results. Initially the soil experienced a compaction load 70 kg (also when dry, just here, for unifying the conditions of this diagram) before setting the 30

kg load (applied while shearing). The soil was tested at the following moisture contents, 0.54, 3.11, 6.33, 9.72, and 12.53 %.

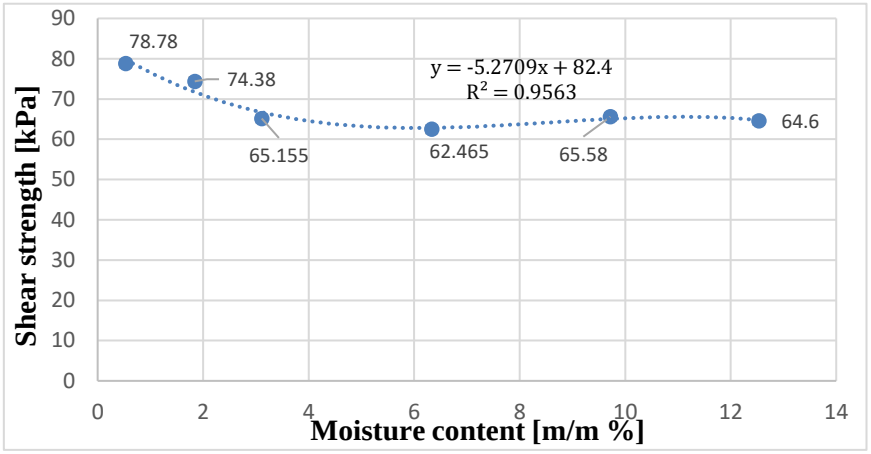

Fig. 5.8. Shear strength of the tested sand soil as function of moisture content (70 kg/223.68 kPa initially applied load/stress, and 30 kg/95.86 kPa is used with shearing); shear strength at 1.84 % is included in the figure.

The equation in the figure belongs to the decay in the shear strength (moisture content, 0.54 % to 3.11 %), since the beyond shear strength is approximately constant.

Knowing that this soil is a frictional soil, the results have shown that with moistening the soil, an apparent cohesion is built up. The term apparent is given to the cohesion, because with the drying of the sand soil, the cohesion decreases, reaching a zero or a neglected value, approximately a total breakdown in the soil particles, the case which is different than when having clay or loam sand soil for example. With reaching high moisture contents in both soils (clay and loam sand), then the drying completion, the particles remain well bonded to each other requiring a force for breaking down the bonding.

The tested soil Mohr-Coulomb line results are shown in Figure 5.9 (moisture contents are mentioned in the graphs), and the shear strength parameters' results are shown in Table 5.2. Tables are used here since the results are close (no significant change), but also the results will be plotted for fitting curves. For the soil at moisture contents beyond 3.11 %, the consolidation stresses considered for drawing the Mohr-Coulomb line are from the masses, 30, 40, 50, 60 kg. Having the soil dry, the masses used are 60, 70, 80 and 90 kg.

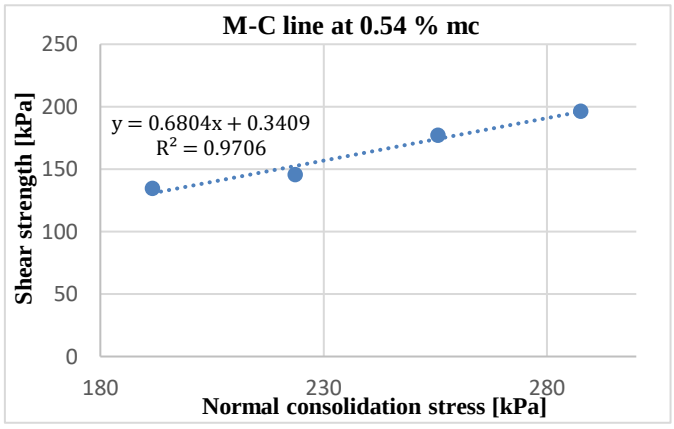

(a)

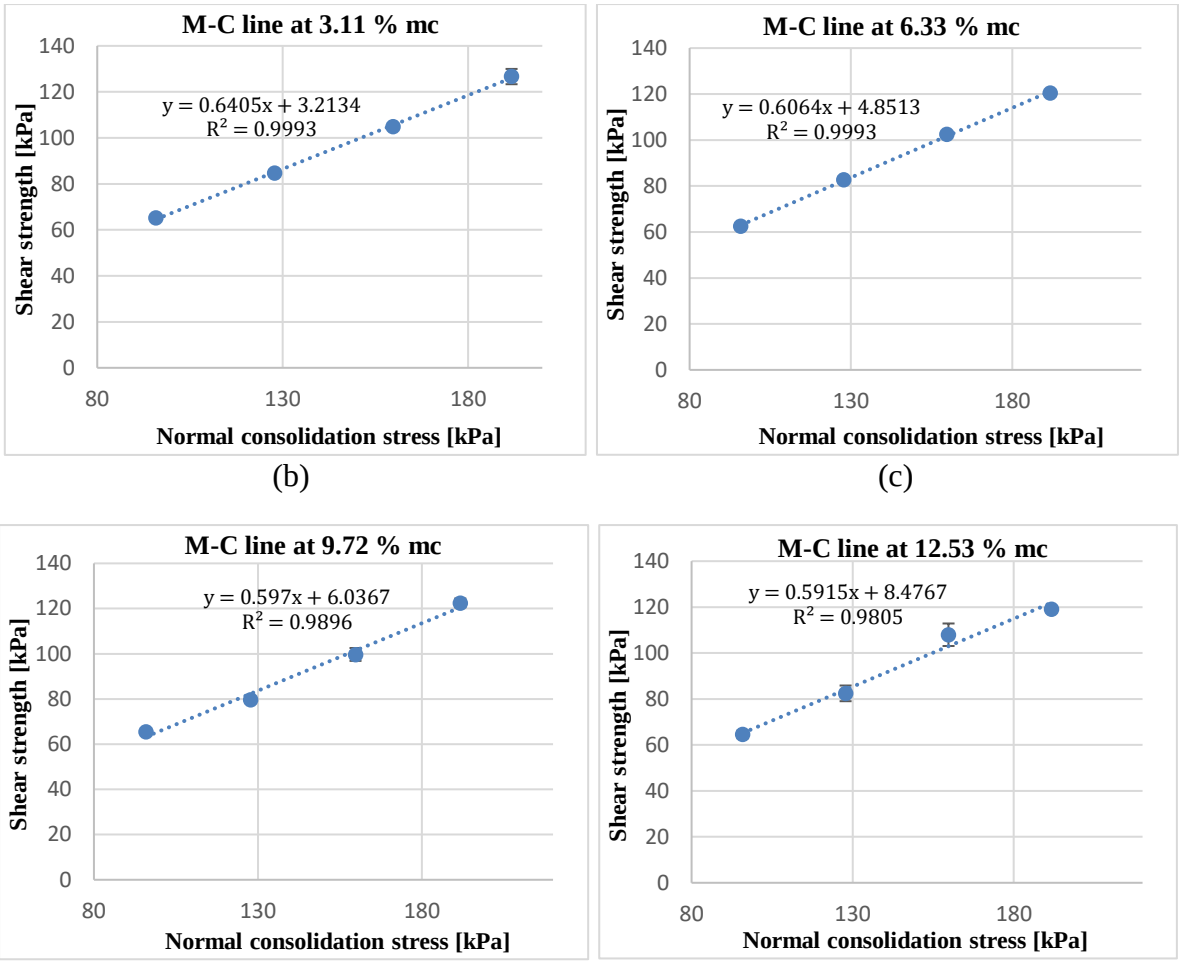

Fig. 5.9. Tested sand soil Mohr-Coulomb line at different moisture contents (for the dry soil, at 0.54 % mc, no higher mass was used, OCR=1, and at the other moisture contents, the initial load/stress used is 70kg/223.68 kPa).

In Figure 5.9, (a) shows that the shear cohesion of the soil when dry is equal to 0.34 kPa. In the work below, the cohesion at 0.54 % mc is considered approximately equal to zero. Having the soil dry at 0.54 %, and considering the cohesion is of null value, also knowing that the shear strength under the 30 kg (95.86 kPa) consolidation stress is 78.78 kPa (Figure 5.8), the internal friction angle can be calculated from the Mohr-Coulomb linear equation. Using the Mohr-Coulomb equation to calculate the internal friction angle, the resulting friction value is 39.41 degree. The sand soil is a frictional soil, thus shows its maximum friction behaviour when dry compared to when moistened. Comparing the friction results in Table 5.2 at different moisture values, having the soil dry (0.54 %) shows that the friction is at its maximum value (39.41 degree).

Table 5.2. Sand soil shear cohesion and internal friction angle as function of moisture content (0.54, 3.11, 6.33, 9.72, 12.53 %).

Moisture content [m/m %]	Shear cohesion [kPa]	Internal friction angle [degree]
0.54	~ 0	39.41
3.11	3.21	32.63
6.33	4.85	31.23
9.72	6.03	30.83
12.53	8.75	30.42

Plotting table 5.2 results in coordinate systems (abscissa and ordinate) aiming to see graphically how the tendency is changing, the shear cohesion and the internal friction angle as function of moisture content are shown in Figure 5.10.

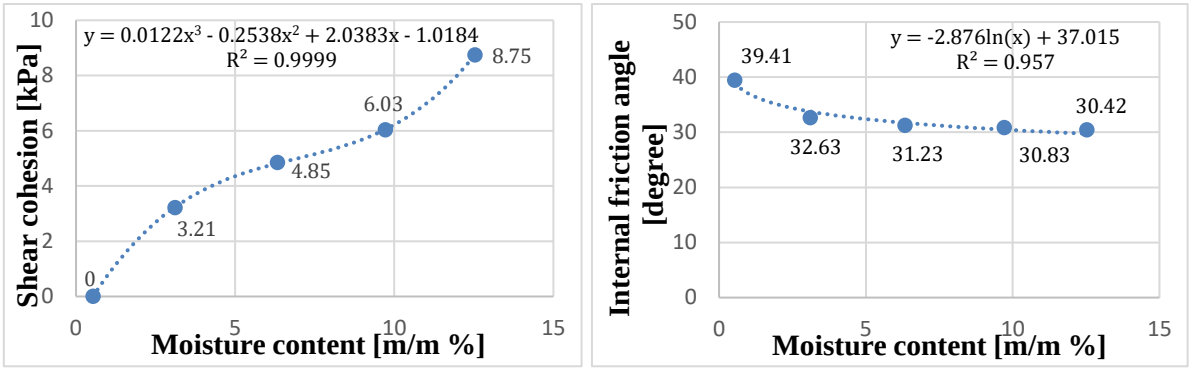

(a) (b)

Fig. 5.10. (a) Sand soil shear cohesion as function of moisture content, (b) internal friction angle as function of moisture content.

5.4.2 Discussion on the sand soil shear strength (with parameters) results

Having a look at the mechanical composition of the tested soil, the sand occupies the highest portion in the texture, these coarse particles lead to the frictional behaviour of the soil. The presence of the small clay and silt percentages (around 2 %) shouldn't have big influence on the cohesion resulting with moistening the soil. Dealing with the soil as approximately pure sand and not taking precisely the influence of the small silt and clay portions on the strength of the soil, the discussion on the tested sand soil shear strength behaviour is given in this section.

The small portion of the silt and clay might be playing a role in keeping the particles bonded when having the compacted moistened sample dried, thus a small excitation force is needed (when dried) for breaking down the sample to separated particles. In some sand soils, as on the shore, when soil is moistened, the soil crumples on each other when captured by hand, but as soon as the soil becomes dry, the structure breaks down alone to separated particles.

With the increase in the moisture content from 0.54 % to 3.11 % mc, the shear strength of the soil decreased from its maximum value, 78.78 kPa, having the soil dry, to a value around 65 kPa. Beyond the moisture content 3.11 %, the shear strength remains of a value around 65 kPa. The measurement was carried out till 12.53 % mc, at which the shear strength result is 64.6 kPa (shear strength results shown in figure 5.8).

It is not easy to end up with precise shear strength parameters (approximately same with repetition) at a moisture content. Results to be used for plotting the Mohr-Coulomb line should be based on averaging the obtained shear strength results at each consolidation stress. Averaging the results will lead to changing the slope and the offset of the line between a measurement and another, the case that will not lead to fixed strength parameters. The soil is a particulate material, and its behaviour is influenced by different factors. Fixing the initial measuring conditions might not end up with accurately the same result upon repetition, but sure a close value. Among the factors influencing the results upon repeating the shear measurement is the unequal density distribution in the soil sample (placed in the shear box), especially at the shearing zone. Despite doing the best for ending with same soil density distribution, but still, this doesn't mean the density is the same at different zones in the sample.

Also dealing with the soil when dry, where there is no cohesion bonding the particles, allows the particles to move freely while shearing and in some cases piling over each other (the case that leads to two peak values on the shear stress-displacement curve, clear on coarse particles soils). This behaviour of the particles (dry soil) while shearing will lead to recognized difference in the shear strength results upon repeating the measurement. These reasons are examples for not ending up with precise shear cohesion and internal friction angle.

In this measurement even though the cohesion results are close, the cohesion (Figure 5.10) was considered in a tendency that occurs on most of the soils, which is the increase in the cohesion with the increase in the moisture content.

Table 5.2 shows that with the increase in the moisture content (disregarding the dry results), the cohesion shows a slight increase in its value, while the internal friction angle shows a slight decrease. The cohesion is increasing from approximately 3.21 to 8.75 kPa, while the internal friction angle decreases from 32.63 to 30.42 degree. The slight increase in the cohesion and decrease in the internal friction angle reflect that the results are approximately equal, since not having a recognized change.

For the internal friction angle, the value at 3.11 % is around 32.63 degree, and with the increase in the moisture content, the value remains approximately constant (around 30 degree).

Table 5.2 results comply with the shear strength tendency of the tested soil as function of moisture content under 30 kg consolidation load, figure 5.3. The stability in the shear strength beyond 3.11 % mc, which is around 65 kPa, is because of the stability in the shear cohesion and the internal friction angle, except for the dry soil, where there is no cohesion and the friction is maximum.

5.5 Silty clay soil shear strength (with parameters) measuring procedure

The tested soil embeds high portions of silt and clay in its texture (relative to the tested soils, sand and loam sand), of mechanical composition (3.34 % sand, 52.05 % silt, 44.61 % clay). The presence of these two soil minerals (in the soil of considered portion) makes the soil cohesive, especially with the increase in the moisture content. The clay particle is of the finest size (among the soil composition particles), then comes the silt. The presence of the small size soil particles will increase the surface area resulting from these particles. With fine particles, more of them (the particles) occupies a specific space when compared to using sand particles (coarse particles, thus more voids). The increase in the amount of the soil particles will increase the summing surface area resulting from the outer surfaces of the particles (each particle is of an outer surface area, then sum the areas). More area surfaces means more polarity between the charges of the water used to moisture the soil and the charges that the surfaces are holding. The increase in the polarity means more cohesion, thus the case that makes the silty and the clay soils of high cohesion when compared to sand soils. The finest the particle (the clay, a soil mineral) is, the highest the cohesion will be. When comparing the two particles' types (or minerals), the silt and the clay, the clay provides higher cohesion keeping the soil particles strongly bonded even when dried, due to the bonding polarity. The strong cohesive bonding resulting with increasing the moisture must lead to decreasing the friction between the particles, since the strong bonding will limit the movement of the particles. At high moisture content the material becomes a paste like material, thus no soil shearing behaviour (no more granular), where the material becomes ductile with high cohesion and null interparticle friction. Reaching the state where the soil becomes paste like material was not considered in the shear strength measurement, considering that it is not applicable in terramechanics study cases, so just dealing with the soil as a granular matter.

The shear strength values were obtained at different moisture contents, starting with the soil of moisture content due to the surrounding humidity. For each shear measurement carried out on a sample (at a moisture content), the soil mass and its initial thickness were fixed in the direct shear box (90 g and 2.88 cm, thus of initial density 0.99 g/cm^3; density before normal consolidation).

After placing a sample in the box, the soil was compacted by initial normal load (mass used 70 kg) for few seconds, and then the required measuring load was applied (removal of the 70 kg, and applying the normal load required during shearing). The shear strength results of the soil at a moisture content (at one moisture content) were obtained under different consolidation masses/stresses (new sample for each consolidation stress).

The masses used for changing the consolidation stresses are 30, 40, 50 and 60 kg. Drawing the Mohr-Coulomb line relying on the obtained shear strength results under the different consolidation stresses, ends up with the shear strength parameters.

Having the soil dry, no 70 kg mass was applied initially, but for providing stability (consolidating the particles) while shearing the loose soil, heavier masses were applied, 50, 60, 70, and 80 kg (70 and 80 are the heavier). This method used on the dry soil ended with accepted shear cohesion that comply with the soil physical status (dry dismantled granular material).

5.5.1 Silty clay soil shear strength (with parameters) results

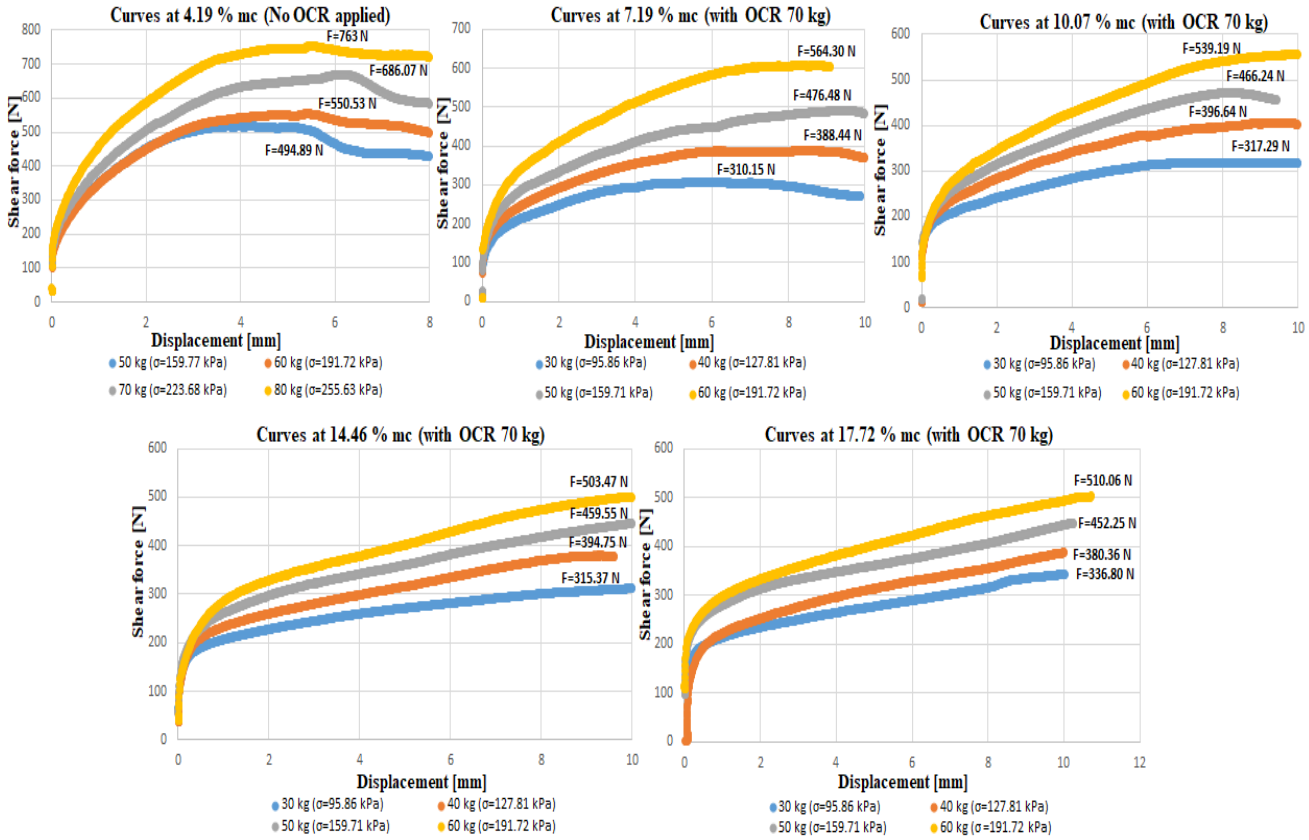

Fig. 5.11. Shear force-displacement curves of the tested silty clay soil under different consolidation stresses, at different moisture contents.

At each of the above moisture contents, it is clear that with the increase in the applied stress value, the shear force increases. For example, at 4.19 % mc, under 50 kg applied mass, the shear force is 494.89 N, while the shear force under 80 kg applied mass is 763 N.

In Figure 5.11, it is recognized that heavier masses were used (50, 60 ,70 , and 80 kg) on the dry soil compared to the rest, and that no heavy mass was applied initially on the dry soil for achieving an OCR value above 1 (that is why no OCR applied is mentioned on dry soil graphs, but in fact it is equal to 1, since the mass applied initially is similar to the mass used for shearing). This result was reached empirically for ending up with low cohesion on dry loose soil. Having the soil moistened, the used OCR is above 1.

In order to understand what is happening to the shear strength with the increase in the moisture value, the maximum shear force under 30 kg normal mass was converted to strength (divided by area) and plotted as function of moisture content.

Figure 5.12 shows the shear strength results under applied consolidation load (from 30 kg). Initially the soil experienced a 70 kg compaction load for few seconds before setting the 30 kg shearing normal load (same on the dry soil, just for this measurement - the shear strength and not the parameters - to compare the results at unified conditions). The soil was tested at the following moisture contents, 4.19, 7.19, 10.07, 14.46, and 17.72 %.

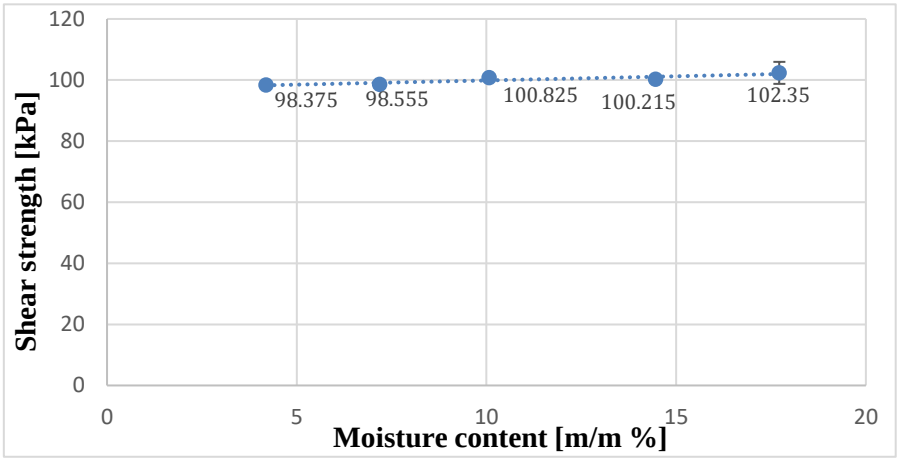

Fig. 5.12. Shear strength as function of moisture content (70 kg/223.68 kPa initially applied load/stress, and 30 kg/95.86 kPa is used with shearing).

In Figure 5.12, under 30 kg applied mass, and at the same shearing speed, the shear strength remains approximately unchanged with the increase in the moisture content. Even though the results show a slight increase in the shear strength, but can be considered approximately constant. The constancy is just on this soil texture among the tested textures in the shear strength measurement (the sand and the loam sand).

The constancy in the shear strength is resulting from the compensation between the shear cohesion and the internal friction angle with moistening. The Mohr-Coulomb equation embeds both, the shear cohesion and the internal friction angle (under normal stress). The two strength parameters, despite one of them is increasing and the other is decreasing, they are changing in a rhythm that keeps the shear strength constant with the increase in the moisture content (results discussed below).

By drawing the Mohr-Coulomb line at the different moisture contents (Figure 5.13), this entitles to plot the shear cohesion and the internal friction angle as function of moisture content.

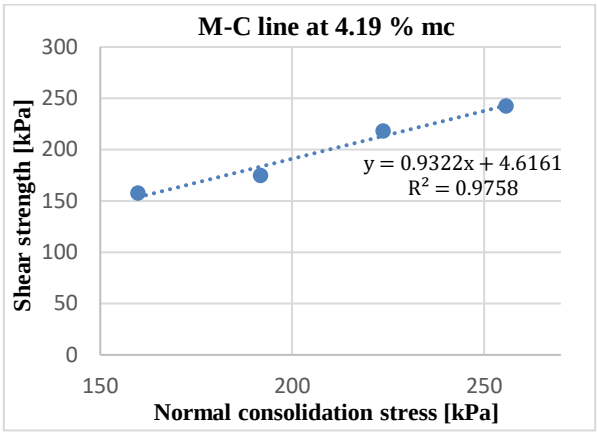

(a)

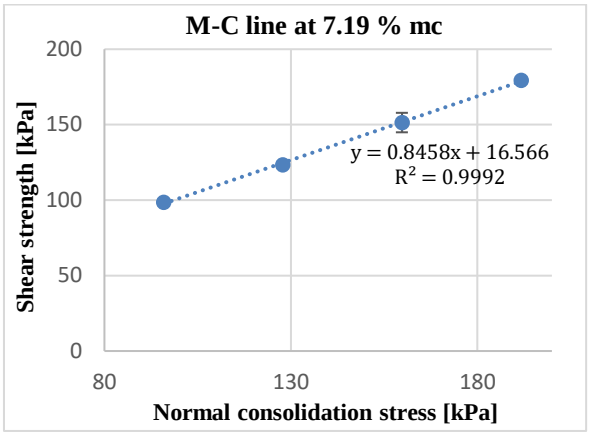

(b)

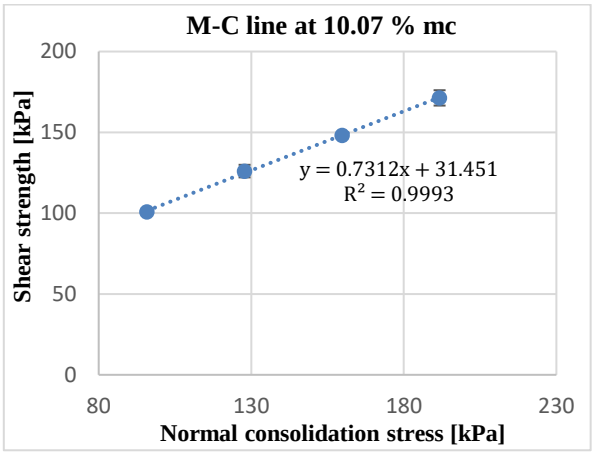

(c)

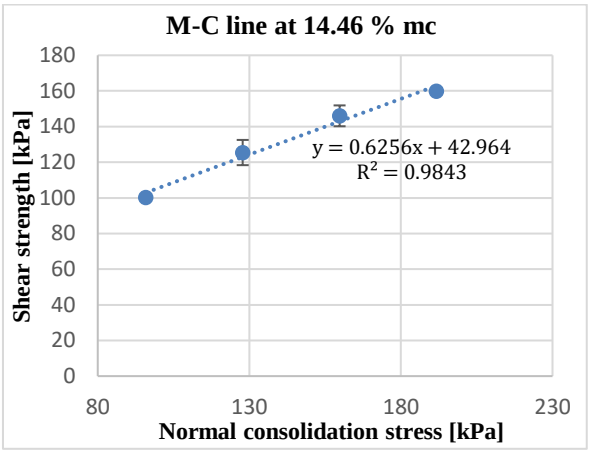

(d)

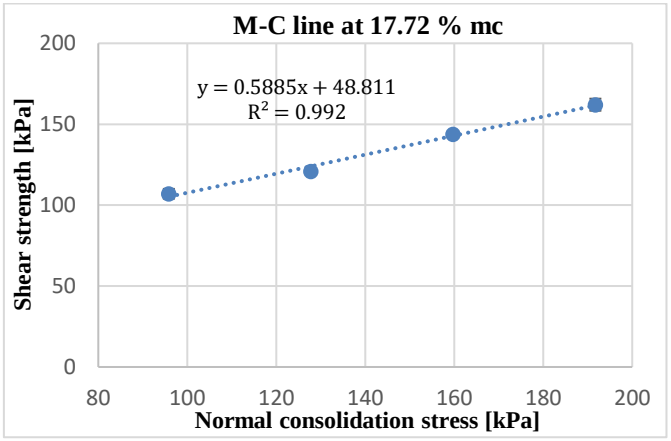

(e)

Fig. 5.13. Tested silty clay soil Mohr-Coulomb line at different moisture contents (for the dry soil, at 4.19 % mc, no higher mass was used, OCR=1, and at the other moisture contents, the initial load/stress used is 70kg/223.68 kPa).

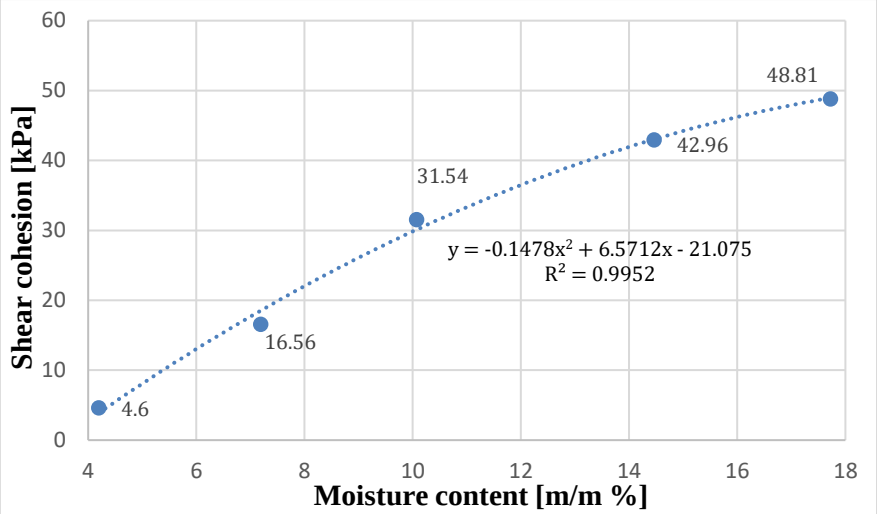

Fig. 5.14. Shear cohesion as function of moisture content.

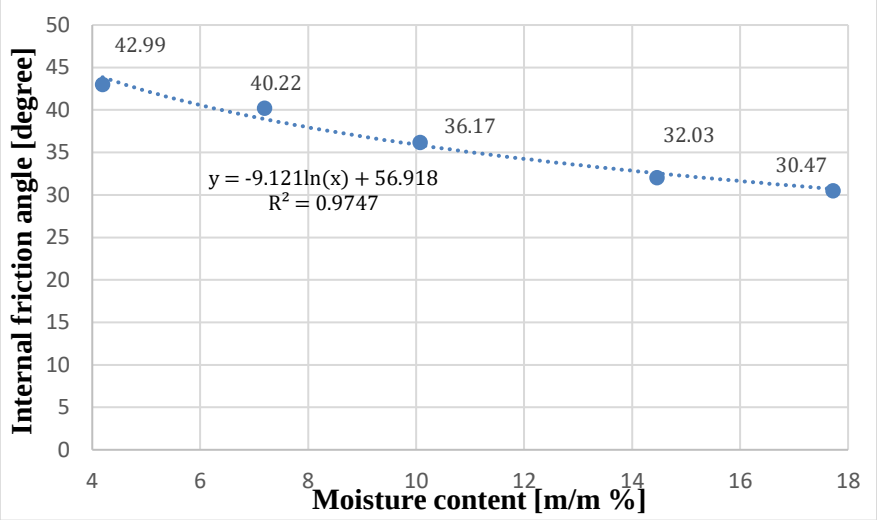

Fig. 5.15. Internal friction angle as function of moisture content**.**

5.5.2 Discussion on the silty clay soil shear strength (with parameters) results

Figure (5.14) shows the shear cohesion results as function of moisture content. With the increase in the moisture content, the shear cohesion increases, applicable till the maximum reached moisture content (at high moisture contents the soil becomes a paste like material, the ignored case, reason mentioned above; check Figures 4.19 and 4.20 for clayey soils physical behaviour at high moisture contents). The shear cohesion tendency complies with the change in the physical behaviour of the soil and with its identity (the clay texture).

For the internal friction angle (Figure 5.15), with the increase in the moisture content, the friction angle decreases, applicable till reaching the maximum considered moisture content. The tendency complies with the physical behaviour of the soil, since the increase in the cohesion limits the interparticles' friction, due to the strong polarity bonding.

Upon having any moisture content provided as input to any of the equations mentioned in the figures (shear cohesion and friction angle), this leads to predicting the parameters at the moisture content used. Using both parameters with the normal stress, the shear strength can be predicted.

Summary of the new approach in the chapter

The important step in this chapter is finding the shear strength, shear cohesion, and the internal friction angle of three soil textures.

Even though finding the shear strength and its parameters using the direct shear test is not a new idea, but the important part in the work is obtaining the results at a speed higher than the speed used in the civil/geo engineering study cases, making the results applicable to be used in terramechanics without difficulties (emulating the study case relative to speed).

The empirical work carried out on each dry loose soil texture for finding accepted shear parameters (null cohesion) that comply with the physical status of the soil, is also an important step.

So, ending with the results in undrained condition (process followed is explained in the chapter), which is not clarified based on checking literatures especially in terramechanics science, is required in vehicle mobility study cases.

6. Soil properties obtained from the colour reflectance

6.1 Shear strength determined from the colour reflectance

As mentioned in the introduction, linking the mechanical properties of the soil to its colour facilitates knowing the infield mechanical properties of the soil from its colour. This work was achieved through laboratory work, and the results should be validated by field measurements. In the case of studying the mobility of a vehicle on a soil terrain, especially for calculating the traction (drawbar pull), some of the shear stress-displacement models require the shear strength and/or its parameters as input data for predicting the traction of the vehicle, as in Ageikin model (shear strength parameters required) shown in Equation 6.1 (Ageikin, 1992), (Ageikin, 1987a), (Ageikin, 1987b), (He et al., 2019).

The shear strength of the soil is calculated using the Mohr-Coulomb model (basic model), having both of the parameters, the shear cohesion and the internal friction angle. This linear Mohr-Coulomb model is the mostly used in terramechanics community. Some scientists worked on modifying this model to fit specific soil types, such as clay soil (Sun et al., 2006), unsaturated soil (Hilf, 1956), and partially saturated soil (Bishop et al., 1960).

The three pioneer scientists that have settled the basics for the development of the shear stress-displacement models are Pokrovski, Bekker, and Janosi (Pokrovski, 1937), (Bekker, 1956), (Bekker, 1969), (Janosi and Hanamoto, 1961).

Oida (1975) proposed a model based on Pokrovski's model that is only applicable on soils that are of shear stress-displacement profile with a hump and residual stress. Certain types of loams are of shear stress-displacement profile having the mentioned characteristic (Wong, 2009).

$$\tau = \frac{1}{\frac{1}{\varsigma c + p\tan(\phi)} + \frac{t_{gr}}{E'.|j|}} \tag{6.1}$$

where:

τ is the shear stress;
j is the shear displacement;
t_{gr} is the grouser pitch;
c is the soil shear cohesion;
p is the average ground pressure;
ϕ is the internal friction angle;
E' is a soil shear parameter;
ς is a model parameter.

This model is not for being used in any of our laboratory measurements or in a field measurement, but it is given as an example on the availability of traction models that require the shear strength parameters as input in field (thus, field onspot calculation), aiming to reach the required (calculated) traction that based on it the performance of a vehicle will be enhanced. So, having the shear strength parameters obtained infield from the colour reflectance, will help in reaching the model result with less time and effort consumed.

Having the equation of the curve fitting the colour reflectance points at 700 nm (section 4, Figurs 4.14-4.18), will help in finding the moisture content of the soil upon substituting the reflectance value in it (new record at 700 nm); thus, the moisture content is obtained.

With the equation of the curve passing through the plotted shear cohesion points as function of moisture content, the shear cohesion can be calculated at the moisture content (predicted from the reflectance). By using the equation of the internal friction angle curve fitting the plotted points, the internal friction angle is obtained at the predicted moisture content. The same process is applicable on the shear strength plotted as function of moisture content (under a normal consolidation stress). Figure 6.1 flowchart shows the correlation process/methodology.

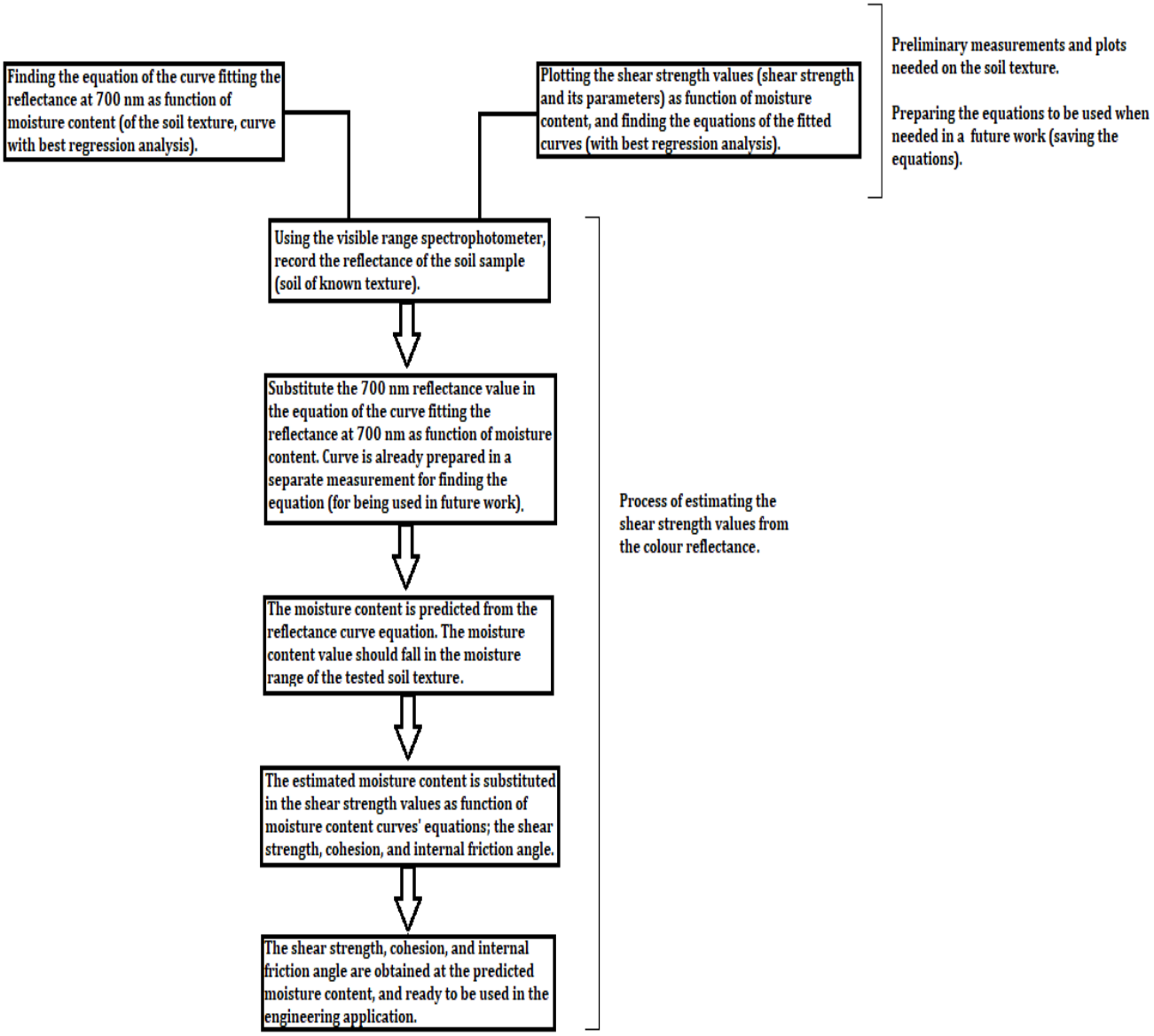

Fig. 6.1. Flowchart showing the process followed for predicting the shear strength values from the colour reflectance.

An example is given on one of the tested soils regarding finding the shear strength and the parameters from the reflectance. Considering the loam sand soil for this example, back to section (colour validity section), relying on the curve equation (section 4.6, Figure 4.22 and

Equation 4.3), the estimated moisture value is 5.07 % mc. The 5.07 % mc is substituted in the loam sand soil shear strength curves' equations (section 5.3.1, Figures 5.3, 5.5, and 5.6).

The strength equations of the loam sand are the following equations, under the condition that the soil is tested as loose soil.

The shear strength equation (under 30 kg mass) as function of moisture content (Figure 5.3) is:

$$Y_1 = 0.2219x^2 - 5.2532x + 105.15 \quad (6.1)$$

The shear cohesion equation as function of moisture content (Figure 5.5) is:

$$Y_2 = 8.9164\ln(x) + 3.3824 \quad (6.2)$$

The internal friction angle equation as function of moisture content (Figure 5.6) is:

$$Y_3 = -5.79\ln(x) + 42.669 \quad (6.3)$$

Solving for the input moisture value (5.07 %, estimated from colour),

$Y_1 =$ 84.22 kPa , $Y_2 =$17.85 kPa , $Y_3 =$ 33.26 degree.

The above work clarifies the correlation process between the colour reflectance and the shear strength values of a soil texture. The same process is applicable on other textures, following the same steps.

By having these values obtained, they can be substituted in a vehicle performance model, ending with the required performance value.

Each shear strength value with the colour reflectance as function of moisture content, the two curves are combined in one figure (Figures 6.2, 6.3, and 6.4). In each of the combined curves figures, upon providing one property as input, the other properties are obtained.

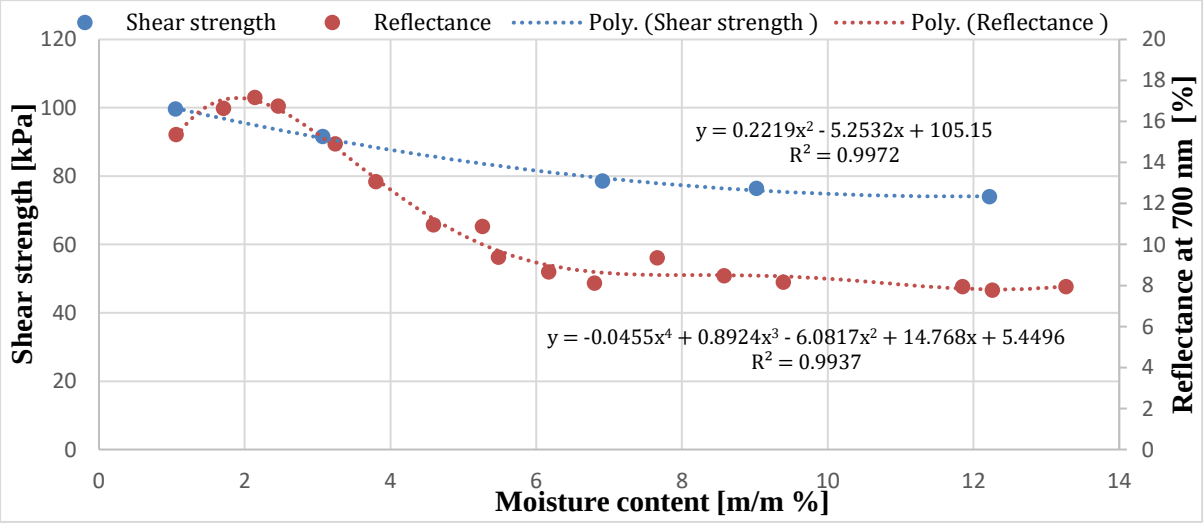

Fig. 6.2. Both curves, the shear strength and the colour reflectance as function of moisture content, are combined in one figure.

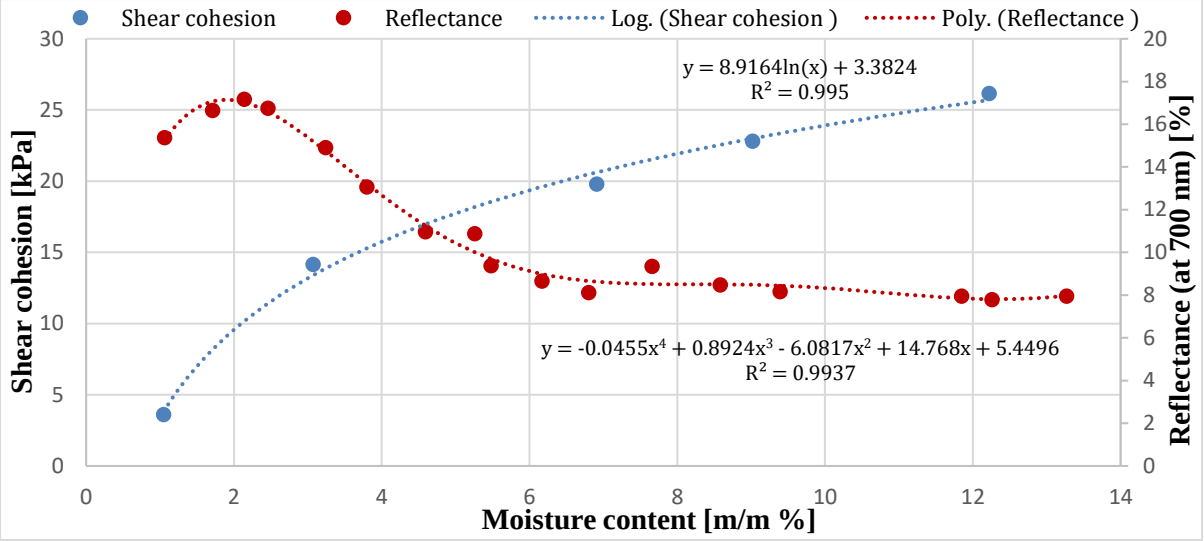

Fig. 6.3. Both curves, the shear cohesion and the colour reflectance as function of moisture content, are combined in one figure.

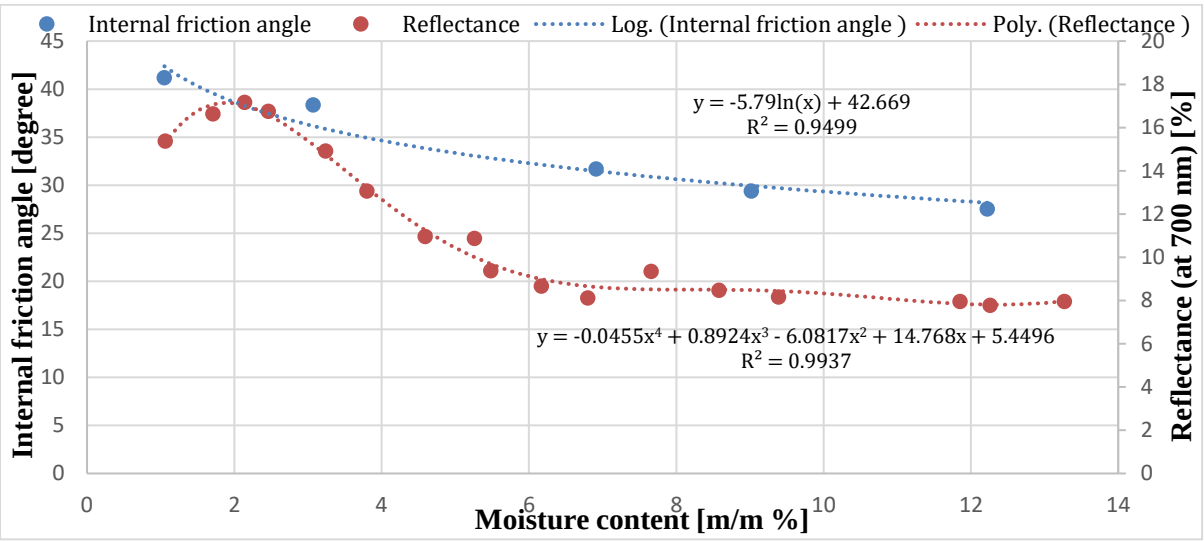

Fig. 6.4. Both curves, the internal friction angle and the colour reflectance as function of moisture content, are combined in one figure.

6.2 Soil moisture content predicted from the colour reflectance *(field test using the reliable equation, thus field validation)*

As mentioned in the previously in the text, that as a major step for relating the soil mechanical properties (shear strength and parameters in my work) to the colour of the soil (spectral behaviour), the reflectance must be related to the moisture content. Both should be prepared, the change in the colour reflectance as funtion of moisture content and the change in the mechanical properties as function of moisture content. Since having the moisture content in common, so it is the major property to be estimated from the reflectance before identifying the required mechanical strength value of the soil. With different trials to relate the colour to the moisture of the soil, through plotting different reflectance parameters, finally it ended that the reflectance at 700 nm as function of moisture content will serve in ending up with the reliable curve for identifying the moisture content from the reflectance.

The colour measurements were carried out on five soil textures, and for each of the tested textures, the validity of its relation (the equation) for estimating the moisture content from the 700 nm curve was checked (check chapter 4).

The colour work was performed dealing with the soil as sieved soil, thus visually homogeneous material with no impurities affecting the measurement.

With validating the colour reflectance equation of each soil having the soil as a visually homogeneous material, the validity has ended with convincing moisture content result of low difference percentage relative to the gravimetric result (percentage of each soil in chapter 4).

In the field, the case is totally different compared to the laboratory work, such as the presence of vegetation and rocks or stones. The question that arises here is, if this work will be applicable in field.

In a separate measurement, one soil type was checked in field and is the loam sand soil, the university's land soil, in Gödöllő. The carried out reflectance measurement deals directly with the soil (spectrophotometer lens is in direct contact), and not a measurement through the vegetation, so before carrying out the field measurement, a spot was prepared by removing the vegetation and the impurities. The soil in this spot was artificially moistened by a hand held water sprinkler.

Different zones in this spot were watered, each with different amount of water, with increasing the water sprinkle from a zone to another.

At these zones, colour records were taken by the spectrophotometer, and in addition to that, samples were collected in covered plastic boxes for checking the moisture content by the moisture analyzer in the laboratory.

Figure 6.5 shows the prepared spot, cleared off vegetation and impurities, ending with a clear soil surface, besides, the usage of the spectrophotometer can be seen in the figure for the colour records.

Fig. 6.5. Soil spot prepared, and the spectrophotometer usage in field.

Relying on the loam sand reflectance equation, and is in Figure 4.22. The resulting curve equation is in a moisture range, and the reason behind considering this moisture range is explained in chapter 4.

Equation 4.3, the loam sand soil equation is:

$$y = -0.0455x^4 + 0.8924x^3 - 6.0817x^2 + 14.768x + 5.4496$$

In Table 6.1, the validity of the equation in the field measurement was checked using three colour records (already knowing that the moisture content falls in the Figure 4.22 moisture range; 1.06 % to 6.80 % mc).

Table 6.1. Shows the colour reflectance records at 700 nm, with the results obtained when the records are substituted in the equation, also shows the gravimetric moisture content results.

Test number	Colour record at 700 nm [%]	Predicted moisture value [%]				Moisture analyzer result [m/m %]	Result % (relative to the highest value)
		x	x	x	x		
Test 1	14.03	3.51	7.63+2.46i	7.63-2.46i	0.83	2.92	83.19
Test 2	14.16	3.46	7.64+2.48i	7.64-2.48i	0.85	3.44	99.42
Test 3	11.72	4.37	7.35+2.26i	7.35-2.26i	0.53	5.24	83.39

Some of the obtained values in the table are complex numbers, and these values cannot be moisture content results. For the first test, two complex numbers are eliminated, and the value 0.83 doesn't fall in the moisture range, thus 3.51 % is the estimated moisture content from the colour equation. This value is close to the moisture content measured by the moisture analyzer, 2.92 %. Comparing the two numbers, the smallest value relative to the highest forms 83.19 %.

For test 2, there are two complex numbers, and they cannot be considered. The 0.85 doesn't fall in the moisture range. The remaining number is 3.46 %, and is close to the moisture analyzer obtained number, 3.44 %, of 99.42 result %.

For test 3, there are two complex numbers and one out of moisture range. The estimated result is 4.37 %, the analyzer result is 5.24 %, and the result relative percentage is 83.39 %.

6.3 Soil texture identified from the colour reflectance

In addition to the original target of the project, which is relating the colour reflectance of the soil to its shear strength, the quantitative spectrophotometric results can be a solution for identifying a dry soil infield.

The reflectance results (in the spectrum range) of a dry soil are tangable values to rely on in another benefit. Having the reflectance of a dry soil (approximately 0 % mc, dried) at 700nm, this value can be used to check a soil identity (texture) infield, applicable by saving the 700nm obtained reflectance result in a properties database.

Comparing the field soil reflectance result (sample taken from field and dried) to the laboratory already obtained one (dried), in case the 700nm records are approximately the same, and both are visually similar when dry (also with sensing the soil by hand), this means that the field soil texture is similar to the one tested in the laboratory. This step saves time instead of taking the field sample for checking its texture in the laboratory by experienced person/s, checked either by the laser particle size analyzer method or by the pipette method (sedimentation based technique). These methods require time, cost and effort, when it comes to carrying out both, the measurement and the analysis. The pippette method takes around two days.

The information about the measurements (laser and the pippette method) used for finding a soil texture, and the textures (the mechanical composition) of the soils used in the project, were taken from the TAKI soil institute in Budapest (Institute for Soil Sciences).

By having the reflectance results (at 700 nm, dried soils) prepared in a laboratory, these results are to be relied on when checking a new field soil sample (knowing that both should be of moisture content approximately zero for having a fixed moisture content, also visually similar). With this important reached step, the texture result is obtained faster. This idea is similar to the Munsells charts usage principle (mentioned in the literature, the qualitative method), that relies on vision by comparing infield soil to samples' pictures in the charts (with codes), but the difference is that with the new process a quantitative reflectance value is available to rely on. Showing the above mentioned work on the soil textures used in the measurement. In Table 6.2, colour reflectance results of the textures are shown at approximately 0 % mc (dried by the moisture analyzer). Figure 6.6 shows the soil textures/samples, and the records in Table 6.2 were taken after completely drying the samples by the moisture analyzer.

Table 6.2. The tested soil textures, each with its reflectance at 700 nm having the soil dry.

Tested soil texture	**Colour reflectance at 700 nm, (totally dried, approximately 0 % moisture content)**
Loam sand soil (90.50 % sand, 3.20 % silt, 6.30 % clay)	13.97
Silty clay loam soil (14.07 % sand, 47.46 % silt, 38.47 % clay)	34.61
Sand soil (94.53 % sand, 4.78 % silt, 0.69 % clay)	42.64
Silt clay soil (3.34 % sand, 52.05 % silt, 44.61 % clay)	17.42
Sand soil (95.68 % sand, 2.12 % silt, 2.21 % clay)	19.70

Fig. 6.6. The soil textures.

Sticking to the above textures (Figure 6.6), if checking a soil infield and it visually complies with one of the prepared soils with having the record of the field soil at 0 % mc (dry by the

moisture analyzer) approximately similar to the soil record in Table 6.2, this means that both are of the same texture.

Summary of the new approach in the chapter

This chapter gives an example on one texture (same process applicable on the other textures) about obtaining the shear strength values from the colour reflectance of the soil.

The correlation is a process that relies on the reflectance and the shear strength curves' equations that might change slightly (equations) with repeating the measurements. With repeating the measurements, the linking process or the methodology remains the same, and the steps are:

- Plotting the reflectance at 700 nm as function of moisture content, with finding the equation of the fitting curve.
- Plotting the shear strength values, each as function of moisture content, and finding the equations of the fitting curves.
- Predict the moisture content from the colour reflectance curve (700 nm).
- Substitute the predicted moisture content in the shear strength equation/s.

Thus, there are no certain equations to be generalized for being used on all textures, since the soil behaviour (reflectance and strength) changes from a texture to another, but the equations obtained on one texture can be generalized just for this texture. With repeating the measurements on a soil for finding the equations, the equations will not be precisely the same, but should end up with approximate predicted results, moisture content and shear strength values. The obtained equations (mainly the strength) are applicable on loose soil, so in case of using these equations infield, the soil should be of loose status (tilled).

In this chapter, a field measurement was carried out on one soil texture, and it has shown convincing results with estimating the moisture content from the colour reflectance.

This chapter has also shown the ability of benefiting from the reflectance at 700 nm (of dried soil) in identifying a soil texture. In this process, soil will not undergo measurements for checking its texture using the methods mentioned (laser and the pipette, or another method if availabe), thus saving time, cost and effort.

7. Soil shear strength parameters from mechanics perspective

7.1 Direct shear test emulating vehicle mobility study case (relative to speed)

The shearing mechanism resulting on soil terrain from the tractive element of a vehicle (wheel or track) is shearing the soil in translational shearing mechanism, and the shearing is occuring at a certain depth, thus inside the soil. The direct shear test machine shears the soil in a mechanism that closely resembles the mechanism of the tractive element on the soil. Focusing on this measurement and ending up with convincing results especially at higher shearing speed/s, relative to the standard method speed, might be a solution for improving vehicle's mobility on soil.

The mechanical properties of a soil are influenced by its initial physical and mechanical conditions (as the particles' bonding and the stress history). In field, having the soil as cohered material is different than having the soil tilled (loose soil). Each soil physical status will yield different strength results when studied. The soil in field falls under two major categories, tilled and cohered soil. Having the soil as cohered differs from a field to another. Totally dried or shrinked soil is different than cohered soil holding an amount of moisture content. The important point to consider when studying the performance of a vehicle on soil, is to know the physical status of the soil in the field where the vehicle is performing. By using the shear strength results of loose soil obtained in the laboratory to be substituted in performance models, the models' results will not be reliable to be used in a field of hard soil layer. Considering that the risky case that puts a vehicle in the zone of performing bad on soil is when having the soil loose, thus in the research the soil is studied as a loose material. With loose soil, at high moisture content, the soil becomes weak (on most of the soils), thus weakening the bearing capacity and the shear strength.

The soil initial stress condition influences the obtained shear strength result. For example, when performing a measurement using the direct shear test, having a high mass applied on the soil (loose soil) before the shearing is run using a lower mass, will make the soil sample of overconsolidation ratio above 1. Testing the soil samples with OCR above 1 (moistened soil), is leading to convincing shear strength parameters results at high shearing speeds (chapter 5).

In this research part, the soil is studied as one body far from the geo-technical and civil engineering work. One of the aims behind this chapter is to end up with the shear strength parameters of the soil in undrained condition relying on mechanics (chapter 7.5). New ideas were invented by researchers aiming to measure the shear strength of the soil at higher speed compared to the speed used in traditional shear test methods (Dudzinski and Damian**,** 2019), but these ideas are limited to finding the shear strength and not the parameters.

The shear strength at high shearing speed measured by a design is applicable under the applied consolidation stress, but when dealing with a normal stress resulting from another tractive element, the case will be different. A measured shear strength (at a speed) is restricted to the normal stress used in the measurement. As long as having the shear strength parameters available in field (belong to a field condition and measured at a speed), these values will lead to finding the shear strength of the soil under another normal stress by relying on the Mohr-Coulomb linear equation.

7.2 Importance of this chapter in terramechanics

Different measurements were carried out in the laboratory on the loam sand soil (texture mentioned above), and there is set of aims behind these measurements. The first target is to show the influence of the density on the shear strength of the soil in both rotational and translational shearing. The results in the measurement have shown that in translational shearing the density (in a certain range) does not have influence on the shear strength of the soil, the case that has clarified the linearity of the Mohr-Coulomb failure in a normal stress range.

As a target, is also to find the shear strength parameters of the soil using a mechanics method far from the Mohr-Coulomb line work, then checking the validity of the parameters results obtained, with comparing the results to the results obtained relying on the Mohr-Coulomb principle. Tests were carried out having the soil in undrained condition (shearing speed 9 mm/min). Finding the friction coefficient (and angle) using the text mechanics method (section 7.5.1, the new proposed method), has lead to understanding why the direct shear test method (the standard method) is carried out in drained condition (low shearing speed).

An additional aim behind ending up with the shear strength parameters at shearing speeds higher than the speed used for draining the soil, is reaching the level of having the shear strength parameters prepared (at high shearing speed) in a database, which will be useful in knowing the shear strength at tested shearing speed under a consolidation stress.

7.3 Translational and rotational soil shear strength measuring techniques

Different shear strength measuring methods are available, where each of them is of a specific mechanism. Based on different literatures, each of these methods ends up with a different shear strength result, despite that some of them are laboratory measurements (as the direct shear test and the triaxial test) and the others are field tests (as the shear vane) (Wroth, 1984), (El Hariri et al., 2023c).

Comparing the direct shear test (laboratory test) to the vane shear test (originally field test). In the direct shear test, a consolidation load is applied on the soil while performing the test, this applied consolidation load affects the frictional part of the shear strength. The Mohr-Coulomb equation shows that the shear strength is resulting from both, the shear cohesion and the internal friction at the particles' level.

The increase in the applied stress leads to an increase in the frictional part of the Mohr-Coulomb equation. High applied stress increases particles' contact friction and interlocking, thus higher shear strength resulting from the friction side of the material.

Inspite the increase in the second part of the equation (frictional part) with increasing the applied stress, an important note should be taken into account, and it is that the internal friction angle (ϕ) remains constant at the applied stresses.

The shear strength parameters denoted by c and ϕ are independent of the applied stresses (while shearing), but are influenced by changing some soil properties (not generalizing all properties), such as the moisture content.

In the Mohr-Coulomb diagram shown in Figure 7.1, increasing the consolidation stress from σ_1 to σ_2, has led to increasing the shear strength from τ_1 to τ_2. It is clear in the figure that the soil

cohesion (c) remained constant with increasing the normal stress, and that what changing is the upper section (above the shear cohesion line, dashed line) at any shear strength. The upper section is the internal friction part of the Mohr-Coulomb linear equation. This part is calculated by multiplying the normal stress with the tangent of the internal friction angle. Having the internal friction angle constant, then the internal friction part of the equation is directly affected by the normal stress.

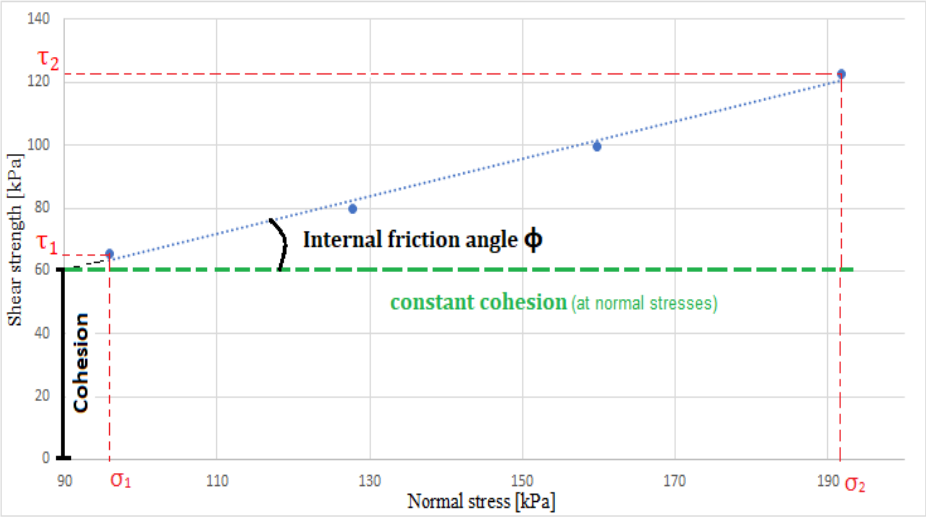

Fig. 7.1. Mohr-Coulomb diagram.

Back to measuring the shear strength using the shear vane, the vane is inserted into the soil to a certain depth and a torque is applied to twist the vane, the torque increases reaching a peak value (it is the shear strength), and beyond this value the shear torque required to twist the vane decreases due to the rupture of the soil. While performing the vane test, no normal load is applied. Omitting the normal stress from the Coulomb equation that is built based on the Mohr's principle (at the failure plane, the applied normal stress is related to the shear strength) (Mohr, 1900), results in the shear strength due to the cohesion of the soil. This test is suggested to be used on soils at high moisture contents (close to saturation), where the cohesion strength is the dominating strength and the frictional influence is low, also suggested to be used on fine soils (cohesive soils).

Based on the above given examples (the tests), it is emphasized that the shear strength is affected by the method used for measuring it. The mechanism of the shearing process influences the shearing strength result.

When it comes to terramechanics science, the shearing mechanism occurring below the tire or the track can be depicted by the mechanism of the direct shear test machine.

7.4 Influence of density on the shear strength

7.4.1 Vane shear test

Soil shear strength was checked at different densities in rotational and translational shearing mechanisms. The aim is to check the influence of the density on the shearing strength. The tested soil texture is loam sand soil, of mechanical composition (90.50 % sand, 3.20 % silt, 6.30 % clay).

Shear vane (20x40 mm), Figure 7.2, was used to perform the shear strength measurement in rotational shearing mechanism, while for the translational shearing, the direct shear test was used.

For the vane test, a bin was filled with soil to initial density (1.32 g cm^{-3}, soil mass 3.87 kg), and the shear strength results were measured at different densities. In each measurement, the soil was compressed starting from the initial density (slight compaction) reaching the required density using the bevameter (hydraulic press). The soil was tested at two moisture contents, 4.04 % and 12 %, sieved before moistening. The reason behind choosing a low and a high moisture content is the difference in the shear strength parameters when comparing the two stages (on most soils), low and high moisture content. Shear strength results were taken at approximately same depth, following the same shearing process (low shearing rate). Results of the vane test at different densities are shown in Tables 7.1 and 7.2.

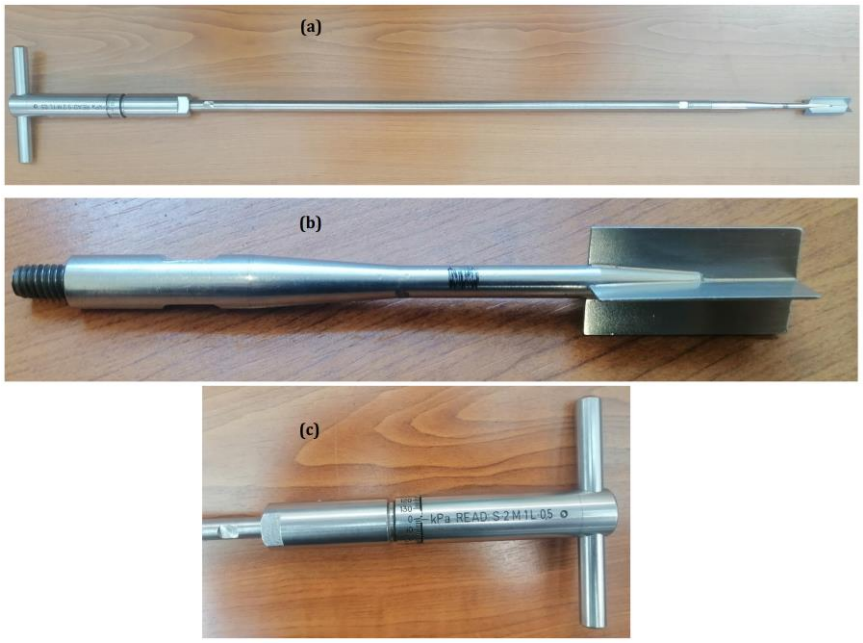

Fig. 7.2. Show the shear vane, (a) the complete instrument, (b) the vane blade of 20×40 mm dimensions, and till the black mark on the vane shaft, is the depth that will be considered in the measurements, (c) the scale and the handle of the vane instrument.

Table 7.**1.** Shear strength of loam sand soil at different densities, of 4.04 % mc, measured using the shear vane.

Loam sand soil at moisture content 4.04 %		
Density [g/cm^3]	**Shear strength [kPa]**	**Shear strength results - sample standard deviation**
1.32	1.66	0.57
1.60	14.66	3.05
1.86	30.66	1.15
2.10	42.00	3.46

Table 7.2. Shear strength of loam sand soil at different densities, of 12 % mc, measured using the shear vane.

Loam sand soil at moisture content 12 %		
Density [g/cm^3]	**Shear strength [kPa]**	**Shear strength results - sample standard deviation**
1.32	2.33	0.57
1.60	5.00	1.00
1.86	9.33	1.15
2.10	14.66	1.15

In the two cases (low and high moisture content), with the increase in the density, the shear strength shows an increase in its result.

7.4.2 Direct shear test

The translational shearing mechanism, direct shear test, was performed on soil samples at different densities having the same consolidation stress σ applied while shearing (from 30 kg mass, 95.86 kPa). Different masses were used for setting the initial density of the soil before shearing. 30 kg, 70 kg, and 90 kg [in term of normal stress, 95.86 kPa, 223.68 kPa, 287.58 kPa] masses were used for the initial compaction of the soil samples. In each measurement, new sample was used, with setting the initial density of the sample (in the shear box) to 1.46 g/cm^3 (for each measurement the soil mass is the same, 110 grams). In each measurement, the soil amount was filled carefully and uniformly in the box without any compaction in the soil, and upon discharging all the amount in the box, the soil was smoothly compacted to the set initial height in the box, thus setting the initial density (same mass and same height, thus same initial density). Preparing the soil to the initial density and then covering it by the covering plate, a mass was applied, thus by the mass the soil will be compacted to a next density (actual density before shearing). Afterthat, the applied mass and the cover were removed for measuring the height from the soil upper surface to the top brink of the shear box. Having the total height of the box and the measured height, the soil thickness can be calculated. With the mass and the thickness of the soil, the density can be calculated. The same procedure was followed using the mentioned masses (30, 70, and 90 kg). The tests were carried out having the soil at 4.38 % mc and 11.51 % mc. Tables 7.3 and 7.4 show the shear strength results at the different densities.

Table 7.3. Shear strength of loam sand soil at different densities, of 4.38 % mc, measured using the direct shear test.

Loam sand soil at moisture content 4.38 %		
Density [g/cm^3]	**Shear strength [kPa] (30 kg is the applied mass while shearing)**	**Shear strength results - sample standard deviation**
1.49 (using 30 kg)	79.28	3.36
1.59 (using 70 kg)	88.18	1.73
1.64 (using 90 kg)	85.40	0.64

Table 7.4. Shear strength of loam sand soil at different densities, of 11.51 % mc, measured using the direct shear test.

Loam sand soil at moisture content 11.51 %		
Density [g/cm^3]	**Shear strength [kPa] (30 kg is the applied mass while shearing)**	**Shear strength results - sample standard deviation**
1.73 (using 30 kg)	62.69	1.00
1.77 (using 70 kg)	64.01	4.33
1.81 (using 90 kg)	62.69	2.12

The results in the two tables show that with the increase in the density and under the same applied normal stress while shearing (from 30 kg), the shear strength is approximately the same. Thus, under these loads that are applied initially to compact the soil there is no change in the cohesion built up, cohesion is approximately the same in the three density cases, and the actual factor that has influence on the translational shearing strength of the soil is the friction part which is due to the applied normal stress (σ). This work complies with Mohr-Coulomb linear equation.

In the Mohr-Coulomb equation, the shear strength is the sum of both, the cohesion and the friction strength at the shearing zone. Having the soil at the same moisture content, the friction angle should be the same (friction between the same material, also as soon as the cohesive bonding breaks, the friction will occur inbetween the soil, mostly it is supposed that there should be friction before and after breaking the cohesion, but is dependent on the study case). Having the same normal stress applied, and with same internal friction angle (soil at same moisture content), this case is occuring at the different tested densities, the shear strength test is yielding approximate results. With the same normal stress and the same friction coefficient ($\tan\phi$), and relying on the Mohr-Coulomb equation, the shear cohesion should be approximately the same. In the Mohr-Coulomb line diagram (Figure 7.1), it is clear that under different normal stresses the cohesion is constant (at a moisture value), and that what changing is the friction part of the equation.

Thus, based on the above paragraph mentioned information, it can be deduced that the applicability of the Mohr-Coulomb line is limited to field work, where in field on-average the cohesion is approximately the same, despite the reason behind building the cohesion in the field, such as polarity, negative pore pressure, and other reasons. The passage of the soil through different natural processes (drying, wetting, and then drying) and external excitations (such as movement of machinery on soil), all these factors have effect on the soil cohesion.

The cohesion built up in the tested loose soil is resulting from the applied initial compaction stress (as a result of polarity and negative pore pressure). In the above work, it is clear that the cohesion is approximately the same under the tested densities. As a result of the work, the linearity of the Mohr-Coulomb failure is applicable in a normal stress range.

Even though polarity plays a role in the cohesion, but this is valid under a consolidation stress, otherwise the particles must attract each other strongly as a magnet when just moistened, and this is not the case in the tested soil (and on most soils). The polarity helps in sticking or creating the tendency of the particles to stick together, but polarity alone (on most soils) is of weak strength, and what strengthens the cohesion is the negative pore pressure built under the normal stress.

The cohesion of the tested soil was measured in another measurement, in a way far from the Mohr-Coulomb line work, by placing the soil in the direct shear box and then shearing the soil with zero applied normal stress, cancelling the friction term from the Mohr-Coulomb equation. Measurements were carried out at 6.3 % moisture content, under different initial compaction densities. Results are shown in Table 7.5.

Table 7.5. Shear cohesion of loam sand soil at 6.3 % mc (measured using the method mentioned above).

Mass used for initial compaction [kg]	30	60	90	200	300
Cohesion [kPa]	7.06	7.85	9.01	9.49	10.77
Cohesion results - sample standard deviation	0.90	0.26	0.67	0.02	0.04

In another measurement, the soil cohesion was measured in two cases (at 11 % mc), one under an initial applied mass, and the second having the soil being compacted by striking it heavily when placed in the shear box, and then measuring the cohesion using the above mentioned method (without normal stress). Results are shown in Table 7.6. The 11 % moisture content (high moisture) was chosen, since at high moisture the soil becomes easy to be compacted (weak bearing capacity).

Table 7.6. Shear cohesion of loam sand soil at 11 % mc (measured using the method mentioned above).

Initial compaction	Using 70 kg	Random, by striking the soil prepared in the box
Cohesion [kPa]	5.90	14.20

In Table 7.5, the results show that between 30 kg and 90 kg the cohesion is approximately of a close value, and with increasing the applied mass, the cohesion keeps on increasing. Thus, constant cohesion (approximate value) is applicable in a certain range, and based on that finding, the Mohr-Coulomb linearity is applicable in a certain normal stress range. With carrying out a measurement in another range, the linearity should be applicable in the other range till a maximum stress/es. In Table 7.6, the difference in the cohesion is clear, thus the Mohr-Coulomb linearity in such case can not be applied, due to the difference in the cohesion. Shifting the cohesion results in Table 7.6 to Figure 7.1, the cohesion will not fall on the same line (or approximate), the dashed line.

When it comes to land locomotion study case, the cohesion is dependent on the field that the machine is moving on. When a vehicle moves on tilled soil, the case is totally different than when having a vehicle moving on shrinked or swelled soil, or soil in any other condition. In most cases the vehicle's mobility is affected when moving on physically loose soil (tilled soil). Having a vehicle moving on such soil, which is of a low cohesion when compared to cohered soil (bonded particles), it is important to mention that the cohesion that is built in the soil is due to the applied pressure (with polarity effect) from the vehicle on the soil at the tractive element contact patch. As mentioned above regarding the tables' results on loose soil, that the cohesion is built under the applied masses, the same is applicable in real-time terramechanics case.

In the case of moving on cohered soil, it is supposed that as long as having the normal stress below the maximum stress that the soil has experienced, the linearity of the Mohr-Coulomb failure should be applicable, this case remains valid with increasing the normal stress, even if slightly exceeding the maximum experienced stress (cohesion remains approximately the

same). The behaviour of a soil under a load is strictly dependent on its initial condition, thus studies should be carried on samples of different cohesion.

7.5 Mechanics implemented for finding the soil shear strength

7.5.1 Principle explained theoretically with procedure

When it comes to a terramechanics scientist it might be challenging to find the cohesion and the internal friction angle, especially if the case requires that the measurement to be carried out at a high shearing speed (compared to the standard shearing method rate).

In this section, the Mohr-Coulomb principle will be treated relying on mechanics and not on the Mohr-Coulomb line for finding the shear strength parameters, the case that might entitle a researcher to measure the parameters at different shearing speeds.

Thinking of a soil sample having a normal load exerted on it, two forces will resist the shearing force, and are the cohesion and the friction. Soil particles are bonded to each other at the shearing plane, thus a force is needed for breaking these bonds (F_1). As long as having a normal force applied, there will be friction at the shearing plane between the particles, and inorder to overcome the material friction shearing resistance (F_2), a force should also be applied.

The major resisting force to shearing that the soil sample holds is the sum of the two forces F_1 and F_2, bonding and the friction, expressed in Equation 7.1.

$$\mathbf{F_{Shear\ strength}} = \mathbf{F_1} + \mathbf{F_2} \tag{7.1}$$

Figure 7.3 shows the forces acting on and from a soil sample while being sheared in the direct shear test.

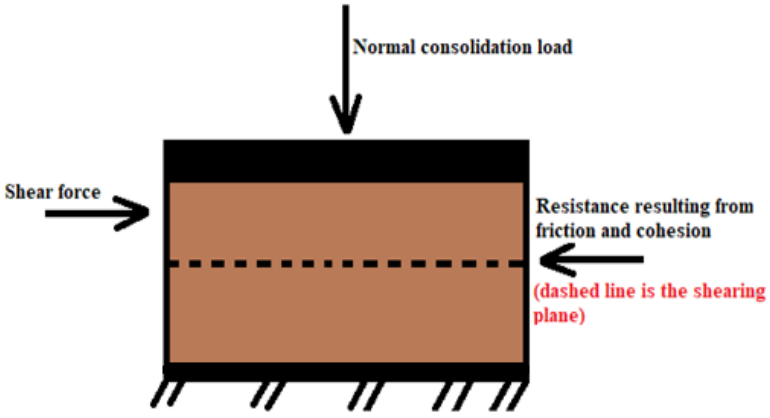

(a)

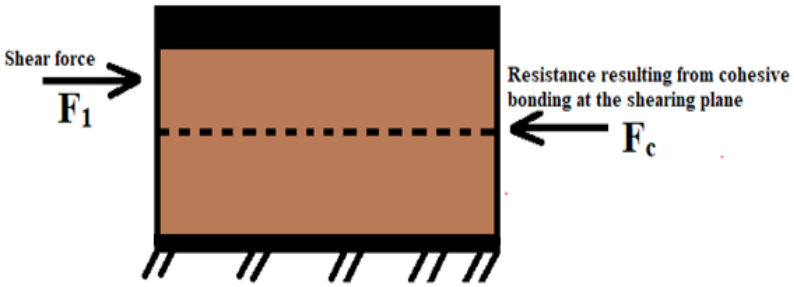

(b)

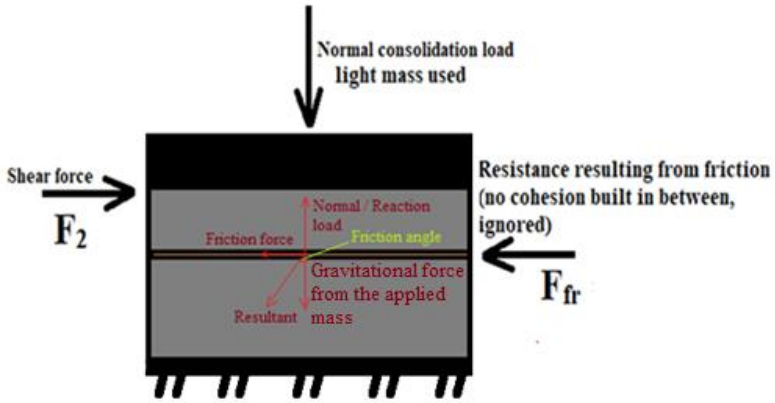

(c)

Fig. 7.3. (a) shows the shear force required to break the cohesion and pass the friction (initially kinetic friction), (b) shear force required to break the cohesion, without normal load applied, (c) shear force required to pass the friction in a thin soil layer under light mass (brown colour shows the thin layer).

In Figure 7.3, it is clear that with removing the normal load applied, and then shearing the sample, the maximum force that will be recorded by the machine is the shear cohesion resistance (F_1). Thus, the cohesion term in the Mohr-Coulomb equation is obtained at the set shearing speed. The second term (F_2) is the friction term, which is the normal stress multiplied by the soil material friction coefficient. In the derivation below, it is clear how the soil shear strength is reached from the forces.

$$\mathbf{F_{shear\ strength} = F_1 + F_2}$$

$$\mathbf{F_{shear\ strength} = F_{cohesion} + F_{friction}}$$

Normal force acting on the shearing plane is equal to the gravitational force.

$$\mathbf{Normal\ force = normal\ mass\ applied \cdot gravity}$$

$$\mathbf{F_{shear\ strength} = F_{cohesion} + Friction\ coefficient(\mu) \cdot Normal\ force}$$

Dividing the equation by the shearing area, will lead to the shear strength (in stress term).

$$\mathbf{\tau_{shear\ strength}[kPa] = Cohesion[kPa] + Friction\ coefficient\ (\mu) \cdot Normal\ stress\ [kPa]} \quad (7.2)$$

$$\mathbf{\mu = \tan\phi}$$

ϕ is the internal friction angle, and is friction parameter between the contacting materials, and in this case between the same soil material at a moisture content, and is independent of the applied normal stress. The cohesion and the friction angle are soil fixed values (dependent on soil condition). It might happen that in case the consolidation stress is above the maximum stress value experienced by the soil, that soil builds up higher pore pressure cohesion, but as long as the stress is below the maximum experienced stress, the soil will be holding the initial material cohesion.

The required value for completing the friction term in the shear strength equation (Equation 7.2) is the friction coefficient.

A new suggested idea for measuring the friction coefficient was tried, yielding (when substituting the obtained friction angle) accepted shear strength results compared to measured results (validated).

The target behind the suggested idea is to achieve the shearing on a thin soil layer, thus shearing against friction without cohesion. The following work was done using the direct shear test machine, but with a small change in the shearing sample design.

Two teflon cylinders were used with double face tape on each, a face is glued on a teflon side, and on the other side, soil (at a moisture content) is placed. When shearing the soil it will shear over each other, with no cohesion built up (might be of a very small value, explained in the text), and in addition to that, a light mass is applied while shearing (5 kg used, and not heavy mass, to avoid the building up of pore pressure cohesion). The steps followed for preparing the shearing soil sample are shown in Figure 7.4.

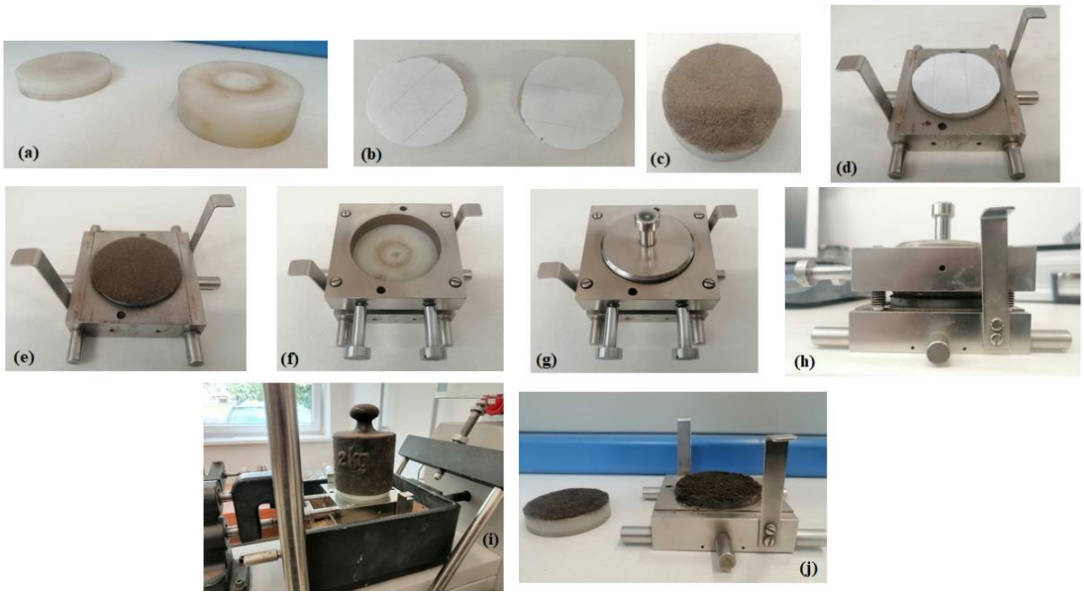

Fig. 7.4. (a, b) show the prepared teflon cylinders, with double face tape used on them, (c) shows the soil sticking on the other face of the tape, this sample is prepared for the upper frame, (d, e) lower frame teflon with soil prepared on it, (f, g, h) frame assembled, shearing zone seen in h, (i) Box installed in the shear machine with normal load applied - all masses applied are considered (with the teflon piece mass), (j) soil of high moisture content on the tape face.

It is worth mentioning that the force measuring sensor should be checked that it is calibrated (no deviation in results), and that the applied normal mass is at 90 degrees, and any small tilt in the angle might yield another friction coefficient value (general information). The original mass loading system in the machine was not used aiming to have the precise mass applied, and as seen in Figure 7.4 (i), the light mass is placed on the shear box centering the teflon piece. All the masses used should be considered (the upper plastic piece and the applied mass), thus having the actual applied mass on the shearing plane. At high moisture content, soil is initially rubbed on the tape face for sticking, and then applying a thin soil layer (see Figure 7.4-j).

7.5.2 Results obtained using the mechanics method

The soil was tested under two light masses (1 kg and 2 kg) at different moisture contents, except for the high moisture value reached, where a 200 g mass was also used. The internal friction angle is independent of the normal load applied, and the aim behind using a light mass is to avoid building up of cohesion between the particles, thus running the friction measurement at the particles' level without any disturbances on the measured friction force value.

The friction coefficients of the soil under the masses at the different moisture contents were calculated.

The loam sand soil is used; friction coefficients obtained at the different moisture contents are shown in Table 7.7.

Table 7.7. Friction coefficients of the tested soil at different moisture contents (112 g teflon piece mass added to the applied mass).

Moisture content [m/m %]	0.62	3.23	6.07	9.64	12.07
Friction coefficient under 1.112 kg	0.89	0.67	0.62	0.67	0.65
Friction coefficient under 2.112 kg	0.86	0.64	0.56	0.69	0.76

In Table 7.7, at the moisture contents, 0.62, 3.23, and 6.07 % mc, the friction coefficient results show an approximation in the results under the two masses. The tendency shows a decrease with the increase in the moisture at the first three moisture contents. At 9.64 % mc and 12.07 % mc, the friction coefficients show an increase in the friction value.

Logically the friction should decrease with the increase in the moisture content, but these two results contradict the logical tendency. The reason behind that might be due to cohesion building up in the soil under the masses used (even if very small cohesion value), the case that is leading to the force being recorded embedding this very small cohesive value, thus yielding a higher force at this stage. At high moisture contents, the plasticity of the soil increases. The main conclusion taken from the obtained results at the high moisture contents might be the main reason behind making the direct shear test, for measuring the cohesion and the friction angle, requiring to be in drained condition for ending up with results of less errors.

Back to the last 2 moisture values in Table 7.7, and trying to reach a way to end up with the actual friction coefficients based on the above work (and shearing speed). For the 9.64 % mc, preparing another sample (soil on the tape), and following the same procedure for measuring the friction, but now applying and then removing the masses (upper teflon with soil layer is kept, is of light mass), so just measuring the built up cohesive force. For the 9.64 % mc, the

cohesive force values built under the used masses are, c = 6.56 N [2.08 kPa] under 1.112 kg [3.55 kPa] and c = 7.03 N [2.23 kPa] under 2.112 kg [6.74 kPa].

It is important to mention that all the results recorded by the force sensor embed the force required for pushing the shear box movable part (upper frame), thus for the accuracy in the results, this force should be deducted from the recorded forces (in all the measurements). Its force value can be obtained in a separate measurement on the box having it empty. This is similar to the idea of using separate masses (not the machine loading system) for knowing the precise light mass used for the consolidation. The friction measurement at a low moisture content should yield a friction curve, while at a high moisture value, it will yield a plasticity curve (elasto-plastic curve).

Having the cohesion force obtained at the 9.64 % mc, also knowing the friction obtained, and as mentioned that it is not the pure friction at this moisture content, the cohesion and the frame forces should be deducted from the measured friction force, this will lead to the precise friction force of the soil. Dealing with the results (at high moisture contents) in the mentioned way, ended with the friction coefficients under the two used masses (1.112 kg and 2.112 kg / 3.55 kPa and 6.74 kPa). The obtained friction coefficients are μ=0.50 (under 1.112 kg) and μ=0.57 (under 2.112 kg). The two results are convincing and fall in the friction change tendency with increasing the moisture content.

For decreasing the error in the measurement, the same work principle was followed for the 12.07 % mc, but this time the mentioned masses were not used (1 and 2 kg), and tried with a very low mass (200 g), considering that this will not build a recognized cohesion. It is a mass that is applied while shearing, and it should yield the same friction coefficient (with friction angle) as when compared to finding the friction using a higher applied mass. The mass was applied on the teflon piece, and 2 records were taken, one for the cohesion (remove the mass then shear), and the second for the friction (embedding the light cohesion). Having the 2 values, then deducting the cohesion and the frame forces (frame should be deducted from both friction and cohesion measurements) from the measured friction value, will yield the actual friction force. Under the 200 g mass (lighter upper teflon piece used, 47 grams, both summing 247g / 0.789 kPa), the obtained friction coefficient is 0.47.

Table 7.8 shows the friction coefficient with the internal friction angle of the tested soil at the different moisture contents.

Table 7.8. The friction coefficient and internal friction angle of the tested loam sand soil at the different moisture contents.

Moisture content [m/m %]	0.62	3.23	6.07	9.64	12.07
Friction coefficient (average results in table 7.7)	0.87	0.65	0.59	0.53	0.47
Internal friction angle [degree]	41.18	33.22	30.54	28.14	25.17

Table 7.8 shows that with the increase in the moisture content, the internal friction decreases. This tendency complies with the actual soil mechanical behaviour with moistening, considering that the water (and the soil hydration) acts as a lubricant between the particles. Having soil particles with less hydration makes the contact or friction tendency higher than when compared to having the soil at high moisture content. Also, it is important to mention that the friction coefficient (even if having the soil dry) should be of a value less than one, this makes the

measuring work sensitive, thus a main reason for checking the accuracy of the force measuring sensor, and to be sure of the actual applied normal stress and its angle.

7.5.3 Validity of the obtained friction results

The obtained friction results were validated under 5 kg (sum 5.112 kg / 16.33 kPa) normal mass applied while shearing. For the cohesive force measurement, place the soil (at a moisture content) in the shear box, then apply 200 kg (623.45 kPa) mass (chosen mass for the cohesion), after that remove the mass and run the machine. The maximum force is recorded by the sensor (the cohesive force).

The shearing force was measured in a new measurement (new sample, same speed) under 5 kg. A 5 kg was applied during shearing, and a 200 kg mass was initially used for building up the cohesion.

Note that 4.6 N is the force required for displacing the empty frame. Table 7.9 shows the cohesion and both, the measured and the calculated shear strength, results are after deducting the 4.6 N force (shear box area 0.003147 m^2).

Table 7.9. Shows the validity of the obtained friction angle results (at moisture contents close to the friction angle results moisture contents).

Moisture content [m/m %]	0.62	3.20	6.40	9.64	12.53
Cohesion [kPa] (under 200 kg)	2.45	10.14	8.80	4.56	5.24
Cohesion results - sample standard deviation	0.15	0.24	0.08	0.45	0.20
Measured shear strength [kPa] (one record considered)	22.04	20.24	16.45	15.25	14.46
Calculated shear strength [kPa] (Mohr-Coulomb equation, using the cohesion and the friction angle)	16.18	20.91	17.76	12.54	12.89
% Relative [relative to the highest value, measured and calculated]	73.41	96.79	92.62	82.22	89.14

7.6 Comparing the obtained results (from the mechanics method) to the Mohr-Coulomb line results

The shear cohesion in Figure 5.5 (chapter 5) shows an increasing tendency with the increase in the moisture content, but the results do not comply with the ones obtained in Table 7.10. The word shear cohesion in translational shearing should be the force that is resisting the shearing process, resulting from the cohesive bonding, thus it should be the value that is resulting from the resistance without the friction term. The additional cohesion recognized in Figure 5.5 results compared to Table 7.10 (at each moisture content) might be due to additional cohesion that is built up with shearing (from the plasticity of the soil, also under normal stress, because when the soil is dry the results are approximate). Further investigation is required on the difference in the results as it is not an aim behind the project.

Since the vane shear does not require a normal load while measuring the soil shear strength, so the friction term is eliminated from the Mohr-Coulomb equation, thus the cohesion should be approximately equal to the shear strength. The cohesion to be used in translational shearing is supposed to be of a value close to the shear strength obtained by the vane shear, this is also applicable on a field sample. In laboratory work, preparing similar to the soil sample in the direct shear box but on a larger scale (both of approximately same physical condition, as density

and cohesion), and by checking its shear strength using the shear vane, the obtained shear strength can be used as the translational direct shear test cohesion.

An additional information to consider, is that when placing soil in a small diameter bin and compressing it to achieve high soil density in the bin, this might increase the error in the measured cohesion (by the vane). The internal stress acting at the particles' level, and resulting from the bin wall pressure (transmitted to the particles), will act as lateral friction (as normal stress friction case). In this case, the shear strength will embed both, the cohesion and the friction resulting from the lateral stresses.

The frame force is included in both tests of this section (the Mohr-Coulomb line and table 7.10 method). The difference in the cohesion results is clear between the two measurements.

Table 7.10. Tested loam sand soil shear cohesion (using the direct shear test machine with no consolidation stress).

Moisture content [m/m %]	1.05	3.12	6.75	9.00	12.07
Shear cohesion [kPa] (frame force included)	4.50	6.23	7.11	7.73	5.80
Cohesion results - sample standard deviation	0.14	0.02	0.06	0.02	0.21

The friction angle results shown in Figure 5.6 (chapter 5, loam sand) approximately comply with the friction angle results obtained using the above method (see Table 7.8).

7.7 Influence of speed on the shear strength parameters (using the mechanics method, section 7.5)

Preparing shear strength results (without parameters) in laboratory and using them in field makes these results just applicable under the applied normal stress.

As the shear strength is influenced by the shearing speed (shearing power, force multiplied by speed), thus both the shear cohesion and the internal friction angle should also be affected by the shearing speed. Soil deformation speed is a factor influencing its strength properties, and that has been indicated in different scientific literatures, as (Taylor and Gill, 1984). Having the shear cohesion and the friction angle at a speed, these values can be saved in a database to be used under any applied consolidation stress by substituting them in the Mohr-Coulomb equation for ending up with the shear strength.

When applying a normal stress that exceeds the maximum stress that the soil has experienced, the cohesion of the soil might be influenced, and that is clear in Tables 7.5 and 7.6. It is obvious that in a certain normal stress range (relative to the actual applied normal stress), the influence of the actual applied normal stress on the cohesion can be neglected. What is important is to have the cohesion of the field status and the internal friction angle at the shearing speed. Having both prepared at the required shearing speed, the shearing strength that the soil can withstand under the tractive element can be predicted.

The shear cohesion and the friction coefficient were measured at three different speeds. The shear cohesion was measured using the direct shear box, but without normal stress applied during shearing. The cohesion was built up in the loose soil placed in the box under 70 kg, so

mass was applied and then removed, after that the cohesion was measured. The friction was measured following the method mentioned in section 7.5.1.

The results of the shear strength parameters at the different shearing speeds are shown in Table 7.11. The moisture content of the tested soil (loam sand soil) is 6.15 % mc (fixing the moisture content).

Table 7.11. Shows the shear cohesion and the friction coefficient of the tested loam sand soil at different speeds.

Shearing speed [mm/min]	1.00	5.00	10.00
Shear cohesion [kPa] (frame force deducted)	5.11	5.88	6.31
Cohesion results - sample standard deviation	0.19	0.34	0.21
Friction coefficient [degree]	0.68	0.82	0.79

Table 7.11 shows that with the increase in the shearing speed, the shear cohesion increases. The friction coefficient increases with the increase in the speed; speed from 1 mm/min to 5 mm/min. At 5 and 10 mm/min (actual value 9.99999 mm/min the friction coefficients are approximately equal.

Reaching the ability of splitting the shear strength measurement at different speeds into cohesion and friction values, is useful in many applications. Here comes an idea, why not designing a bin that works similar to the mechanism of the direct shearing test machine, but is of the tractive element contact patch size (similar to the bevameter technique), with shearing at higher speeds. Emulating the real case interaction mechanism might facilitate studying terramechanics cases.

In real-time terramechanics case, the soil shearing speed is much higher than when testing the soil using the geotechnical and the civil engineering methods such as, the direct shear test and the shear vane, the case that arises questions about the applicability of the results obtained from these methods in vehicle mobility study cases.

Summary of the new approach in the chapter

The work has clarified different points that are important when it comes to measuring the shear strength of the soil to be used in vehicle mobility study cases:

- The idea behind the linearity of the Mohr-Coulomb failure criterion was clarified through measuring the translational shear strength of a soil at different densities under the same consolidation stress. The sensitivity of the density influence on the shear strength is dependent on the shearing mechanism. A small change in the density leads to changing the shear strength of the soil when being measured using the shear vane, but when it comes to the direct shear test, the density in a certain range does not influence the shear strength, where the shear strength is tremendously affected by the normal load applied while shearing, affecting the friction term in the soil.

- A new method was used for measuring the friction coefficient of a soil in undrained condition. The method yielded convincing results that comply with the results obtained using the Mohr-

Coulomb line in undrained condition. The results obtained using the mechanics methods in the chapter were validated by comparing the calculated shear strength to the measured value at the different moisture contents (same shearing speed).

- Considering the shear strength parameters results of the tested soil obtained using the method in section 7.5 and the Mohr-Coulomb line principle, the results of each parameter in both tests fall in the logical tendency change with moistening (on most soils), which is the decrease in the friction coefficient and the increase in the cohesion with moistening.

- The measurements have shown the ability of having the soil shear strength parameters at speed higher than the value followed in the standard direct shear test measuring method (thus finding the shear strength under a consolidation stress).

8. Conclusion on the research

The main target behind the research has been achieved, which is relating the shear strength of the soil to its colour reflectance. This target was reached and checked on five different soil textures. As a preliminary step for relating the shear strength to the colour reflectance, it is to predict the moisture content from the colour reflectance of the soil.

For each soil texture, relying on the colour reflectance records captured by the spectrophotometer and dealing with them empirically and mathematically, it has appeared that plotting the reflectance records at 700 nm as function of moisture content is ending with a curve that is of reliable equation to be used in predicting the moisture content from the colour reflectance. This reached finding was validated through laboratory work by using new samples' reflectance records, also was checked infield. Predicting the soil moisture content from its colour reflectance might be helpful in different fields such as, terramechanics, agriculture, civil and geotechnics. The tendency of the change in the colour reflectance as function of moisture content is dependent on the soil type, as sand or silty clay, which is specified by its texture. In a chapter, it is mentioned the ability of determining the soil texture of a sample from the colour reflectance record (at 700 nm) when having the soil dry (0 % mc, dried), and is achieved by saving the record in a properties database to return back to it as an identity of the soil.

Using the direct shear test machine, the shear strength results of three different soil textures were found in undrained condition (higher speed compared to the standardized method shear speed, the speed used in civil and geotechnical engineering). The shear strength parameters obtained, shear cohesion and internal friction angle, show convincing curves changing tendencies as function of moisture content in the three tested textures. In each tested texture, the change in the shear strength results as function of moisture content comply with how the soil is physically changing with moistening. Having the moisture content estimated from the colour reflectance, it can be substituted in a shear strength value equation (shear strength, shear cohesion, or internal friction angle) as function of moisture content for ending with the required shear strength value, also applicable infield, but under the condition that the physical status of the soil infield is similar to the tested in the laboratory (loose soil in this project).

The linearity of the Mohr-Coulomb failure was clarified based on empirical work, and it is that the Mohr-Coulomb line (the linear equation) is applicable in a normal stress range (range relative to normal stresses used for finding the shear strength parameters), due to the influence that might result from the normal stress (initially before shearing) on the cohesion.

Dealing with soil from mechanics perspective for finding its shear strength parameters at a shearing speed that might be helpful in terramechanics study case, was given in a chapter. This method splits the shear strength to two terms, the shear cohesion and the friction, with finding each of the them in a separate measurement at the required speed.

Finally, as the main target is achieved, and is determining the shear strength or it parameters from the colour reflectance, this step will serve in saving time, cost, and effort. When it comes to finding the moisture content or the required shear strength value infield, this work will be performed using a remote sensor, thus no strength machines or instruments, or a moisture analyzer to be used infield. In vehicle mobility study science, with this reached target, a step is leaped for enhancing the mobility of a vehicle on soil terrains, thus at least taking the no-go decision to avoid having the vehicle getting stuck infield incase of not adjusting the tractive element contact patch area or its driving torque.

9. New scientific findings

As the main target behind the research work is to relate the soil shear strength values to its colour, new important scientific results were reached during dealing with the project, and the most important scientific findings are *(5 scientific findings)*:

9.1- The reflectance at 700 nm is used for predicting the moisture content from the colour.

Determining the correlation between the spectrophotometric colour reflectance records and the moisture content of the soil. Plotting the reflectance colour records at the **wavelength 700 nm as function of moisture content**, the equation of the curve fitting the plotted points with the best regression analysis is a reliable equation to estimate the moisture content from the colour reflectance of the soil.

I obtained the connection that relates the colour to the moisture content of the soil as a preliminary step for connecting the colour to the shear strength *(scientific finding 9.4)*. Based on my measurements, I state reaching the ability of estimating (predicting) the moisture content from the colour in a visually homogenous soil (no impurities and vegetation). I measured the colour using a visible range spectrophotometer (measures in the visible spectrum). Five different soil textures were tested.

Dealing with the records taken by the spectrophotometer mathematically and empirically by plotting different reflectance parameters at different moisture contents, I was able to reach the reliable curve (for each tested soil) that relates the colour to the moisture content, which based on it the moisture content is estimated.

Each soil has its initial colour when dry, and has its colour (reflectance) change behaviour (colour change tendency) with moistening. The amount of moisture a soil holds from humidity (when dry) differs from a type (specified by texture) to another, that is why the starting soil moisture content differs in the measurements, also the soil moisture content at saturation level (approximately maximum moisture content reached in each colour measurement) is affected by the type (curves below; findings in 9.2).

9.2- The reflectance-moisture content curve tendency changes with the change in the soil texture (type).

a- Colour-moisture curve tendency in loam sand soil (the tendency is showing stability in the reflectance beyond a moisture value).

By relating the colour to the moisture content, I figured out that the soil texture (mainly the type which is based on texture) plays an important role in the colour-moisture curve tendency, this can be recognized in the tested soils, and among them the loam sand soil. Figure 9.1 shows the curve tendency of the tested loam sand soil.

In the loam sand soil, the tendency of the curve has shown a decrease in the reflectance (on average) with the increase in the moisture content, and this is applicable till a certain moisture range (around 6 % moisture content), and beyond this range the reflectance becomes constant. The tendency is shown in Figure 9.1. For resulting with the best curve fitting of the best regression analysis, the constancy part was removed and the equation of the

curve in the first moisture range was taken into account as the reliable equation for estimating the moisture content from the colour reflectance.

I have reached out that in the first moisture range the colour reflectance is decreasing with the increase in the moisture content (on average) due to the darkening in the soil colour, but beyond approximately 6 % moisture content, the results become constant (visually stable colour).

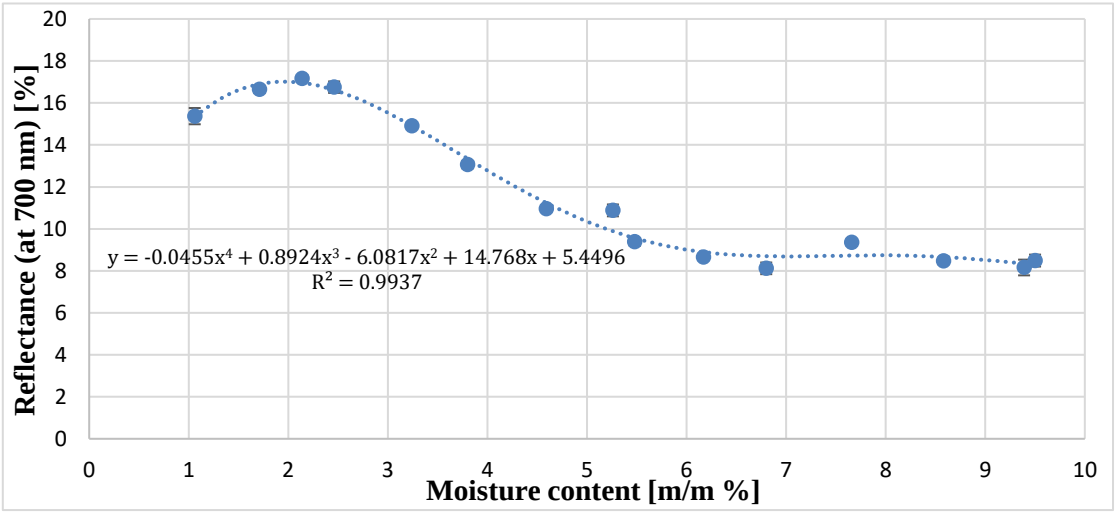

Fig. 9.1. Colour reflectance (at 700 nm) as function of moisture content, loam sand soil (90.50 % sand, 3.20 % silt, 6.30 % clay), the equation is of the curve in the range 1.06 to 6.80 %.

The equation (of the curve in the range 1.06 to 6.80 %, Figure 9.1) was validated resulting in moisture values close to the moisture content obtained by the gravimetric measurement (moisture analyzer).

b- Colour-moisture curve tendency in silty clayey soils (the tendency is showing an increase in the reflectance at high moisture content).

Two of the investigated textures are silty clayey soils (embedding high amount of clay and silt in the texture), and based on the colour obtained results a new finding was reached out.

I have found that in silty clay soils (based on the tested textures), at high moisture content, the reflectance shows a slight increase, and that can be seen in Figure 9.2. Another silty clay soil texture was tested, its tendency is in chapter 4 (of similar curve tendency).

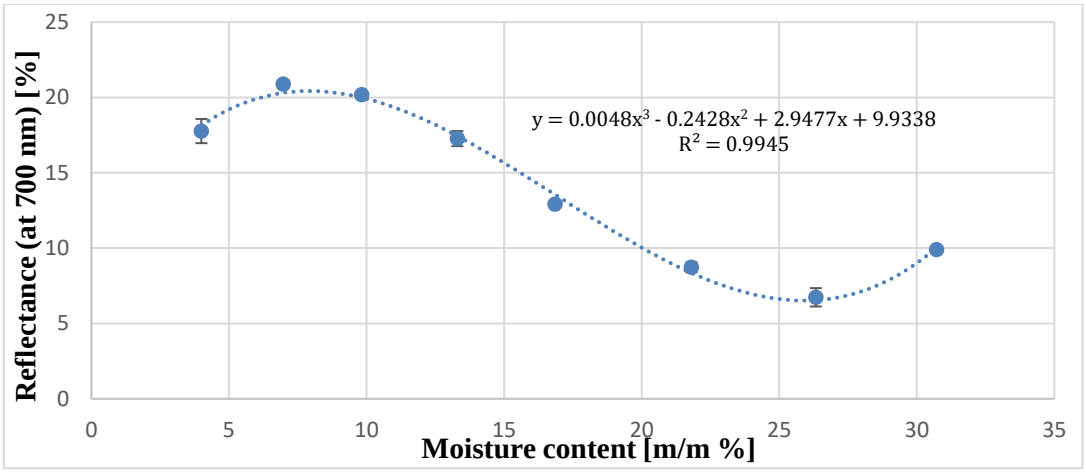

Fig. 9.2. Colour reflectance (at 700 nm) as function of moisture content, silty clay soil (3.34 % sand, 52.05 % silt, 44.61 % clay).

The presence of silt and clay, mostly clay, will lead to the particles bonding each other forming one face at high moisture content, the case that prevents (or decrease its ability) the spectrophotometric sent light wave from entering the particles' level and getting scattered and absorbed (maybe small portion), leading to increasing the reflectance. At high moisture contents (beyond the minimum point) the colour visually reaches stable level (pictures in the dissertation), and what dominates the reflectance of the sent light wave is the physical behaviour of the material (paste like material, which is not applicable in terramechanics), which becomes of high cohesion at the particles' level.

c- Colour-moisture curve tendency in sandy soils (the tendency is decreasing in logarithmic function).

I have reached based on the colour-moisture curves tendencies of the two tested sand soils, that with the increase in the moisture content, the reflectance keeps on decreasing (logarithmic change) despite the moisture content reached (close to saturation level). Figure 9.3 below shows the colour change tendency as function of moisture content. Another sand soil texture was tested, its tendency is in chapter 4 (of similar curve tendency).

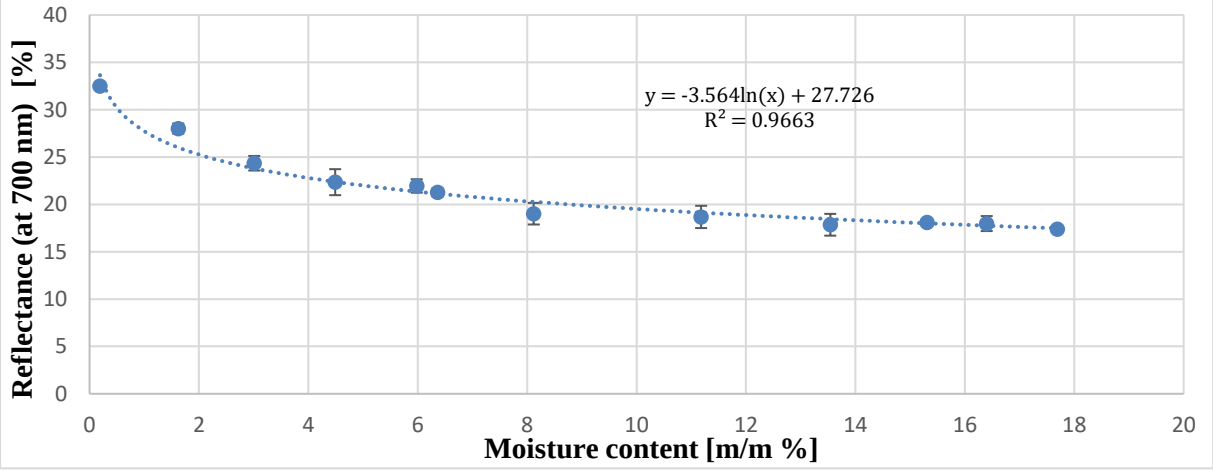

Fig. 9.3. Colour reflectance (at 700 nm) as function of moisture content, sand soil (94.53 % sand, 4.78 % silt, 0.69 % clay).

The tendencies in the two curves show that the colour of a sand texture (based on the tested soils) keeps on decreasing with moistening, meaning that the colour keeps on darkening (due to increase in absorbtivity) till reaching the moisture content close to the saturation level.

9.3- Determining the shear strength values of three soil types in undrained condition using the Mohr-Coulomb failure criterion, also reaching a new idea (with new design) for finding the shear strength parameters.

a- **I determined the shear strength parameters of three tested soil textures (loose soils, the physical status) using the direct shear test in undrained condition. I obtained that for finding the shear strength parameters by ending up with the Mohr-Coulomb line result (angle and intercepting the y-axis), the soil sample (each tested sample) should be of OCR >1.** Testing the soil samples with over consolidation ratio (OCR) above 1, which is the maximum effective stress that soil has experienced in the past over the current stress, is leading to realistic shear strength parameters' results at higher shearing speeds (compared to drained; 9 mm/min is used in the measurement) when loose soil is tested (my study case).

The direct shear test is geo-civil engineering test (but used in terramechanics), and for finding the shear strength parameters (cohesion and internal friction angle), this test should be carried out in drained condition (less than 1 mm/min shearing speed). The shear strength (alone and not the parameters) can be measured at any shearing speed, even if in undrained condition (higher speed), but upon plotting the shear strength results obtained under different consolidation stresses for reaching the Mohr-Coulomb line, the cohesion and the internal friction values might be unrealistic (such as negative cohesion or a high value).

The results (based on this finding) are ending up with accepted cohesion and internal friction angle curves' tendencies (plotted as function of moisture content) in the three tested soil types, knowing that finding the shear strength results at a shearing speed higher than in drained condition complies with vehicle mobility study cases (wheel/track shearing speed).

b- Since the usage of the Mohr-Coulomb line for finding the shear strength parameters is limited to testing the soil in drained condition (very low shearing speed), that case might not be too helpful in some terramechanics studies.

I ended up with a new method that based on it the shear strength parameters will be obtained from a mechanics perspective far from drawing the Mohr-Coulomb line. For shearing the soil and going over the resisting shear strength, two forces are needed (convert to stress), one for breaking the cohesion and the second for going over the friction resistance (due to the normal stress).

The new method sums the results of two measurements, one measurement results in the cohesive force (bonding) and the second in the friction resisting force.

From a mechanics side, I was able to find the cohesive bonding force by shearing a soil sample in the shear test machine (at a speed) with having no consolidation stress, the case that will cancel the friction term from the equation leading to just finding the cohesion in the soil (force over area, the cohesion in kPa). With this process the cohesion is obtained. For finding the friction term in the soil, normal stress multiplied by tangent friction angle $\boldsymbol{\sigma \cdot \tan\phi}$, the internal friction angle is needed. The friction angle at the shearing zone has to do with the friction between the contacting materials (in the soil shearing case, same soil type), and is independent of the applied stress.

I was able to end up with a design/idea for finding the friction angle, and it is by using two plastic cylinders and placing on each a double face tape. Face for sticking to the cylinder, and the second for placing a thin soil layer on (same for the second piece). The soil layers will contact each other at the shearing zone (at a speed that can be higher than the drained shearing speed), and a small mass (to avoid cohesion building up) as a normal stress (gravitational force over area) is applied during shearing the soil. The maximum recorded force is the friction resisting force that based on it and on the normal applied force the material friction angle can be obtained (friction force equalizes the friction coefficient μ multiplied by the normal force). Figure 9.4 below shows the design idea and the preparation steps. Friction results obtained from this finding are similar to the results obtained from the Mohr-Coulomb line.

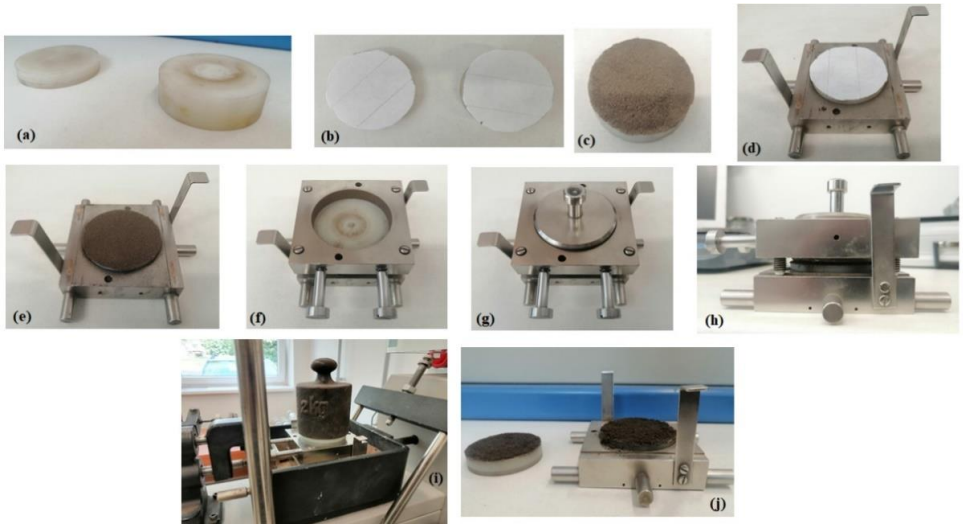

Fig. 9.4. (a, b) show the prepared teflon cylinders, with double face tape used on them, (c) shows the soil sticking on the other face of the tape, this sample is prepared for the upper frame, (d, e) lower frame teflon with soil prepared on it, (f, g, h) frame assembled, shearing zone seen in h, (i) Box installed in the shear machine with normal load applied - all masses applied are considered (with the teflon piece mass), (j) soil of high moisture content on the tape face.

9.4- Relating the shear strength values of a soil texture to its colour reflectance.

I have correlated the shear strength values to the colour of the soil. **Since the colour is plotted as function of moisture content, also the shear strength results, the cohesion, internal friction angle, and the shear strength are plotted as function of moisture content, thus the moisture content is in common.**

Having the moisture estimated from the colour-moisture curve *(scientific result 9.1)*, this moisture content can be substituted in the curves' equations of the shear strength values. Plotting the results of each strength value (shear strength, cohesion, and internal friction angle) as function of moisture content, will lead to ending up with the equation of the curve fitting the plotted results (function relating the strength term to the moisture content). These curves equations are reliable to substitute the estimated moisture content in, and thus predicting the shear strength values (or a required value) at the moisture content obtained from the colour reflectance. The flowchart in Figure 9.5 shows the correlation methodology.

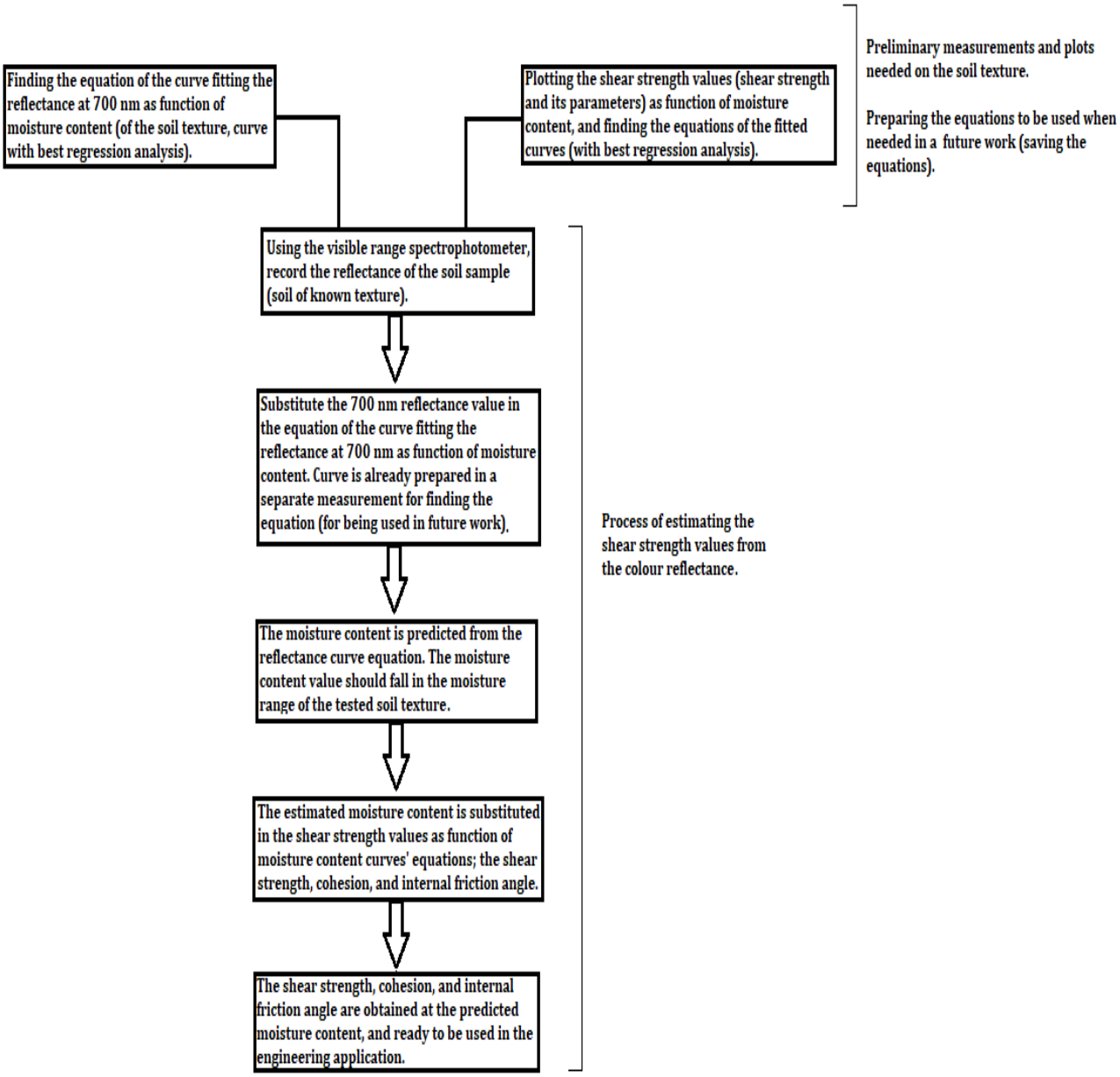

Fig 9.5. Flowchart showing the process followed for predicting the shear strength values from the colour reflectance.

9.5- Explaining/Elucidating the linearity of the Mohr-Coulomb failure criterion.

Clarifying the constancy in the Mohr-Coulomb diagram cohesion, which is applicable in a normal consolidation stress range.

I determined that the consolidation stress (as initial stress on a soil) affects the soil cohesion (affecting case explained below), recognized clearly on a loose soil, thus the incapability of relating the shear strength, at a normal stress, linearly to the shear strength, at another normal stress, of the soil that is of another cohesive strength (Mohr-Coulomb linearity).

I have checked the soil translational shear strength at different densities (using the direct shear machine at same shearing speed), and I obtained that the linearity of the Mohr-Coulomb failure is applicable in a normal stress range which is dependent on the actual applied normal stress

(for obtaining the shear strength under it). When it comes to relating a shear strength linearly to shear strengths obtained under different applied normal stresses (using the direct shear test) based on the cohesion and the internal friction angle, these parameters can be used to find the shear strength resulting under a mass that is of a value close the tested masses (converted to stresses, used for finding the parameters, fitting the Mohr-Coulomb line). For example, considering the mass range [30 kg to 90 kg], if finding the shear strength parameters using 40, 50, 60, 70 kg masses (stress, weight over the area, for the Mohr-Coulomb line), then the allowed mass to be used for predicting the shear strength from the parameters should fall in the mentioned range (for example under 90 kg).

The initial normal stress applied on the soil might (depends on normal stress) affect its cohesion (negative pore pressure), especially if the soil is loose (tilled), thus exceeding a certain normal stress range will lead to a recognized change in the cohesion affecting the linearity of the Mohr-Coulomb failure. Within a stress range, the cohesion change will be so small (neglected), thus not influencing the Mohr-Coulomb linearity (passing through the shear strength-normal stress plots of the close masses).

10. Suggestions for future work related to the research

a- Checking the validity of the colour reflectance (700nm)-moisture content curve reliable equation of each of the other soil textures infield. In the research, the reliable curve equation of the loam sand soil (university soil) was checked infield, and ended with moisture results that are close to the results obtained by the moisture analyzer.

b- It is mentioned that in the loam sand soil, the reflectance reaches constancy in the result beyond a moisture value, meaning that either the colour is no more changing with moisture content, or the used spectrophotometric measuring range (400-700 nm) is not ending with precise results beyond a moisture value in the tested soil, the case that bestirs to use another spectrophotometric range (beyond 700nm), the infrared range. Research is restricted to the usage of the visible range spectrophotometer.

c- It is mentioned in the colour reflectance chapter (chapter 4) that the reflectance reaches a peak value (the hump, check loam sand soil curve). To avoid the conflict when choosing the moisture content, the soil conductivity or resistivity should be measured at the peak reflectance moisture content, to be used as a border for choosing the right moisture content among the two choices.

d- The work has been carried out on each soil as a visually homogeneous material (sieved) for the sake of simplifying the case of study, since the correlation is a new idea (relating the mechanical properties to the colour reflectance), and the measurements were carried out on samples in the laboratory. Thus, it is suggested to carry out the reflectance measurement on the soil in its natural field condition for checking the deviation in the results, following the obtained colour-strength relating methodology.

e- For the mechanics perspective method used for finding the shear strength and parameters at higher shearing speed, it is suggested to be validated under higher masses relative to the mass used in the measurement. The new method was checked on soil in laboratory studycase, where the cohesion is built up under an applied mass (having the soil loose). Work should be checked on field samples of different physical conditions and at different shearing speeds.

f- The colour reflectance is related to the moisture content through direct process, so just dealing directly with the soil body. Infield there might be vegetation covering the surface, thus ideas should be settled prior to using the reached correlation finding in fields with vegetation. Also, the spectrophotometer lense should be inserted in the soil or used at the required depth, since the moisture content changes with depth infield and is not similar to the moisture content at the surface (mostly), the case that is different than the laboratory test where the prepared moistened soil sample holds approximately the same moisture amount.

11. Summary

In the literature review, the importance of studying the performance of a vehicle over soil terrain is considered, starting with an introduction showing the role of terramechanics science in studying the interaction between the vehicle and the terrain. The methods of approach for studying the vehicle interaction with the terrain are discussed, then the main target behind the research is mentioned (to be used in autonomous vehicles). Modelling the terrain behaviour is discussed, with how the terrain will behave upon being stimulated by an excitation load (from a wheel or track). The influence of moisture content on the soil properties is written in a section, and is based on results of researchers and scientists. The gravimetric method, the method that will be used for measuring the moisture content in soil samples, is mentioned in a paragraph explaining the method's working principle. The basic terramechanics instruments and machines used for measuring the terrain strength properties are mentioned, the cone penetrometer and the bevameter, in addition to mentioning the geo/civil engineering machines and instruments for measuring the shear strength of soil (also used in terramechanics), and are the direct shear test, in-situ shear vane, and the tri-axial test. Since the main target behind the research is relating the soil colour to its shear strength, a soil colour section is written showing the methods used for measuring the soil colour (Munsell chart and the spectrophotometer). The soil bearing capacity and shear strength are discussed in a section, where the bearing capacity is related to the speed of the vehicle (Grahn model based on Bekker's pressure sinkage relationship), and in the shearing strength part, some new inventions for measuring the soil shear strength are mentioned. The three element Maxwell model is used for calculating the normal stress distribution at the interaction zone (wheel/track and terrain), while the tangential stress distribution is calculated using analytical diagram of rigid wheel on soft terrain, relying on the Mohr-Coulomb model. Finally, numerical methods are discussed, with details on finite and discrete element methods, and findings of some researchers that used these methods are mentioned.

In chapter four, the colour reflectance results of five different soil textures were obtained using a visible range spectrophotometer, that measures in the spectrum range 400 to 700 nm. In each soil, dealing with the records taken by the spectrophotometer at different moisture contents mathematically and empirically, has led to ending up with the reliable curve that based on its equation the moisture content can be estimated. Plotting the reflectance at 700 nm as function of moisture content, the equation of the curve fitting the plots is the reliable equation to be used in predicting the moisture content. The curve's equation of each tested soil texture was validated.

In chapter five, the shear strength and its parameters of three soil textures were determined using the direct shear test in undrained condition. In each texture, for ending up with convincing shear strength parameters (having the soil moistened) that comply with the soil physical status, the soil was tested with an overconsolidation ratio above 1. This process was used on the three textures, and all have ended with realistic parameters' results.

In chapter six, the colour reflectance was correlated to the shear strength and its parameters. The moisture content is estimated from the colour reflectance-moisture curve (at 700 nm) by substituting a 700 nm colour reflectance record in the curve's equation. The estimated moisture content can be substituted in any shear strength value-moisture curve equation as input, thus predicting the shear strength value.

Field measurement was carried out for checking the validity of the reflectance-moisture curve equation (at 700 nm), the reliable equation, in the field. The field tested soil texture is the loam sand soil, the soil of the university's land. The field estimated moisture content results from the colour reflectance comply with the results measured using the gravimetric method (moisture analyzer).

The colour reflectance record at 700 nm, having the soil dry at approximately 0 % mc (dried by the moisture analyzer then taking the record), is saved in a database to be used in the future for predicting a soil texture (new field sample). The record is saved as a soil identity.

In chapter seven, a proposed mechanics method was used for measuring the soil shear strength parameters in undrained condition, the case that will help in having the shear strength parameters at a speed higher than the speed used in the standard direct shear test method (used in geo/civil engineering). Also, the applicability of the Mohr-Coulomb linearity was clarified (applicable in a normal stress range). With having the shear strength parameters at higher speed, the shear strength can be obtained at this speed under a consolidation stress (changeable normal stress).

Finally, a small conclusion on the research work is given with some suggestions to be condsidered in any upcoming research work related or close to this research.

11. Összefoglalás

A szakirodalmi részben áttekintettem a járművek terepen való haladásával kapcsolatos szakirodalmat. Bemutattam a talajmechanika szerepét a jármű és a terep kölcsönhatásában. Vizsgálat alá vettem a járművek és terepviszonyok kölcsönhatásának különböző megközelítési módszereit. Kutatásom fő célja az önvezető járművek irányító rendszeréhez szükséges bemeneti információval kapcsolatban a talaj nyírószilárdságának távérzékeléssel történő közvetett meghatározása. Bemutattam a terep viselkedésének modellezési lehetőségeit. Végül a nedvességtartalom talajmechanikai tulajdonságokra gyakorolt hatását is leírtam.

A negyedik fejezetben öt különböző textúrájú talaj színreflexiós eredményeit mutattam be a fény látható tartományban (400-700 nm), amelyet spektrofotométerrel határoztam meg. Minden egyes vizsgált textúrához különböző nedvességtartalom mellett mértem a színspektrumot. A mérési eredmények kiértékelése olyan empirikus összefüggésre vezetett, amely egyenlet alapján megbecsülhető az adott textúrájú talaj nedvességtartalma a színspektrum alapján. A nedvességtartalom előrejelzésére a 700 nm-en mért reflektancia görbék a legalkalmasabbak.

Az ötödik fejezetben három talajtextúrához tartozó nyírószilárdság értékeket és további talajmechanikai paramétereket közvetlen nyírási kísérlettel határoztam meg a talaj száraz állapotában. A talaj fizikaiállapotának megfelelő nyírószilárdsági paraméterek biztos meghatározásához a talajt egy feletti túlterhelési aránnyal vizsgáltam. Mindhárom textúra esetén reális paramétereket mértem.

A hatodik fejezetben a színreflexiót összepárosítottam a nyírószilárdsággal és annak paramétereivel. A nedvességtartalmat a színreflexió-nedvesség görbéből becsültem meg úgy, hogy a görbe egyenletébe a 700 nm-es színreflexiós adatokat helyettesítettem. A becsült nedvességtartalom bármely nyírószilárdság-nedvesség görbe egyenletébe behelyettesíthető bemenetként, így kiszámolható a nyírószilárdság értéke.

Terepi mérést végeztem a korábban laborban feltárt összefüggés terepen való érvényességének ellenőrzésére. A vizsgált talajszerkezet a vályogos homoktalaj volt, amely az egyetem területén található. A színreflexióból származó terepi becsült nedvességtartalom-eredmények megegyeznek a gravimetriás módszerrel (laboratóriumiban) mért eredményekkel.

A mért színreflexiós adatokat egy adatbázisba mentettem, amelyet a jövőben a talaj állapotának előrejelzésére használhatunk.

A hetedik fejezetben javaslok egy új mérési módszert a talaj nyírási paramétereinek mérésére, amely abban segít, hogy a nyírószilárdság paramétereit nagyobb nyírási sebességek mellet is meg lehessen határozni, szemben a hagyományos (földrajzi/építőmérnöki) közvetlen nyírási vizsgálati módszernél alkalmazott sebességnél. A Mohr-Coulomb linearitás alkalmazhatósági határait is tisztáztam.

Végül a következtetések és javaslatok fejezetben a kutatási munkához kapcsolódó tanácsokat és tanulságokat közlők, amelyeket érdemes figyelembe venni ezen kutatáshoz hasonló vizsgálatok során.

12. References

[1] Atkinson, J.H., and Lau, W.H.W., Measurement of soil strength in simple shear tests, Geotechnical engineering research centre, the City university, London EC1V 0HB, U.K., 1990.

[2] Ageikin, J.S., Physical and mathematical soil parameters for evaluation of wheeled vehicle-terrain interaction, In International Symposium "Optimal Interaction", Russian Terramechanics Committee: Syzdal, pp. 3-9, Russia, 1992.

[3] Ageikin, J.S., Off-the-road wheeled and combined traction devices: theory and calculation, Amerind Pub. Co., New Delhi, India, 1987a.

[4] Ageikin, J.S., Off-the-road mobility of automobiles, Amerind Pub. Co., New Delhi, India, 1987b.

[5] American Society of Agricultural Engineers, Soil cone penetrometer, recommendation ASAE R313, Agricultural engineers yearbook, Am. Soc. Agric. eng., St. Joseph, pp. 296-297, 1969.

[6] Abeels, P., and Declercq, D., La lacomotion tout terrain. la compaction du sol, (Off-road locomotion and soil compaction) rev. Agric., 1, 131-150, 1977.

[7] Aitkenhead, M., Coull, M., Towers, W., Hudson, G., Black, H., Prediction of soil characteristics and colour using data from the national soils inventory of Scotland, Geoderma 200-201, 99-107, 2013.

[8] Agui, J.H., Bucek, M., DeGennaro, A., Wilkinson, R. A., Zeng, X., Lunar excavation experiments in simulant soil test beds: revisiting the surveyor Geotechnical data, J. Aerosp. Eng, 26, 117-133, special issue: in situ resource utilization, 2013.

[9] Abo-elnor, M., Hamilton, R., Boyle, J.T., Simulation of soil-blade interaction for sandy soil using advanced 3D finite element analysis, Soil Tillage res. 75 (1), 61-73, 2004.

[10] Ayers, P.D., Moisture and density effects on soil shear strength parameters for coarse grained soils, Trans. Am. Soc. Agric. Engrs, 30 (5), 1282-1287, 1987.

[11] Angelopoulou, T., Balafoutis, A., Zalidis, G., Bochtis, D., From laboratory to proximal sensing spectroscopy for soil organic carbon estimation - a review, Sustainability 12, 433, 2020.

[12] Al-Abbas, A.H., Swain, P.H., Baumgardner, M.F., Relating organic matter and clay content to the multi-spectral radiance of soils, Soil Sci. 1972, 114, 477-485.

[13] Ahmed, A.E.E., El Hariri, A., Kiss, P., Soil spectral behavior related to its load-bearing capacity based on moisture content, Applied Sciences, 13, 3498, 2023.

[14] Ahmed, A.E.E., El Hariri, A., Kiss, P., Soil strength and load bearing capacity measurement techniques, HAE 2021, 40, 16-27.

[15] ASTM D3080/D3080M-23, Standard test method for direct shear test of soils under consolidated drained conditions, American Society for Testing and Materials, Book of standards vol 04.08, last update 06 Dec 2023.

[16] Baladi, G.Y., Terrain evaluation for off-road mobility, J. Terramechanics, 24, 127-157, 1987.

[17] Baladi, G.Y., and Meier, R.W., General soil model for calculating tractive forces between the terrain and a given vehicle, proc. 9th int. conf. ISTVS, Barcelona. pp. 826 833, 1987.

[18] Bekker, M.G., Theory of land locomotion, University of Michigan Press, Ann Arbor. Michigan, 1956.

[19] Bekker, M., Terrain evaluation in automotive off-the-road operations, SAE technical paper 570340, 1957.

[20] Bekker, M. G., Off-the-road locomotion: research and development in terramechanics, Ann Arbor, USA, University of Michigan, 1960.

[21] Bekker, M.G., Introduction to terrain-vehicle systems, University of Michigan Press, Ann Arbor, Mi, 846 pp, 1969.

[22] Bhadra, S.K., and Bhavanarayana, M., Estimation of the Influence of soil moisture on soil color, division of agricultural physics, Indian Agricultural Research Institute, India, New Delhi, J. of Plant Nutrition and Soil Science, volume 160, p. 401-405, 1997.

[23] Bell, F.G., Engineering Geology, Rock properties and their assessment, Butterworth-Heinemann is an imprint of Elsevier, 2007 (second edition).

[24] Brady, N., and Weil, R., Elements of the nature and properties of soils, Pearson Prentice Hall: Boston, Ma, USA, 2008.

[25] Bloch, I., Hosen, J., Kracht, E., Lefebvre, M., Jazmine-Lopez, C., Woodcock, R., Keegan, W., Is it better to be objectively wrong or subjectively right?: testing the accuracy and consistency of the Munsell capsure spectrocolorimeter for Archaeological applications, adv. Archaeol. pract, 9, 132-144, 2021.

[26] Bentaher, H., Ibrahmi, A., Hamza, E., Hbaieb, M., Kantchev, G., Maalej, A., Amold, W., Finite element simulation of moldboard-soil interaction, Soil Till res. 134, 11-16, 2013.

[27] Bishop, A.W., Alpan, I., Blight, G.E., Donald, I.B., Factors controlling the strength of partly saturated cohesive soils. In Research Conference on Shear Strength of Cohesive Soils; American Society of Civil Engineers: Boulder, CO, USA, pp. 503-532, 1960.

[28] Bishop, A.W., and Heknel, D.J., The measurement of soil properties in the triaxial test, Edward Arnold, London, 1964.

[29] Blaisdell, G.L., Chamberlain, E.L., Mellor, M., Evaluation of the cold regions aspects of mobility and hardening of the mobile test bed at Malmstrom Air Force base, Final report for U.S. air force ballistic missile office, 1987.

[30] Bowers, S.A., and Hanks, R.J., Reflection of radiant energy from soils, Soil Science, 100 (2), 30-138, 1965.

[31] Boussinesq, J., Application des potentials a l'etude de l'equilibre et due mouvement des solides elastique, Gauthier-Villars, Paris, 1885.

[32] Berenyi, T., and Pershing, R. L., and Romig B.E., Vehicle Mission Simulation, SAE Mississippi Valley Section Meeting, 1972.

[33] Baumgardner, M.F., Sylva, L.F., Biehl, L.L., Stoner, E.R., Reflectance properties of soil, Advances in Agronomy, 38, 1-44, 1985.

[34] Coulomb, C.A., Essai sur une application des regles des maximis et minimis a quelques problemes de statique relatifs a l "A r c h i e c t u r e" Mem. acad. roy. pres divers savants, vol.7. Paris, 1776.

[35] Changbin, H., Yong, Y., Decheng, W., Hongjian, W., Estimating soil failure due to torsion via vane shear test by varying vane diameter and soil properties, Soil and Tillage research 177 68-78, 2018.

[36] Chew, S., Bharati, K., Chua, K., Lim, J., Effect of large diameter sample testing for offshore site investigation, Housing Development Board, Singapore, 2011.

[37] Cundall, P.A., Strack, O.D.L., A discrete numerical model for granular assemblies, Géotechnique 28 (1), 47-65, 1979.

[38] Chamberlain, E.J., Mellor, M., and Abele, G., Frozen ground strength characterization and grouser cutter design for hardening transition, and mobility over snow-covered terrain for the mobile test bed, draft report to U.S. air force, ballistic missile office, 1988.

[39] Carter, W.T., Color analysis with spectrophotometer, Amer. Soil Surv. Assoc. Bull., 12, 169-170, 1931.

[40] Dudzinski, P.A, Steering: state-of-the-art report, J. Terramechanics, 21, 215-235, 1984.

[41] Dudzinski, P.A., and Damian, S., Method for predicting dynamic shear strength in soils-part ii:validation of the new criterion using an innovative test device, Journal of Terramechanics 86, 39-46, 2019.

[42] Damian, S., Dudzinski, P.A., Soil shear strength determination methods - state of the art, Soil and Tillage research 208, 104881, 2021.

[43] Dafalla, M.A., Effects of clay and moisture content on direct shear tests for clay-sand mixtures, Adv. Mater. Sci. Eng., 1-8, 2013.

[44] Dwyer, M.J., Comely, D.R., Everaden, D.W, The field performance of some tractor types related to soil mechanical properties, J. Agric res., 19, 35-50, 1974.

[45] Deepak, A.M., and Ivan, J., Laboratory triaxial testing - from historical outlooks to technical aspects, Procedia Engineering 191, 342-351, 2017.

[46] Dickinson, J., Zuckerberg, B., Bonter, D., Citizen science as an Ecological research tool: challenges and benefits, 41, 149-172, 2010.

[47] Doi, R., Wachrinrat, C., Teejuntuk, S., Sakurai, K., Sahunalu, P., Semiquantitative colour profiling of soils over a land degradation gradient in Sakaerat, Thailand. Environ. Monit. Assess, 170, 301-309, 2010.

[48] Dimitrios, Z., George, A.A., Jonathan, D.B., Athena, G., Andreas, T., Large-scale direct shear testing of municipal solid waste, Waste Management 30, 1544-1555, 2010.

[49] Das, B., Shallow foundations: bearing capacity and settlement, CRC press, 1999.

[50] El Hariri, A., Ahmed, A.E.E., Kiss, P., Sandy loam soil shear strength parameters and its color, Appl. Sci., 13, 3847, 2023a.

[51] El Hariri. A., Kiss. P., Soil shear strength values obtained from its color, 16th European-African Regional Conference of the ISTVS, Poland, 2023b.

[52] El Hariri, A., Ahmed, A.E.E., Kiss, P., Review on soil shear strength with loam sand soil results using direct shear test. J. Terramechanics, 107, 47-59, 2023c.

[53] Freitag, D.R., A dimensional analysis of the performance of pneumatic tires on soft soils, Tech. Rep. no. 3-688, U.S. army engineer waterways Exp. Stat., Vicksburg, Ms, 141 pp, 1965.

[54] Franco, Y., Rubinstein, D., Shmulevich, I., Prediction of soil-bulldozer blade interaction using discrete element method, Trans, ASABE, 50 (2), 345-353, 2007.

[55] Fervers, C.W., Improved FEM simulation model for tire-soil interaction, Journal of Terramechanics, 41(2 & 3), 87-100, 2004.

[56] Franzmeier, D.P., and Yahner, J.E., Steinhardt, G.C., Sinclair Jr., H.R., Color patterns and water table levels in some Indiana soils, Soil Sci. Soc. Am. J., 47, 1196-1202, 1983.

[57] Gee-Clough, D., The Bekker theory of rolling resistance amended to take account of skid and deep sinkage, J. Terramechanics, 13, 87-105, 1976.

[58] Gee-Clough, D., Mcallister, M., Pearson, G., and Everaden, D.W., The empirical prediction of tractor-implement field performance, J. Terramechanics 15 (2), 81-94, 1978.

[59] Gee-Clough, D., The effect of wheel width on the rolling resistance of rigid wheels in sand, J. Terramechanics, 15, 161-184, 1978.

[60] Gholizadeh, A., Saberioon, M., Viscarra Rossel, R., Boruvka, L., Klement, A., Spectroscopic measurements and imaging of soil colour for field scale estimation of soil organic carbon, Geoderma, 357, 113972, 2020.

[61] Gómez-Robledo, L., López-Ruiz, N., Melgosa, M., Palma, A., Capitan-vallvey, L., Sánchez-marañon, M., Using the mobile phone as Munsell soil-colour sensor: an experiment under controlled illumination conditions, Comput. Electron. Agric, 99, 200-208, 2013.

[62] Golob, T.B., Development of a terrain strength measuring system, Journal of Terramechanics, 18(2), 109-118, 1981.

[63] Grahn, M., The influence of penetration velocity on the pressure sinkage relationship, Proc. 4th European conf. ISTVS, Wageningen, Netherlands, vol. i, pp. 54-61, 1989.

[64] Grahn, M., Prediction of sinkage and rolling resistance for off-the-road vehicles considering penetration velocity, Journal of Terramechanics, vol. 28, no. 4, pp. 339-347, 1991.

[65] Grujicic, M., Marvi, H., Arakere, G. and Haque, I., A finite element analysis of pneumatic-tire/sand interactions during off-road vehicle travel, Multidiscipline Modeling in Materials and Structures, vol. 6 No. 2, pp. 284-308, 2010.

[66] Goriatchkin, V.P., Harvester wheels [orig. in Russian: Kolesa zhatvennih mashin]. Sob. Soch., Moscow, 1937.

[67] Harrison, W.L.Jr., Soil strength prediction by use of soil analogs, in Proc. Hist. Environ. Sci, Ann. Tech. Mtg, San diego, CA, pp. 577-581, 1966.

[68] Hernanz, J.L., Peixoto, H., Cerisola, C., Sánchez-girón, V., An empirical model to predict soil bulk density profiles in field conditions using penetration resistance, moisture content and soil depth. J. Terramech. 37 (4), 167-184, 2000.

[69] Hiroma, T., and Ota, Y., Analysis of normal stress distribution under a wheel using viscoelastic-model of soils, Proc. 10 th int. conf. of the ISTVS, Kobe, Japan, vol. 1,24, 1990.

[70] Hemmat, A., Nankali, N., Aghilinategh, N., Simulating stress–sinkage under a plate sinkage test using a viscoelastic 2d axisymmetric finite element soil model, Soil Till, 107-166, 2012.

[71] Hallquist, J.O., Nike3d - An implicit, finite-deformation finite element code for analyzing the static and dynamic response of three-dimensional solids, University of California, Lawrence Livermorenational laboratory, report UCID-18822, 1981.

[72] Hallquist, J.O., Nike3d - A vectorized implicit, finite deformation finite element code for analyzing the static and dynamic response of 2-d solids with interactive rezoning and graphics, University of California, Lawrence Livermore National Laboratory, report UCID-19677, 1983.

[73] Hao, L., and Christian, S., Analysis of soil compaction and tire mobility with finite element method, Proc imeche part k: Journal of multi-body dynamics227(3), 275-291, IMechE, 2013.

[74] Hu, W., Dano, C., Hicher, P.Y., Le Touzo, J.Y., Derkx, F., Marliot, E., Effect of sample size on the behavior of granular material, Geotech. Testing J., 34 (3), 1-12, 2011.

[75] HE 53 Halogen moisture analyzer user manual, Mettler-Toledo GmbH, Switzerland, 2021.

[76] He, R., Sandu, C., Khan, A.K., Glenn Guthrie, A., Schalk Els, P., Hamersma, H.A., Review of terramechanics models and their applicability to real-time applications. J. Terramechanics, 81, 3-22, 2019.

[77] Hoffer, R. M., and Johannsen, C.J., In "Remote Sensing in Ecology" (P.L. Johnson, ed.), Athens, Univ. Of Georgia Press, pp. 1-29, 1969.

[78] Hilf, J.F., An investigation of pore water pressure in compacted cohesive soils, University of Colorado at Boulder: Denver, CO, USA, 1956.

[79] IUSS working group (WRB), World reference base for soil resources, World Soil Resources reports no. 103, FAO: Rome, Italy, 2006.

[80] IUSS Working Group WRB, World reference base for soil resources 2014, update 2015, International soil classification system for naming soils and creating legends for soil maps, World Soil Resources Reports no. 106. FAO, Rome, 2015.

[81] Janosi, Z., and Hanamoto, B., The analytical determination of drawbar pull as a function of slip for tracked vehicles in deformable soils, Proc. 1st int. conf., Soil-Vehicle Mechanics, Torino, pp. 707-736, 1961.

[82] Karafiath, L.L., Analysis of stress distribution beneath wheels by the theory of plasticity with respect to Lunar locomotion, Proc. ISTVS-TRW off-road mobility Syrup, Los Angeles, CA, 1970.

[83] Karafiath, L.L., and Nowatzki, E.A., Soil mechanics for off-road vehicle engineering, Trans. Tech Publ., Clausthal, Germany, 515 pp, 1978.

[84] Kurtay, T., and Reece, A.R., Plasticity theory and critical state soil mechanics, Journal of Terramechanics, 7(3 & 4), 23-56, 1970.

[85] Komandi, G., On the mechanical properties of soil as they affect traction, Journal of Terramechanics, vol. 29, no. 4/5, pp. 373-380, 1992.

[86] Konen, M., Burras, C., Sandor, J., Organic carbon, texture, and quantitative colour measurement relationships for cultivated soils in north central Iowa, Soil Sci. Soc. Am. J., 67, 1823, 2003.

[87] Kirillova, N., Vodyanitskii, Y., Sileva, T., Conversion of soil colour parameters from the Munsell system to the CIE-LAB system, Eurasian Soil Sci. 48, 468-475, 2014.

[88] Kirillova, P., Zhang, Y., Hartemink, A.E., Zhulidova, D.A., Artemyeva, Z.S., Khomyakov, D.M., Calibration methods for measuring the color of moist soils with digital cameras, CATENA, volume 202, 2021.

[89] Kogure, K., and Sugiyama, N., A study of soil thrust exerted by a tracked vehicle, J. Terramechanics, 12, 225-238, 1975.

[90] Kogure, K., Yamaguchi, H., and Ohira, Y., Comparison of strength and soil thrust characteristics among different soil shear tests, J. Terramechanics, 25 (3), 201-221, 1988.

[91] Kolk, H., Hoope, J., Ims, B., Evaluation of offshore in-situ vane test results, vane shear str. test, Soils: field lab, stud, 339-353, 1988.

[92] Kantaris, P. F. H., The universal equation solver by basic, Keigaku publishing, Tokyo, 1987.

[93] Kahle, G.W., and Hung, H. M., Economic assessment of turbine powered industrial vehicles, SAE Trans. 75 Paper 66-6-5, 1967.

[94] Kim, J., Hwang, H., Lee, H., Park, Y., Development of DEM–ANN-based hybrid terramechanics model considering dynamic sinkage, J. Terramechanics, 116, 2024.

[95] Laib, L., Analysis of the vibration-excitation effect caused by deformable soil surfaces, Journal of Terramechanics, volume 32, issue 3, pages 151-163, May 1995.

[96] Liljedahl, J. B., Carlenton, W. M., Turnquist, P. K., Smith, D.W., Tractors and their power unit, 3rd edn. John Wiley & sons, New York, p. 237-239, 1979.

[97] Lambe, W., Soil testing for engineers, New York, 1964.

[98] Liles, G., Beaudette, D., O-geen, A., Horwath, W., Developing predictive soil c models for soils using quantitative colour measurements, Soil Sci. Soc. Am. J., 77, 2173-2181, 2013.

[99] Landry, H., Lague, C., Roberge, M., Discrete element modelling of machine-manure interactions, Comput. Electron. Agric. 52, 90-106, 2006.

[100] Liu, C.H., and Wong, J.Y., Numerical simulations of tire-soil interaction based on critical state soil mechanics, Journal of Terramechanics, 33(5), 209-221, 1996.

[101] Liu, C.H., Wong, J.Y., Mang, H.A., Large strain finite element analysis of sand: model, algorithm and application to numerical simulation of tire-soil interaction, Computers and Structures, 74, 253-265, 2000.

[102] Liu, Y., Qiu, M., Liu, C., Guo, Z., Big data challenges in ocean observation: a survey, Pers. Ubiquitous Comput, 21, 55-65, 2017.

[103] Lyne, P.W.L., and Burt, E.C., Real time optimization of tractive efficiency, ASAE paper No.87-1624, 1987.

[104] Liston, R.A., The land locomotion laboratory, Journal of Terramechanics, volume 2, Issue 4, Pages 69-81, 1965.

[105] Lan, Q., Wang, Z., Ding, L., Yang, H., Gao, H., Richter, L., Deng, Z., DEM simulation and continuation algorithm of granular physical field for planetary wheel-terrain interaction, Powder Technology, 433, 2024.

[106] Mohr, O. Welche Umstände bedingen die Elastizitätsgrenze und den Bruch eines Materials? Z. Ver. Dtsch. Ing., 44, 1524-1530, 1900.

[107] Mulqueen, J., Stafford, J.V., Tanner, D.W., Evaluation of penetrometers for measuring soil strength. J. Terramechanics, 14, 137-151, 1977.

[108] Murakami, H., Terrain evaluation-ii, Journal of Terramechanics, vol. 28, no. 2/3, pp. 123-135, 1991.

[109] Máthé, L., and Kiss, P., Determination of rolling losses of a towed vehicle, In proceedings of the 13th ISTVS European conference, Rome, October 21-23, 2015.

[110] Meirion-griffith, G., and Spenko, M., A modified pressure-sinkage model for small rigid wheels on deformable terrains, J. Terramech. 48 (2), 145-155, 2011.

[111] Mobility and Environmental Systems Laboratory (U.S.), Studies of aerial cone penetrometer, report 2, field tests, U.S army engineer Waterways Experiment Station, Vicksburg, Mississippi, 1958.

[112] Meyer, M.P., and Knight, S.J., Trafficability of soils: soil classification, U.S. army engineer, Waterways Experiment Station, Vicksburg, Mississippi, 1961.

[113] Meyer, M.P., Ehrlich, I.R., Sloss, D., Murphy, N.R., Jr., Wismer, R.D., Czako, T., International society for terrain-vehicle systems standards, Journal of Terramechanics, 14(3), 153-182, 1977.

[114] Marqués-mateu, A., Moreno-ramón, H., Bbalasch, S., Ibáñez-asensio, S., Quantifying the uncertainty of soil colour measurements with Munsell charts using a modified attribute agreement analysis, CATENA, 171, 44-53, 2018.

[115] Mouazen, A., Karoui, R., Deckers, J., De Baerdemaeker, J., Ramon, H., Potential of visible and near-infrared spectroscopy to derive colour groups utilising the Munsell soil colour charts, Biosyst. Eng, 97, 131-143, 2007.

[116] Morris, R., Spectrophotometry, Curr. Protoc. Essential lab. tech. 11:2.1.1-2.1.30, 2015.

[117] Momozu, M., Oida, A., Yamazaki, M., Koolen, A.J., Simulation of a soil loosening process by means of the modified distinct element method, J. Terramech, 207-220, 2003.

[118] Muro, T., Tractive performance of a bulldozer running on weak terrain, J. of Terramechanics, vol. 26, no. 3/4, pp. 249-273, 1989.

[119] Mootaz, A.E., Hamilton, R., Boyle, J.T., Simulation of soil-blade interaction for sandy soil using advanced 3d finite element analysis, Soil Till. res. 75, 61-73, 2004.

[120] Mak, J., Chen, Y., Sadek, M.A., Determining parameters of a discrete element model for soil-tool interaction, Soil Tillage res. 118, 117-122, 2012.

[121] Micklethwait, E.W.E., Soil Mechanics in Relation to Fighting Vehicles, British School of Tank Technology, Military College of Science, 1944.

[122] McKeys, E., Soil Cutting and Tillage, Elsevier Science Publishers B.V., Amsterdam, 1985.

[123] Munsell Color, Munsell Soil Color Charts, Machbeth Div. of Kollmorgen Corp: Baltimore, MD, USA, 1975.

[124] Mokma, D.L., Water tables and color patterns in sandy soils in Michigan, Soil Surv. Horiz., 38, 54-59, 1997.

[125] Muller, E., Decamps, H., Modeling soil moisture-reflectance, Remote Sensing of Environment, vol. 76 (n°2), pp. 173-180, 2001.

[126] Nakashima Y., Fujii H., Sumiyoshi S., Wight T.N., Sueishi K. Early human atherosclerosis: accumulation of lipid and proteoglycans in intimal thickenings followed by macrophage infiltration, Arterioscler Thromb Vasc Biol., 27(5):1159-65, 2007.

[127] Oida, A., Study on equation of shear stress-displacement curves., J. Jpn. Soc. Agric., 37, 20-25, 1975.

[128] Oida, A., Soil Rheology in Terramechanics, Journal of the Japanese Society of Agricultural Machinery, 41(3), 369-373, 1986.

[129] Osman, M.S., The measurement of soil shear strength, Journal of Terramechanics, volume 1, issue 3, pages 54-60, 1964.

[130] Pershing, R. L., Simulating tractive performance, Earthmoving industry conference, Central Illinois Section, Peoria, Illinois, April 5-7, 1971.

[131] Pan, J., The general Rheological model of paddy soil in south China, Journal of Terramechanics, 23(2), 59-58, 1986.

[132] Pokrovski, G.I., Issledovanie no Fizike Gruntov, CHT: Moscow, Russia, 1937.

[133] Persson, M., Estimating surface soil moisture from soil color using image analysis, Vadose Zone J., 4 (4), 1119-1122, 2005.

[134] Post, D.F., Levine, S.J., Bryant, R.B., Mays, M.D., Batchily, A.K., Escadafal, R., Huete, A.R., Correlations between field and laboratory measurements of soil color, In: Bigham, J.M., Ciolkosz, E.J. (Eds.), Soil Color. Soil Science Society of America, Madison, WI, pp. 35-50, 1993.

[135] Perumpral, J. V., Liljedahl, J. B., Perloff, W. H., A numerical method for predicting the stress distribution and soil deformation under a tractor wheel, Journal of Terramechanics, 8(1), 9-22, 1971.

[136] Payne, .P.C.J., The relationship between the mechanical properties of soil and the performance of simple cultivation implements, Jou. Agric. Engr. research, vol.1, 1956.

[137] Prandtl, L.,"Über die Härte plastischer Körper" Nachr. Ges. Wiss. Goettingen, 1920.

[138] Pillinger, G., Kiss, P., Géczy, A., Hudoba, Z., Determination of soil density by cone index data, Journal of Terramechanics 77, 69-74, 2018.

[139] Perdok, U.D., A prediction model for the selection of tyres for towed vehicles on tilled soil, J. Agric. Eng. res., 23, 369-383, 1978.

[140] Raper, R. L., Johnson, C. E., Bailey, A. C., Coupling normal and sheaing stresses to use in finite element analysis of soil compaction, ASAE paper no. 90-1086, 1990.

[141] Reece, A.R., Problems of soil vehicle mechanics, U.S. army O.T.A.C. Land Locomotion laboratory report, 1964.

[142] Reece, A. R., and Peca, J. O., An assessment of the value of the cone penetrometer in mobility prediction, Proceedings of the 7th international conference of the international society for terrain–vehicle systems, iii, a1-a33, 1981.

[143] Roscoe, K. H., Schofield, A.N., Wroth, C. P., On yielding of soils, Geotechnique, 8(1), 22-53, 1958.

[144] Ralph, A., and Volker, W., An empirical method of predicting traction, Journal of Terramechanics, vol. 29, no. 4/5, pp. 381-394, 1992.

[145] Rabenhorst, M., Schmehling, A., Thompson, J., Hirmas, D., Graham, R., Rossi, A., Reliability of soil colour standards, Soil Sci. Soc. Am. J, 79, 193-199, 2015.

[146] Rajapakse, R.A., Geotechnical engineering calculations and rules of thumb, Butterworth-Heinemann, 2015.

[147] Sitkei, G.Y., Die viskoelastischen Eigenschaften von Ackerböden und deren Einfluss auf die Boden-Rad Wechselwirkung, In: Proceedings of the 4th. Int. Conf. of the ISTVS, Stockholm, 1972b.

[148] Sitkei G.Y., Non-linear viscoelastic-plastic model describing compaction processes, In: Proc. of 2nd IFAC/IMACS Conf., pp. 105-112, 1997.

[149] Sitkei G., Further studies on the characterization of wood colors, Department of wood engineering, University of Sopron, Hungary, 2020.

[150] Salman, N.D., and Kiss, P., Survey: Effect of bulk density and moisture content of soil on the penetration resistance and penetration depth, MEL, 17, 109-118, 2018.

[151] Sallberg, R.J., Shear Strength, U.S Department of Transportation, Bureau of Public Roads: Washington, WA, USA, 1965.

[152] Sun, D., Yao, Y.P., Matsuoka, H., Modification of critical state models by Mohr-Coulomb criterion, Mech. Res.Commun, 33, 217-232, 2006.

[153] Sugiyama, N., and Kondo, H., Basic study in the turning resistance of track, Proc. 8th int. conference of ISTVS, Cambridge, 1984.

[154] Sohne, W., Fundamentals of pressure distribution and soil compaction under tractor tires and 290, Agricultural Engineering, 39, 276-281, 1958.

[155] Schofield, A.N., and Wroth, C. P., Critical state soil mechanics, McGraw-Hill, London, 1968.

[156] Shoop, S.A., Thawing soil strength measurements for predicting vehicle performance, Journal of Terramechanics, vol. 30, no. 6, pp. 405-418, 1993.

[157] Shoop, S.A, Terrain characterization for trafficability, CRREL report 93-6, 1993a.

[158] Sela, A.D., and Ehrlich, I.R., Load support capability of flat plates of various shapes in soils, Journal of Terramechanics 8, 39-69, 1972.

[159] Society of Automotive Engineers, Off-road vehicle mobility evaluation, SAE j939, handbook supplement, SAE international, New York, 1967b.

[160] Smith, P., Soussana, J., Angers, D., Schipper, L., Chenu, C., Rasse, D., Batjes, N., Egmond, F., Mcneill, S., Kuhnert, M., et al., How to measure, report and verify soil carbon change to realize the potential of soil carbon sequestration for atmospheric greenhouse gas removal, Glob. Chang. Biol, 26, 219-241, 2019.

[161] Sánchez-marañón, M., Delgado, G., Delgado, R., Pérez, M., Melgosa, M., Spectroradiometric and visual colour measurements of disturbed and undisturbed soil samples, Soil Sci, 160, 291-303, 1995.

[162] Sánchez-marañón, M., Huertas, R., Melgosa, M., Colour variation in standard soil-colour charts, Aust. J. Soil Resour, 43, 827-837, 2005.

[163] Sánchez-marañón, M., García, P., Huertas, R., Hernández-andrés, J., Melgosa, M., Influence of natural daylight on soil colour description: assessment using a color-appearance model, Soil Sci. Soc. Am. J., 75, 984-993, 2011.

[164] Stiglitz, R., Evaluation of an inexpensive sensor to measure soil color, all theses 2016.

[165] Soane, B.D., Blackwell, P.S., Dickson, J.W., Painter , D.J., Compaction by agricultural vehicles: a review, Soil and Tillage research, 1, 207-237, Elsevier scientific publishing company, Amsterdam -- printed in Belgium, 1980/1981.

[166] Song, G., and Malla, R., Earth and space 2010 - engineering, science, construction and operations in challenging environments, in: proceedings, 12th ASCE Aerospace Div. Internat. conf. on engineering, construction and operations in challenging environments, 2010.

[167] Seta, E., Kamegawa, T., Nakajima, Y., Prediction of snow/tire interaction using explicit FEM and FVM, Tire Science and Technology, TSTCA, 31(3), 173-188, 2003.

[168] Soil survey staff, Soil Taxonomy: a basic system of soil classification for making and interpreting soil surveys, 2nd ed., U.S. dept. of agriculture, natural resources conservation service: Washington, DC, USA, 1999.

[169] Spectrophotometer CM700d/600d, Instruction manual, KONICA MINOLTA, 2008.

[170] Tao, G., Lei, D., Liu, L., Li, Y., Zhu, X., Prediction of soil water characteristic curve based on soil water evaporation, Advances in Civil Engineering, 2021.

[171] Tan, T.K., Three-dimensional theory of the consolidation and flow of clay layers, Scientia Sinica, 6, 1, 1957.

[172] Tanaka, T., Operation in paddy fields: state-of-the-art report, J. Terramechanics 21, 153-179, 1984.

[173] Tanaka, H., Momozu, M., Oida, A., Yamazaki, M., Simulation of soil deformation and resistance at bar penetration by the distinct element method, Journal of Terramechanics, 37(1), 41-56, 2000.

[174] Taylor, J.H., and Gill, W.R., Soil compaction: state-of-the-art report, J. Terramechanics 21, 195-213, 1984.

[175] Taghavifar, H., and Mardani, A., Off-road vehicle dynamics, Studies in systems, decision and control 70, Springer International Publishing Switzerland, 2017.

[176] Torrent, J., and Barrón, V., Laboratory measurement of soil color: theory and practice, Soil Sci. Soc. Am, 31, 21-33, 1993.

[177] Turnage, G. W., Prediction of in-sand tire and wheeled vehicle drawbar performance, proceedings of the 8th international conference of the international society for terrain-vehicle systems, i, 121-150, 1984.

[178] Turk, J., and Rebecca, Y., Field conditions and the accuracy of visually determined Munsell soil color, Soil Sci. Soc. Am. J, 84, 163-169, 2020.

[179] Terzaghi K., Theoretical Soil Mechanics, John Wiley & Sons, Inc., New York, 1943.

[180] United States Department of Agriculture (USDA), Soil color, 2020.

[181] Upadhyaya, S.K., Rosa, U.A., Wulfsohn, D., Application of the finite element method in agricultural soil mechanics, Adv. Soil Dyn. 2, 117-153, ASAE, 2002.

[182] Uffelman, F.L., Proc.int.conf., Soil vehicle systems, 1961.

[183] Viscarra Rossel, R.A., Minasny, B., Roudier, P., Mcbratney, A., Colour space models for soil science, Geoderma, 133, 320-337, 2006.

[184] Vodyanitskii, Y., and Savichev, A., The influence of organic matter on soil colour using the regression equations of optical parameters in the system cie - l*a*b*, Ann. Agrar. Sci, 15, 380-385, 2017.

[185] Vanderlinde, J., Discrete element modeling of a vibratory subsoiler, Ms thesis thesis, department of mechanical and mechatronic engineering, University of Stellenbosch, Matieland, South Africa, Matieland, 2007.

[186] Wong, J.Y., Discussion on ‘prediction of wheel-soil interaction and performance using the finite element method’, Journal of Terramechanics, 14(4), 240-250, 1977.

[187] Wong, J.Y., Terramechanics and off-road vehicles, Amsterdam: Elsevier, 1989.

[188] Wong J.Y., Terramechanics and off-road vehicle engineering, Terrain behaviour, off-road vehicle performance and design, second edition, Ottawa-Canada, 2010.

[189] Wong, J.Y., Terramechanics and Off-road vehicle engineering:terrain behaviour, off-road Vehicle Performance and Design, 2nd ed.; Butterworth-Heinemann: Oxford, UK, 2009.

[190] Wanjii, S., Hiroma T., Ota Y., and Kataoka T., Prediction of wheel performance by analysis of normal and tangential stress distributions under the wheel-soil interface, Journal of Terramechanics, vol. 34, no.3, pp.165-186, 1997.

[191] Wismer, D., and Luth, H.J., Off-road traction prediction for wheeled vehicles, Journal of Terramechanics, vol. 10, no. 2, pp. 49-61, 1973.

[192] Wills, B.M.D., The load sinkage equation in theory and practice, proc. 2nd int. conf. Int Soc Terrain-Vehicle Systems, Quebec, pp. 199-246, 1966.

[193] Wills, S., Sandor, J., Burras, L., Prediction of soil organic carbon content using field and laboratory measurements of soil color, Soil Sci. Soc. Am. J, 71, 380-388, 2007.

[194] Warr, B., Soil colour, INSEAD: Fontainebleau, Singapore, 2015.

[195] Wroth, C.P., The interpretation of in-situ soil tests, Geotechnique, 34: 449-489, 1984.

[196] William, S., and Huei, P., Modeling of wheel-soil interaction over rough terrain using the discrete element method, Journal of Terramechanics, 50, 277-287, 2013.

[197] Winters, E., The measurement of soil color, Amer. Soil surv. Assoc. Bull. 11, 34-37, 1930.

[198] Winters, E., The measurement of soil color, Soil Science of America Journal 11, 34-37, 2001 (1930).

[199] Yong, R.N., and Windish, E.J., Determination of wheel contact stresses for measured instantaneous soil deformation, J. of Terramechanics, vol. 7, no. 3/4, pp. 57-67, 1970.

[200] Yong, R.N, and Warkentin B.P, Soil properties and behaviour, Elsevier, Amsterdam, 1975.

[201] Yong, R.N., and Fattah, E.A., Prediction of wheel-soil interaction and performance using the finite element method, Journal of Terramechanics, 13(4), 227-240, 1976.

[202] Yong, R.N., and Fattah, E.A., Boosinsuk, R., Analysis and prediction of tyre-soil interaction and performance using finite elements, Journal of Terramechanics, 15(1), 43-63, 1978.

[203] Yong, R. N., and Fattah, E.A, Boonsinsuk, P., Analysis and predictions of tracked vehicles: theoretical prediction versus field measurements, Proc. 7th int. conf ISTVS, Calgary, 1981.

[204] Yokoi, H., Relationship between soil cohesion and shear strength, Soil Sci. Plant Nutr., 14, 89-93, 1968.

[205] Zydron, T., and Zgoda, J., The influence of moisture content on shear strength of soils from the Carpathians, Acta Sci. Pol.,11 (2), 75-84, 2012.

[206] Zhang, B., Zhao, Q.G., Horn, R., Baumgartl, T., Shear strength of surface soil as affected by soil bulk density and soil water content, Soil Tillage res. 59 (3), 97-106, 2001.

[207] Zhang, T., Lee, J.H., Liu, Q., Finite element simulation of tire-snow interaction under combined longitudinal and lateral slip condition, Proceedings of the 15th international conference of the international society for terrain-vehicle systems, 2005.

[208] Zhou, Q., Shen, H., Helenbrook, B., et al., Scale dependence of direct shear tests, Chinese Sci. Bull., 54, 4337-4348, 2009.

[209] Zanetti, S.S., Cecílio R.A., Alves, E.G., Silva, V.H., Sousa, E.F., Estimation of the moisture content of tropical soils using color images and artificial neural networks, CATENA, volume 135, Pages 100-106., 2015.

13. Publications and conferences

- **List of English language publications:**

Publication 1 : Soil Strength and Load Bearing Capacity Measurement Techniques - **Hungarian Agricultural Engineering / (**co-author).

Publication 2 : Review on Soil Shear Strength with Loam Sand Soil Results Using Direct Shear Test - **Journal of Terramechanics** / (author), **Impact factor:** 2.4 (Q1).

Publication 3 : Sandy Loam Soil Shear Strength Parameters and its Colour - Applied Sciences **MDPI /** (author), **Impact factor:** 2.7 (Q1).

Publication 4 : Load Bearing Capacity of Sandy Loam Soil Related to its Colour at Different Moisture Contents - Applied Sciences **MDPI** / (co-author), **Impact factor:** 2.7 (Q1).

Publication 5 : Visible Range Spectrophotometric Colour Results and Shear Strength Data of Sandy Loam Soil - **Mechanical Engineering Letters** / (author).

- **List of Hungarian language publications:**

Publication 1 : Homokos Vályogtalaj Nyírószilárdságának Meghatározása / **Mezőgazdasági Technika** (author).

- **Conferences - proceedings:**

Conference paper : Soil Shear Strength Values Obtained from its Color - **ISTVS,** 16-th European African Regional Conference, Poland, Lublin, 2023 / (author).

- **Conferences - abstracts:**

Abstract : Determination of Soil Shear Strength by Remote Sensing - International Conference and Workshop on Alternatives to Reduce Soil Degradation, Hungary, Budapest, 2024 / (author).

14. Acknowledgement

I would like to thank my supervisor, Prof. Dr. Péter Kiss, for assisting and guiding me during the research period, beside that benefiting from his experience in the field of study. In addition to working on the research, also getting the opportunity to teach at the university (PhD teaching activity), the case that has also helped me to nourish my knowledge in engines and automotive field theoretically and practically under the supervision of the Professor.

I would like to thank Dr. György Pillinger for providing me with help on the research, in the terramechanics field, thus also benefiting from his experience in the field.

I would like to thank the laboratory technician, Tamás Török, for assisting me in the laboratory and field experiments, also for providing me with practical knowledge on engines and automotive systems relying on the laboratory available systems and parts, thus robusting my practical knowledge, where some of it was provided to the students during the lessons (teaching activity).

I would like to thank the PhD school and the Head of the school, Prof. Dr. Gábor Kalácska, for assisting and guiding the students during the PhD journey by following each student's research progress through presentations.

I would like to thank the TAKI soil institute in Budapest (Institute for Soil Sciences) for providing us with information about the measurements (laser and the pippette method) used for finding a soil texture, and with the textures of the soils used in the project.

I would like to thank the university PhD administration team for assisting the students in the administrative issues during the program.

Finally, I would like to thank the Stipendium Hungaricum foundation for funding my PhD program, thus awarding me the opportunity to pursue my education.

Project no. 2022-2.1.1-NL-2022-00012 has been implemented with the support provided by the Ministry of Culture and Innovation of Hungary from the National Research, Development and Innovation Fund, financed under the 2022-2.1.1-NL funding scheme.

Thank you

Alaa El Hariri

Gödöllő, March 2025